ANTIBACTERIAL AND BIODEGRADATION PERFORMANCE FOR POLY(LACTIC ACID) AND WOOD FLOUR/POLY(LACTIC ACID) COMPOSITES

MR. CHANA PRAPRUDDIVONGS

A DISSERTATION SUBMITTED IN PARTIAL FULFILLMENT OF REQUIREMENTS
FOR THE DEGREE OF DOCTOR OF PHILOSOPHY (MATERIALS TECHNOLOGY)
SCHOOL OF ENERGY, ENVIRONMENT AND MATERIALS
KING MONKUT'S UNIVERSITY OF TECHNOLOGY THONBURI
2013

Antibacterial and Biodegradation Performance for
Poly(lactic acid) and Wood Flour/Poly(Lactic Acid) Composites

Mr. Chana Prapruddivongs M.Eng. (Chemical Engineering)

A Dissertation Submitted in Partial Fulfillment of the Requirements for
the Degree of Doctor of Philosophy (Materials Technology)
School of Energy, Environment and Materials
King Mongkut's University of Technology Thonburi
2013

Dissertation Committee

……...…… Chairman of Dissertation Committee
(Prof. Dr. Suda Kiatkamjornwong, Ph.D.)

……...…… Member and Dissertation Advisor
(Prof. Dr. Narongrit Sombatsompop, Ph.D.)

……...…… Member
(Assoc. Prof. Dr. Jatuphorn Wootthikanokkhan, Ph.D.)

……...…… Member
(Assoc. Prof. Dr. Benjaphorn Prapagdee, Ph.D.)

Dissertation Title	Antibacterial and Biodegradation Performance for Poly(Lactic acid) and Wood Flour/poly (Lactic Acid) Composites
Dissertation Credits	42
Candidate	Mr. Chana Prapruddivongs
Dissertation Advisor	Prof. Dr. Narongrit Sombatsompop
Program	Doctor of Philosophy
Field of Study	Materials Technology
Department	Materials Technology
Faculty	School of Energy, Environment and Materials
Academic Year	2013

Abstract

This work aimed to study the properties of poly(lactic acid) (PLA) and wood/poly (lactic acid) (PLA) based composites including mechanical, thermal, antibacterial, barrier properties and biodegradable performance. The first part of this work, Poly(lactic acid) (PLA) and wood flour/PLA composites were prepared and blended with two antimicrobial agents, triclosan and silver-substituted zeolite (Zeomic), using a twin-screw extruder. The mechanical and thermal properties, antimicrobial activity, and biodegradation performance were investigated. The addition of wood was found to increase the Young's modulus of the composites, whereas the tensile strength, elongation at break, and impact strength dropped because of its incompatibility. The mechanical properties of the PLA and wood/PLA composites filled with Zeomic were also found to drop, especially at a presence of 10 %wt wood, because of the degradation of the PLA matrix as a result of a hydrolysis reaction between PLA, water molecules in the zeolite structure and absorbed water molecules by the wood particles. However, the mechanical properties of PLA and wood/PLA loaded with triclosan did not show any definite trends. Differential scanning calorimeter (DSC) data indicated that the T_g value of neat PLA was 63^oC, whereas those of wood/PLA composites were lower. When wood and Zeomic were incorporated, PLA exhibited double melting peaks. For triclosan system, *Escherichia coli* (*E. coli*) and *Staphylococcus aureus* (*S.aureus*) growth appeared to increase with contact time for PLA, but to decrease with contact time for the wood/PLA composites. Based on the results and quantitative evidence, it

was proposed that the wood flour acted as an "antibacterial promoter" for triclosan blended wood/PLA composites, which facilitated triclosan migration onto the wood/PLA composite surfaces to kill the bacteria. The molecular interactions between PLA, triclosan and wood were quantitatively characterized experimentally by water contact angle and Fourier transform infrared spectroscopy (FTIR). However, Zeomic did not show antibacterial performance under the test condition. Biodegradation tests of neat PLA and wood/PLA composites showed that after a 60-day incubation period the biodegradation rate of wood/PLA was higher than that of PLA. PLA and wood/PLA containing Zeomic were found to degrade more quickly, suggesting that wood and Zeomic acted as biodegradation promoters. On the other hand, triclosan could be considered a biodegradation retarder, since no biodegradation was observed for any triclosan-loaded samples during the initial 20 days of incubation, while neat PLA and wood/PLA composites began to degrade within the first few days.

For the second part, the PLA, triclosan, wood and Cloisite® 30B were compounded using twin screw extruder. This part focused on determinations of mechanical, antibacterial, thermal and barrier properties of PLA composites. It was found that only the tensile modulus of PLA composites increased while the others decreased when 10 %wt wood was loaded. The effect of triclosan and Cloisite® 30B compounding did not change the mechanical properties and glass transition temperature. However, by the presence of wood and Cloisite® 30B, T_m values of the composites exhibited double peak characteristic which was related to an increase in crystallinity level. Antibacterial activity of the PLA composites was improved with the Cloisite® 30B content, and this was attributed to cationic bactericide quaternary ammonium group between the silicates layers. Hydrophobic material triclosan obviously changed water vapor permeability (WVP) of the PLA from 8.24×10^{-11} to at 7.26×10^{-11} g.mm/mm^2.h.Pa for triclosn/PLA specimens. All PLA composites samples with 0.5 %wt clay content showed a significant increase in oxygen barrier property as a result of the exfoliate dispersion.

Keywords: Antibacterial Agent/Biodegradation/Organoclay/Poly(Lactic Acid)/ Wood polymer composite

หัวข้อวิทยานิพนธ์ :	ความสามารถในการยับยั้งเชื้อแบคทีเรียและการย่อยสลายทางชีวภาพสำหรับพอลิแลคติกแอซิดและวัสดุเชิงประกอบระหว่างผงขี้เลื่อยไม้กับพอลิแลคติกแอซิด
หน่วยกิต	42
ผู้เขียน	นายชนะ ประพฤทธิ์วงศ์
อาจารย์ที่ปรึกษา	ศ. ดร. ณรงค์ฤทธิ์ สมบัติสมภพ
หลักสูตร	ปรัชญาดุษฎีบัณฑิต
สาขาวิชา	เทคโนโลยีวัสดุ
สายวิชา	เทคโนโลยีวัสดุ
คณะ	พลังงานสิ่งแวดล้อมและวัสดุ
ปีการศึกษา	2556

บทคัดย่อ

จุดประสงค์ของงานนี้คือเพื่อทำการศึกษาสมบัติของพอลิแลคติกแอซิด และวัสดุเชิงประกอบระหว่างผงขี้เลื่อยไม้และพอลิแลกติกแอซิด ซึ่งประกอบไปด้วยสมบัติเชิงกล เชิงความร้อน การยับยั้งเชื้อแบคทีเรีย การป้องกันการซึมผ่าน และประสิทธิภาพในการย่อยสลายทางชีวภาพ ในส่วนแรกของงานนั้นเป็นการเตรียม พอลิแลกติกแอซิด และวัสดุเชิงประกอบของผงขี้เลื่อยไม้และพอลิแลกติกแอซิด โดยการผสมกับสารยับยั้งเชื่อแบคทีเรีย 2 ชนิด คือ triclosan และ Zeomic โดยใช้เครื่องอัดรีดผสมชนิดเกลียวหนอนคู่ จากนั้นทำการศึกษาสมบัติเชิงกล เชิงความร้อน การยับยั้งเชื่อแบคทีเรีย และประสิทธิภาพในการย่อยสลายทางชีวภาพ การผสมผงขี้เลื่อยทำให้มอดูลัสของยังมีค่าเพิ่มขึ้น ในขณะที่สมบัติการต้านทานแรงดึง การยืดตัว ณ จุดขาดและสมบัติการต้านทานแรงกระแทกลดลงเพราะการเข้ากันระหว่างผงขี้เลื่อยไม้และพอลิแลกติกแอซิดที่ไม่ดีนัก สมบัติเชิงกลของพอลิแลกติกแอซิดและวัสดุเชิงประกอบระหว่างผงขี้เลื่อยไม้และพอลิแลกติกแอซิดที่ผสม Zeomic มีค่าลดลง โดยเฉพาะอย่างยิ่งเมื่อมีการผสมผงขี้เลื่อยไม้ 10 % โดยน้ำหนัก ทั้งนี้เนื่องจากการเสื่อมสภาพของพอลิแลกติกแอซิดอันเนื่องมาจากการเกิดปฏิกริยาไฮโดรไลซิสระหว่างพอลิแลกติกแอซิดกับโมเลกุลของน้ำภายในโครงสร้างของ Zeomic และโมเลกุลของน้ำที่ถูกดูดซึมไว้โดยผงขี้เลื่อยไม้ อย่างไรก็ตามสมบัติเชิงกลของพอลิแลกติกแอซิดและวัสดุเชิงประกอบระหว่างผงขี้เลื่อยไม้และพอลิแลกติกแอซิดที่ผสม triclosanไม่ได้มีการเปลี่ยนแปลงที่ชัดเจนนัก ข้อมูลจาก DSC บ่งชี้ว่า อุณหภูมิการเปลี่ยนสถานะคล้ายแก้ว (T_g) ของพอลิแลกติกแอซิดคือ 63 องศาเซลเซียส ในขณะที่อุณหภูมิการเปลี่ยนสถานะคล้ายแก้วของวัสดุเชิงประกอบระหว่างผงขี้เลื่อยไม้และพอลิแลกติกแอซิดที่มีค่าลดลง นอกจากนี้พอลิแลกติกแอซิดแสดงพีคการสลายผลึกแบบสองพีก (double melting peak) เมื่อมีการ

ผสมขี้เลื่อยและ Zeomic ในระบบที่มีการผสม triclosan นั้นพบว่า *E.coli* และ *S.aureus* มีการเจริญเติบโต แต่การเจริญเติบโตของเชื้อแบคทีเรียลดลงเมื่อมีการเติมผงขี้เลื่อย ทำให้เกิดเป็นข้อสรุปว่าผงขี้เลื่อยไม้ทำหน้าที่เป็น "ตัวส่งเสริมการยับยังการเจริญเติบโตของเชื้อแบคทีเรีย" เนื่องจากผงขี้เลื่อยไม้ช่วยให้ triclosan เคลื่อนที่ออกจากผิวของพอลิแลกติกแอซิดเพื่อฆ่าเชื้อเบคทีเรียได้ง่ายขึ้น การเกิดอันตกริยาระหว่างพอลิแลกติกแอซิด triclosan และผงขี้เลื่อยนั้นสามารถตรวจสอบได้โดยการวัดค่ามุมสัมผัสของน้ำ และ FTIR อย่างไรก็ตาม Zeomic ไม่ได้แสดงสมบัติในการยับยั้งเชื้อแบคทีเรียภายใต้ภาวะที่ทดสอบ การทดสอบการย่อยสลายทางชีวภาพของพอลิแลกติกแอซิด และวัสดุเชิงประกอบระหว่างผงขี้เลื่อยไม้กับพอลิแลกติกแอซิดแสดงให้เห็นว่า เมื่อเวลาผ่านไป 60 วัน การย่อยสลายทางชีวภาพของวัสดุเชิงประกอบระหว่างผงขี้เลื่อยไม้กับพอลิแลกติกแอซิดมีค่าสูงกว่าของพอลิแลกติกแอซิด สำหรับพอลิแลกติกแอซิดและวัสดุเชิงประกอบระหว่างผงขี้เลื่อยไม้และพอลิแลกติกแอซิดที่มีการผสม Zeomic นั้นพบว่าการย่อยสลายทางชีวภาพจะเกิดขึ้นอย่างรวดเร็ว ซึ่งแสดงให้เห็นว่าผงขี้เลื่อยและ Zeomic สามารถทำหน้าที่เป็นตัวส่งเสริมการย่อยสลายทางชีวภาพ ในทางตรงกันข้าม triclosan สามารถประพฤติตัวเสมือนเป็นสารช่วยยับยั้งการย่อยสลายทางชีวภาพ เนื่องจากไม่พบการย่อยสลายของพอลิแลกติกแอซิดภายในช่วงเวลา 20 วันแรกของการทดสอบ หลังจากนั้นการย่อยสลายทางชีวภาพจึงเกิดขึ้นอย่างรวดเร็ว

สำหรับงานในส่วนที่ 2 พอลิแลกติกแอซิด triclosan ผงขี้เลื่อยและ Cloisite® 30B จะถูกนำมาผสมกันด้วยเครื่องอัดรีดผสมชนิดเกลียวหนอนคู่ งานในส่วนนี้จะสนใจศึกษาสมบัติเชิงกล การยับยั้งเชื้อแบคทีเรีย สมบัติทางความร้อน และสมบัติการต้านทานการซึมผ่านของพอลิแลกติกแอซิดวัสดุเชิงประกอบของพอลิแลกติกแอซิด ผลการทดลองพบว่ามีเพียงค่ามอดุลัสเท่านั้นที่มีค่าเพิ่มสูงขึ้น ในขณะที่สมบัติอื่นๆมีค่าลดลงเมื่อผสมขี้เลื่อย 10 % โดยน้ำหนัก การเติม triclosan และ Cloisite® 30B ไม่ส่งผลต่อสมบัติเชิงกลอย่างมีนัยสำคัญ และเมื่อมีการผสมขี้เลื่อยและ Cloisite® 30B จะทำให้อุณหภูมิการสลายผลึกมี 2 ค่า และส่งผลให้มีปริมาณความเป็นผลึกของพอลิแลกติกแอซิดเพิ่มสูงขึ้น สมบัติการยับยั้งเชื้อแบคทีเรียของวัสดุเชิงประกอบพอลิแลกติกแอซิดเพิ่มขึ้นเมื่อมีการผสม Cloisite® 30B เนื่องจาก Cloisite® 30B มีหมู่ cationic bactericide quaternary ammonium อยู่ภายในชั้นซิลิเกตซึ่งมีความสามารถในการฆ่าเชื้อแบคทีเรีย การผสม triclosan ทำให้ค่าการซึมผ่านของน้ำ ลดลงอย่างชัดเจนจาก 8.24×10^{-11} เป็น 7.26×10^{-11} g mm/mm^2 h Pa วัสดุเชิงประกอบทั้งหมดที่มีการผสม Cloisite® 30B ที่ปริมาณ 0.5 % โดยน้ำหนัก เกิดการกระจายตัวแบบ exfoliation และทำให้ค่าการซึมผ่านของออกซิเจนลดลงอย่างชัดเจน

คำสำคัญ: การย่อยสลายทางชีวภาพ/พอลิแลกติกแอซิด/ออร์แกโนเคลย์/สารยับยั้งเชื้อแบคทีเรีย/วัสดุ-เชิงประกอบของผงขี้เลื่อยไม้และพอลิเมอร์

ACKNOWLEDGEMENTS

It is great opportunity for me to express my sincere gratitude to all of the people mentioned below. I would like to express my gratitude to my supervisor, Professor Dr. Narongrit Sombatsompop, for providing me an opportunity to work in the P-PROF research group and also the invaluable constructive guidance and encouragement throughout my study. Sincere gratitude is extended to Professor Dr. Suda Kiatkamjornwong, Associate Professor Dr. Jatuphorn Wootthikanokkhan, Associate Professor Dr. Benjaphorn Prapagdee for helps and providing useful suggestions and discussions. The College of Industrial Technology, King Mongkut's University of Technology North Bangkok (KMUTNB) is also acknowledged for the biological laboratory facilitations. I gratefully acknowledged Associate Professor Dr. Krishnan Jayaraman for his kindness, useful suggestions and advised me during my international internship period at the Centre for Advanced Composite Materials (CACM) the University of Auckland, New Zealand. I would also like to thank the Office of the Higher Education Commission (OHEC) under the National Research University Program, and the Thailand Research Fund (TRF Research Senior Scholar; RTA5280008) for financial co-support throughout this work. I am also obliged all staffs and members of P-PROF group, especially Mr. Apisit Kositchaiyong, for friendliness and supports. I would like to thank my mom and my family, for always standing by my side even though I was facing the hard time.

Finally, from the bottom of my heart I would like to thank my passed away father who always supported and gave me everything until his last breath.

CONTENTS

		PAGE
ENGLISH ABSTRACT		ii
THAI ABSTRACT		iv
ACKNOWLEDGEMENTS		vi
CONTENTS		vii
LIST OF TABLES		x
LIST OF FIGURES		xii
1. INTRODUCTION		**1**
1.1	Introduction	1
1.2	Objectives	4
1.3	Scope of Work	4
2. THEORIES AND LITERATURE REVIEWS		**6**
2.1	Biodegradable polymers	6
2.2	Polylactic acid (PLA)	7
2.3	Poly (lactic acid) based composites	10
2.4	Biodegradation	21
2.5	Standard test methods for biodegradation of biopolymers	29
2.6	Bacteria and biochemical target for drugs action	33
2.6.1	Bacterial cell structure	33
2.6.2	Biochemical target for drugs action	37
2.6.3	Mechanism of selected antibacterial action	40
2.7	Active polymeric materials	46

PAGE

2.7.1	Using of sachets or pads containing volatile antimicrobial agents into material packages	46
2.7.2	Antimicrobial agents Incorporated into polymer directly	47
2.7.3	Coating or adsorbing antimicrobial agents to polymer surface	48
2.7.4	Immobilized antimicrobial agents to polymers by inorganic or covalent linkages	49
2.7.5	Inherently antimicrobials polymer	50
2.8	Standard test methods for evaluation active materials effectiveness	50
2.8.1	Inhibition zone test (Agar Diffusion)	50
2.8.2	Minimal inhibitory concentrations (MIC)	52
2.8.3	Shake flasks test or Plate count agar (PCA)	52
2.9	Literature review	54
3. RESEARCH METHODOLOGY		**58**
3.1	Materials, chemicals and testing bacteria	58
3.2	Research plans	59
3.3	Experiment	62
3.3.1	Specimen preparation	62
3.3.2	Antibacterial activity evaluations	65
3.3.3	The biodegradation test	66
3.3.4	Barrier properties test	68
3.3.5	Characterizations	69
3.4	Experimental problems and solutions during the work	71
3.4.1	Problems and solutions	71

PAGE

4. RESULT AND DISCUSSION **77**

4.1 Effect of wood flour and antibacterial agents loading on the mechanical, antibacterial and biodegradable properties of PLA and PLA based composites 77

4.1.1 Mechanical properties 77

4.1.1.1 Effect of wood flour loading 77

4.1.1.2 Effect of antibacterial agents loading 79

4.1.2 Antibacterial property 84

4.1.2.1 Qualitative antibacterial test 84

4.1.2.2 Quantitative antibacterial test 85

4.1.2.3 Assumption proofs 95

4.1.3 Biodegradable property 107

4.2 Effect of Organoclay Incorporation on Mechanical, Barrier and Thermal Properties and Anti-bacterial Performance of PLA and PLA composites with triclosan and Wood Flour 114

4.2.1 Mechanical properties 114

4.2.2 Thermal property and Clay dispersion analysis 117

4.2.3 Antibacterial properties 121

4.2.4 Barrier properties 126

5. CONCLUSIONS AND FUTURE WORKS **129**

5.1 Conclusions 129

5.2 Future works 131

REFERENCES **132**

BIOGRAPHY **145**

LIST OF TABLES

TABLE		PAGE
2.1	The relationship of wood content and percent crystallinity	15
3.1	Materials, chemicals and testing bacteria used in this work	58
3.2	Composite formulations and symbols used for work flowcharts 1-2	63
3.3	Composite formulations and symbols used for work flowcharts 3	64
3.4	Properties of soil composed in this study	67
4.1	Effect of triclosan content on the changes in mechanical properties of PLA and wood/PLA composites	83
4.2	Percentage of *S.aureus* bacterial reductions at different contact times for PLA and wood/PLA composites with Triclosan and Zeomic loadings of 0.5 - 1.5%wt	89
4.3	Percentage of *E.coli* bacterial reductions at different contact times for PLA and wood/PLA composites with Triclosan and Zeomic loadings of 0.5 - 1.5%wt	94
4.4	Percentage of *E.coli* bacterial reductions at different contact times for PLA with Zeomic loadings of 0.5 - 1.5%wt prepared by quenching process	98
4.5	Water contact angle of PLA and wood/PLA incorporated with triclosan and Zeomic loadings of 0 and 1.5%wt	101
4.6	Appearance of PLA and PLA based composites before and after biodegradation test	108

LIST OF TABLES (Cont.)

TABLE		PAGE
4.7	Biodegradation rates for PLA and wood/PLA composites with and without the addition of Zeomic or triclosan (1.5 % wt)	109
4.8	Thermal properties of PLA and PLA based composites	118
4.9	Percentage of bacterial reductions at different contact times for PLA, W_{10}/PLA and 1.5% triclosan/ W_{10}/PLA composites with Cloisite® 30B loadings of 0.0 – 2.0 wt%	125

LIST OF FIGURES

FIGURE		PAGE
2.1	Classification of the biodegradable polymers	7
2.2	Chemical structure of PLA	7
2.3	PLA synthesis schematic	9
2.4	The chemical structure of cellulose	11
2.5	Hydrogen bond of intra- and inter-molecular of cellulose	11
2.6	The chemical structure of hemicelluloses	12
2.7	The chemical structure of Lignin	13
2.8	Tensile stress–strain curves of the PLA and WF/PLA composites	14
2.9	Structure of 2:1silicate layers	16
2.10	Relationship of transmission electron microscopic of TEM images and the expected wide angle X-ray scans for nanocomposite materials	18
2.11	Schematic presentation of the formation of tortuous path in Polymer/clay nanocomposite	19
2.12	Relationship of Molecular weight and hydrolysis time of PLA and PLA/nano clay composites	20
2.13	General mechanism of plastics biodegradation	21
2.14	Mechanism of hydrolysis reaction of poly (lactic acid)	23
2.15	The model of enzymatic polyester depolymerase	24
2.16	Mechanism of Enzymatic degradation	25
2.17	Effect of pH against hydrolysis reaction on poly (lactic acid)	26

LIST OF FIGURES (Cont.)

FIGURE		PAGE
2.18	Possible mechanism of hydrolysis	28
2.19	Schematic diagram of carbon dioxide evolution measuring system	31
2.20	Bacterial cell structure	33
2.21	Comparison of cell wall of Gram positive and Gram negative bacteria	35
2.22	Target for drug action	37
2.23	Molecular structure of Nisin	41
2.24	Mechanism of action for cationic biocides	42
2.25	Molecular structure of triclosan	43
2.26	Structure of FabI-NAD1-triclosan complexes	43
2.27	Transmission electron micrograph of E. coli cell treated with silver nanoparticles	45
2.28	Antimicrobial agent incorporated for packaging system	47
2.29	Antimicrobial agent coated for packaging system	48
2.30	Antimicrobial agent immobilized for packaging system	49
2.31	Model of inhibition zone	51
3.1	Work flowcharts for the studies of the effect of wood flour and antibacterial agents loading on PLA and wood/PLA composites properties	60
3.2	Work flowcharts for the studies of the effect of wood flour and antibacterial agents loading on biodegradable performance of PLA and wood/PLA composites	60

LIST OF FIGURES (Cont.)

FIGURE		PAGE
3.3	Work flowcharts for the studies the effect of organoclay loading on mechanical, thermal, antibacterial properties and barrier properties of PLA and PLA based composites	61
3.4	Arrangement of the biodegradation test for PLA and wood/PLA composites (modified from ASTM D5338-1)	67
3.5	Over melted PLA during high speed mixing process	71
3.6	Over melted PLA loaded with 20 and 40 %wt wood flour during extrusion process	72
3.7	Bubble evolved across the wood/PLA sheets	73
3.8	Cutting maching with a cooling unit	74
3.9	Broken Zeomic/PLA composite sheets	74
3.10	Over melted wood/PLA loaded with 1.5% Zeomic composites during extrusion process	75
3.11	Fermented soil for biodegradation test	76
4.1	Mechanical properties of PLA and wood flour/PLA composites in terms of: (a)Young's modulus and tensile strength; (b) elongation at break and impact strength	78
4.2	Young's modulus of PLA and wood/PLA composites with different wood contents, different types and amounts of antibacterial agents	79
4.3	Tensile strength of PLA and wood/PLA composites with different wood contents, different types and amounts of antibacterial agents	81

LIST OF FIGURES (Cont.)

FIGURE		PAGE
4.4	Elongation at break of PLA and wood/PLA composites with different wood contents, different types and amounts of antibacterial agents	81
4.5	Impact strength of PLA and wood/PLA composites with different wood contents, different types and amounts of antibacterial agents	82
4.6	Inhibition zone test against *E.coli*	84
4.7	Viable cell count of *S. aureus* with triclosan loadings of 0.5–1.5 %wt for different contact times	86
4.8	Viable cell count of *S. aureus* with Zeomic loadings of 0.5–1.5 %wt for different contact times	87
4.9	Viable cell count of *E.coli* with triclosan loadings of 0.5–1.5 %wt for different contact times	91
4.10	Viable cell count of *E.coli* with Zeomic loadings of 0.5–1.5 %wt for different contact times	92
4.11	Silver ions releasing mechanism of Zeomic	96
4.12	DSC thermograms of PLA, W_5P and $W1_0P$ composites with and without the addition of 1.5 %wt triclosan or Zeomic	97
4.13	Viable cell count of *E.coli* for PLA sample with Zeomic loadings of 0.5–1.5 %wt at different contact time prepared by quenching process	98
4.14	Intermolecular hydrogen bonds of PLA with triclosan	102

LIST OF FIGURES (Cont.)

FIGURE		PAGE
4.15	A possible model of moisture regain by presence of wood in triclosan/PLA blends	102
4.16	FTIR spectra for PLA and wood/PLA composites filled with triclosan	105
4.17	Cumulative CO_2 evolutions during the test	107
4.18	Degree of biodegradation for PLA and wood/PLA composites	111
4.19	Degree of biodegradation for PLA and wood/PLA composites with Zeomic	112
4.20	Degree of biodegradation for PLA and wood/PLA composites with triclosan	113
4.21	Young's modulus of PLA and PLA based composites with different concentration of triclosan and Cloisite® 30B	115
4.22	Tensile strength of PLA and PLA based composites with different concentration of triclosan and Cloisite® 30B	116
4.23	Elongation at break of PLA and PLA based composites with different concentration of triclosan and Cloisite® 30B	116
4.24	Impact strength of PLA and PLA based composites with different concentration of triclosan and Cloisite® 30B	117
4.25	XRD patterns of Cloisite® 30B and PLA based composite with Cloisite® 30B loading of 0.5–2%wt	119
4.26	Viable cell count of E.coli with 0.5–2%wt Cloisite® 30B loading for 0–240 min. contact time	123

LIST OF FIGURES (Cont.)

FIGURE		PAGE
4.27	Water vapor permeabilities of PLA and PLA based composites as a function of Cloisite® 30B loading	127
4.28	The effect of Cloisite® 30B loading on oxygen permeabilities of PLA and PLA based composites	128

CHAPTER 1 INTRODUCTION

1.1 Introduction

Because of health and environmental concerns, many researchers have focused on the modification of antibacterial packaging made from different materials. Various thermoplastics have been used for these applications, e.g. poly(vinyl chloride), polyethylene, polypropylene, polyurethane and polystyrene [1, 2]. To produce active packaging, many techniques have been employed, such as melt-mixing of antimicrobial agents with polymers, applying a coating on polymer surfaces, and immobilizing polymers by covalent bond linkages [3]. After their service life, however, these types of non-biodegradable packaging become plastic garbage which ultimately is colonized by microorganisms. Thus, the use of a biodegradable polymer like poly(lactic acid) (PLA) has received much attention. Since PLA has sufficient strength, high modulus, and the ability to be fabricated, it has become one of the most popular biodegradable polymers for packaging applications [4].

Wood flour, a biodegradable reinforcing material, is one of the most widely used materials for producing wood–polymer composites (WPC) because it possesses several advantages, e.g. high modulus, low density, reduced material use, and low cost. Wood/PLA composites are of great interest because wood and PLA are not only environmentally friendly materials but they are also expected to degrade completely after disposal at the end of their service lives. However, the incompatibility between wood and PLA is a major problem that must be overcome, usually by means of chemical modification [5, 6].

Barrier property is one of important properties for food packaging because good barrier property can potentially extend food quality and shelf life [7]. PLA is an appropriate candidate for packaging end-use application and has limitations in gas barrier property which should be improved [8]. This drawback can be enhanced by general technique of copolymerization, blending and filling techniques. But, the filler incorporation, especially organoclay into the PLA matrix, has been the most attention because of cost-saving and good barrier property [9]. These clay/polymer composites have strong barrier properties because the clay layers retard the diffusing molecule pathway due to tortuosity. Clays are essentially impermeable inorganic crystals, gas molecules have to permeate around the crystals instead of permeation in a straight line path which takes longer mean path and time for gas absorption though these clay/polymer composites [10]. Cloisite® 30B is an organo-modified montmorillonite having two hydroxyl groups, and the reaction between hydroxyl groups of Cloisite® 30B and PLA makes this clay more compatibility for producing PLA-clay composites [11]. Moreover, Cloisite® 30B could also reduce permeability of PLA [12] and also showed a bacteriostatic function against Listeria monocytogenes [13]. There are three main techniques that can be used for composites preparation, including in-situ polymerization, solution intercalation and melt intercalation. The melt intercalation is preferred for industrial applications because of the absence of solvent and compatibility with current processing techniques [14]. Three types of composites derived from interaction between clays and polymers are immiscible, intercalated, and exfoliated. These factors can be characterized by X-ray diffraction (XRD).

Biodegradation properties of biomaterials have been becoming an interesting research. Many techniques have been employed to study the biological degradation behavior of

"green" biomaterials, including visual observation, weight loss measurement, and detection of changes in mechanical properties, CO_2 evolution, and clear zone formation [15]. Among these, CO_2 evolution is generally preferred because the results of the test are usually more accurate. Using this technique, PLA powders with sizes of 60 and 120 mesh were found to be degraded by up to 91% after 35 days at 58 °C in controlled compost [16]. However, the degree of biodegradability of PLA loaded with antimicrobial agents remains unclear. In this work, it was assumed that PLA could lose some of its natural biodegradability after blending with antibacterial agents because the agents might also kill microorganisms that play a key role in the biodegradation process.

Therefore, the first part of this study primarily focused on the effects of the incorporation of two different antibacterial agents on the antibacterial properties and biodegradability of PLA and wood/PLA composites. Triclosan and Zeomic were selected as representative organic and inorganic antibacterial agents, respectively. Antibacterial activity against *S. aureus* and *E. coli* was evaluated by plate count agar (PCA) method. CO_2 evolution technique was used to determine the biodegradation performance of PLA and wood/PLA composites. Mechanical properties of PLA and wood/PLA composites were measured by a universal testing machine and an impact tester. Thermal properties were studied using differential scanning calorimetry (DSC) technique. The second part of this work concentrated on the effects of organoclay loading on barrier-mechanical and antibacterial properties of organoclay/PLA and organoclay/wood/PLA composites incorporated with triclosan prepared by melt blending.

1.2 Objectives

1. To study the effect of wood flour and antibacterial agents loading on the mechanical, thermal, antibacterial properties and biodegradation performance of PLA and wood/PLA composites.
2. To study the mechanical, thermal, antibacterial properties and barrier properties of PLA and PLA based composites by addition of organclay.

1.3 Scope of work

Materials:

- Polymer: Poly(lactic acid) 2002D, 2003D (NatureWorks, USA) was used in this work, having a specific gravity of 1.24 and a melt flow rate of 4
- Wood flour: wood flour with an average particle size of 100–300 μm

  Antibacterial agents: triclosan (2,4,4'-trichloro-2'-hydroxydiphenylether), 24 USP and silver-substituted zeolite (Zeomic) having a structural formula of $MX_{2/n}O{\cdot}Al_2O_3{\cdot}YSiO_2{\cdot}ZH_2O$ (where M is Ag, Na or other ions, and X, Y and Z are the ratio of components, in mol)
- Organoclay: Cloisite® 30B
- Coupling agent: N-(2-aminoethyl)-3-aminopropyltrimethoxysilane (KBM 603)

Testing bacteria:

- *Staphylococcus aureus* ATCC6538 (Gram positive)
- *Escherichia coli* ATCC25922 (Ggram negative)

Experimental Variables:

- Antibacterial agent : triclosan and Zeomic as organic and inorganic antibacterial agent
- Antibacterial agents concentration: 0.0, 0.5, 1.0 and 1.5 %wt
- Antibacterial test period (contact time): 0, 60, 120, 180, 240 minutes
- Biodegradation test period: 60 days
- Wood flour loading: 0, 5 and 10%wt
- Organoclay content: 0, 0.5, 1.0, 2.0%wt

Experiments and characterizations

- Compounding and forming materials: Twin screw extruder and hot press.
- Mechanical properties: Universal testing machine (ASTM D638-8) and notched Izod impact tester (ASTM D625-06a).
- Antibacterial evaluation :Plate count agar method (ASTM E2149 (2001))
- Biodegradation test: Carbon dioxide measurement (ASTM D5338)
- Water vapor permeability: Environmental chamber (ASTM E96-95)
- Oxygen permeability: Oxygen permeation tester (ASTM D3985-5)
- Wettability: Water contact angle
- Thermal property: Differential scanning calorimetry (DSC)
- Chemical interaction examination : Fourier transform infrared spectroscopy (FTIR)

CHAPTER 2 THEORIES AND LITERATURE REVIEW

2.1 Biodegradable polymers

The field of biopolymers is still in early stage but keeps growing in its popularity every day. Normally, biopolymers mean the polymers that are generated from renewable natural sources, be able to biodegradable but non-toxic. They can be produced by biological systems (i.e. microorganisms, plants and animals) or chemically synthesized from biological materials. Two strategies are applied in converting these raw materials into biodegradable polymers: extraction of the native polymer from plant or animal tissue and a chemical or biotechnological route of monomer polymerization. The classification of biodegradable polymers is usually depending upon their synthesis process.

(i) polymers from biomass such as agro-polymers from agro-resources (e.g., starch or cellulose)

(ii) polymers obtained by microbial production such as the polyhydroxyalkanoates (PHAs)

(iii) polymers conventionally and chemically synthesized from monomers obtained from agro-resources e.g., the poly(lactic acid) (PLA)

However, it is possible to classify biodegradable polymers into two main categories: the agro-polymers and the biodegradable polyesters or bio-polyesters as shown in Figure 2.1.

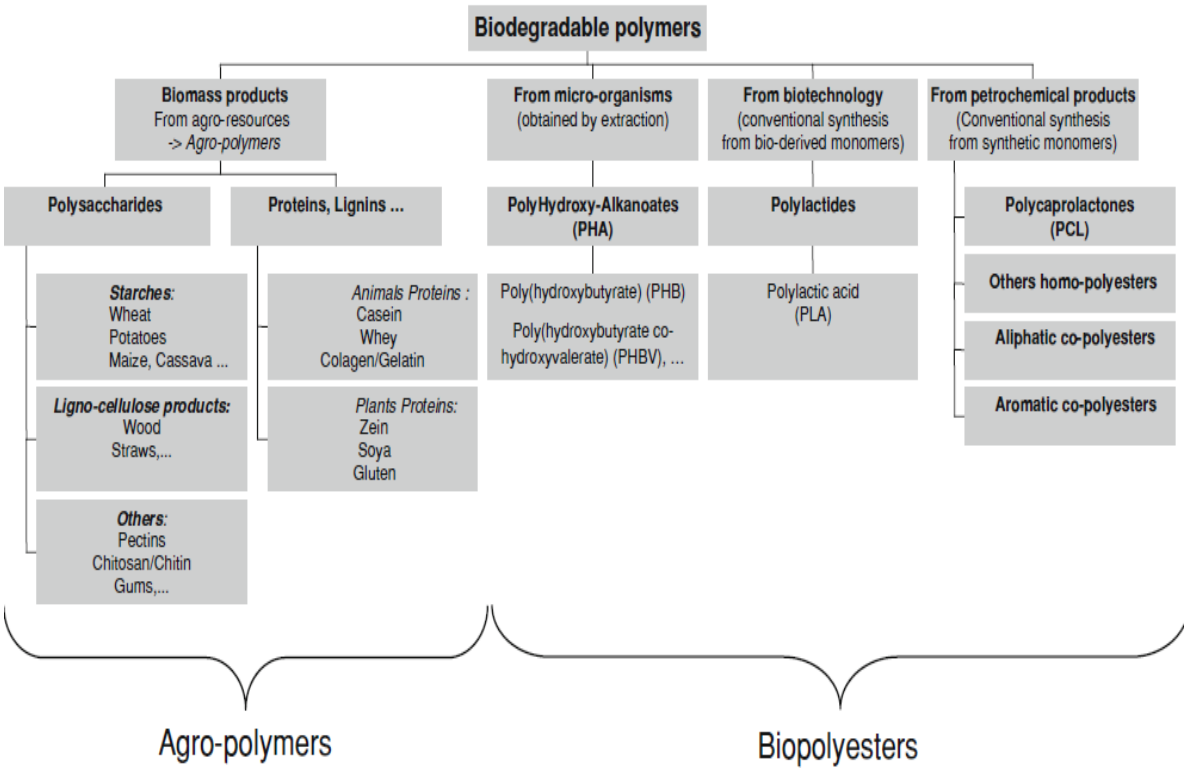

Figure 2.1 Classification of the biodegradable polymers [17]

2.2 Poly(lactic acid) (PLA)

PLA is a biodegradable aliphatic polyester (its structure is shown in Figure 2.2) derived from renewable sources, such as, corn, potato and sugar. Lactic acid (2-hydroxy propionic acid) provided from the fermentation of renewable resources such corn, potato, cane molasses and beet is used as feedstock of PLA production. Lactic acid has D and L stereoisomers which results to the difference in crystallinity level of PLA in the final stage.

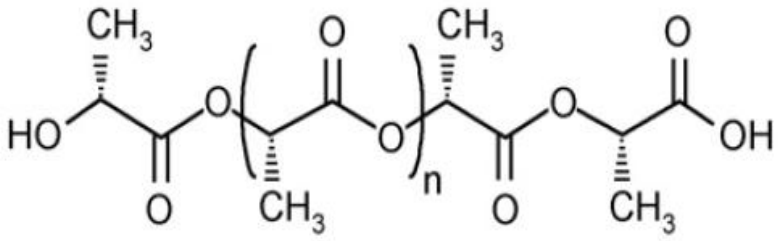

Figure 2.2 Chemical structure of PLA [18]

Biomass is distilled for lactic acid production at the 90 to 99% purity. Currently, the majority of lactic acid production is depended on the fermentation method. The PLA molecular weight for economical production is greater than 100,000 Da. Commercial PLA can be produced by several techniques including azeotropic dehydrative condensation, direct condensation polymerization, and/or polymerization through lactide formation (Figure 2.3). However, direct polycondensation has been extensively used because of its disadvantage. The PLA from direct polycondensation has lower molecular weight because it is hard to remove water content completely from the highly viscous reaction mixture [13]. Either an organic solvent or a multifunctional branching agent (e.g. dipentaerythritol) is used to overcome this difficulty. But, using organic solvent is also difficult to remove it from the PLA end product.

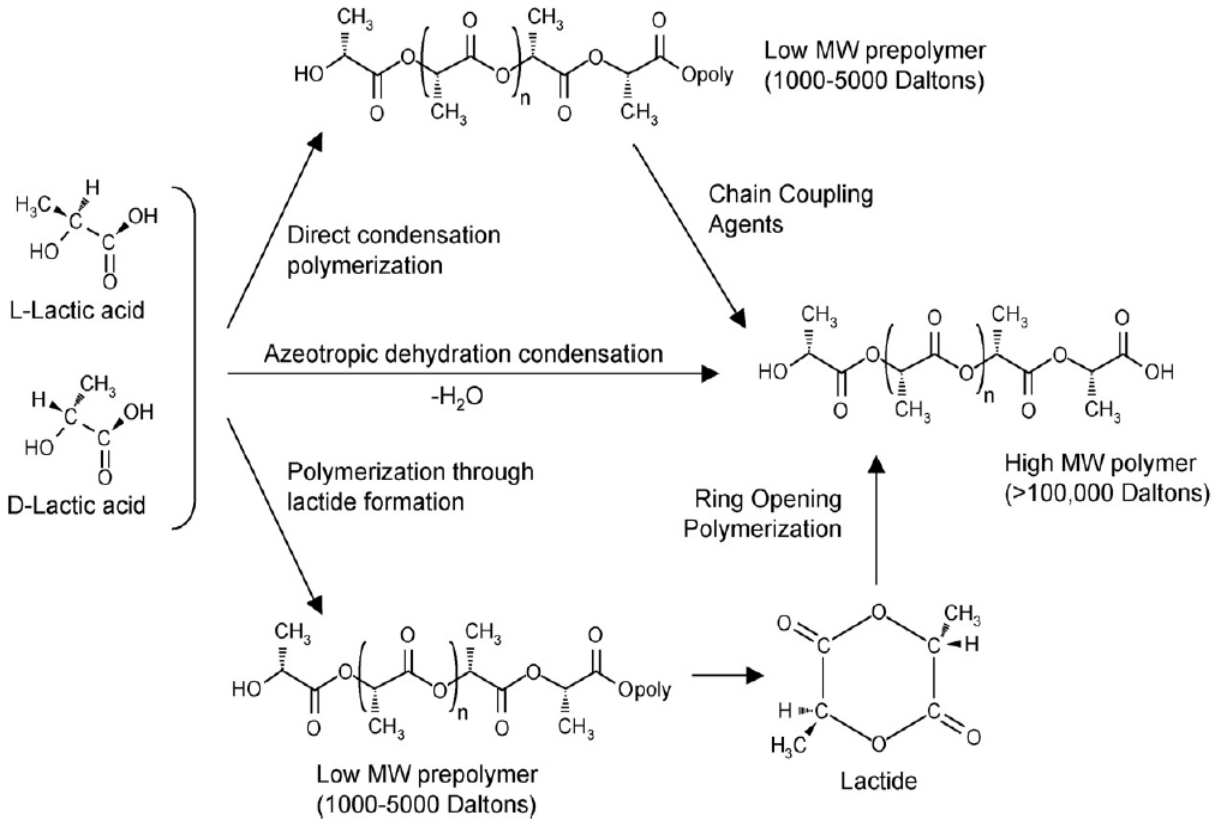

Figure 2.3 PLA synthesis scheme [19]

At present, PLA is large availability on the market and its price is relatively low [20, 21], PLA becomes one of the highest potential biodegradable polymer among bio-polyesters, particularly for packaging and medical applications [19, 20]; nevertheless, PLA consumption is only around 200,000 tons/year and only 30 % of lactic acid is used for PLA production. Thus, this biopolymer presents a high potential for development. The properties of PLA are hugely dependent on the ratio and distribution of the two stereoisomers of LA within the polymer chains. PLA with high l-isomer content produces crystalline product, whereas high d-isomer (>15%) leads to an amorphous product [22]. Commercial PLLA products are semicrystalline polymers with a melting temperature of 180°C and glass transition temperature in the range 55-60°C.

The higher the crystalline region of the PLA, the better the properties of the PLA final products. The crystallinity level of the PLA usually depends upon many factors, such as molecular weight, thermal and processing history, and the temperature and time of annealing treatments. PDLA is completely amorphous which the mechanical properties are quite different. The mechanical and thermal properties of PLLA become almost constant when its M_W is more than 70,000 Da

2.3 Poly(lactic acid) based composites

Wood/poly(lactic acid) composites

Biodegradable reinforcing materials, such as, wood flour is extensively used for producing wood polymer composites (WPC) due to its several advantages, for example, reduce polymer matrix used, increased modulus, lower density and cost [23]. Wood flour (WF) is commonly used as filler for wood plastic composites (WPCs). The use of WF can reduce material costs and make the WPCs to be specific properties, such as, low density, high specific stiffness, and biodegradable. Especially, WPCs with 50 wt% wood have been used in the construction industry such as, fencing, roofing, automotive and window profile [24]. The wood/PLA composites do not only change the physical PLA to be more like wood, but are also expected to be more environmentally friendly and higher tendencies to biodegrade after their shelf life. The main chemical composition of wood is consisted of cellulose, hemicellulose and lignin.

- **Cellulose**

Cellulose is the major chemical component of wood (40-45% of the wood dry weight). It composes of linear chains of D-glucose linked by ß-1, 4-glycosidic bonds (**Figure 2.4**)

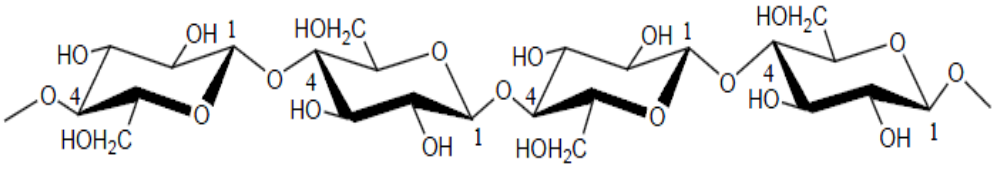

Figure 2.4 The chemical structure of cellulose [25]

Cellulose is mostly linear structure which is a high crystalline structure but also has some amorphous region. Cellulose has the strong hydrogen bond because of the interaction of hydroxyl groups of intra- and inter-molecular structure (illustrated in Figure 2.5). Cellulose has a very limited accessibility to water and chemicals, therefore, chemical attack can be expected to occur primarily on amorphous cellulose and crystalline surface.

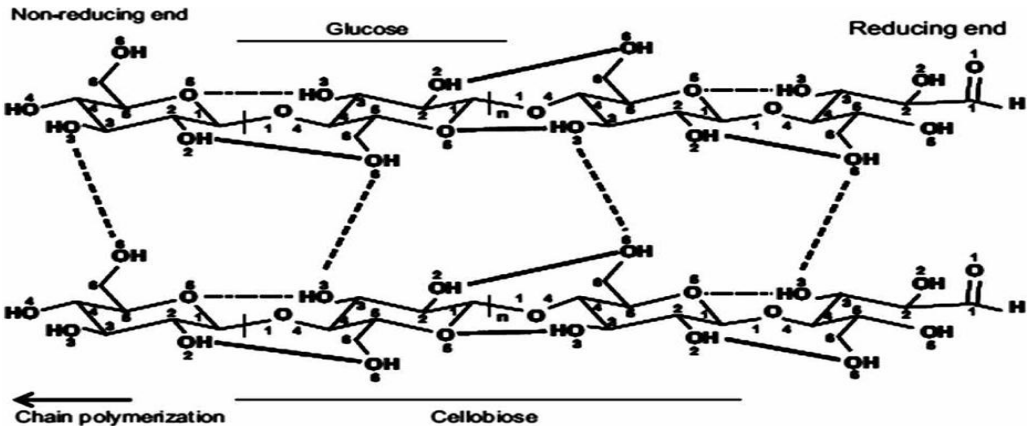

Figure 2.5 Hydrogen bond of intra- and inter-molecular of cellulose [25]

- **Hemicellulose**

Hemicellulose consists of pentose and hexose which degree of polymerization is lower than cellulose (only 50-300). Hemicellulose is more amorphous as compared to the cellulose because of its side groups on the main chain. Chemical structure of hemicelluloses is shown in Figure 2.6.

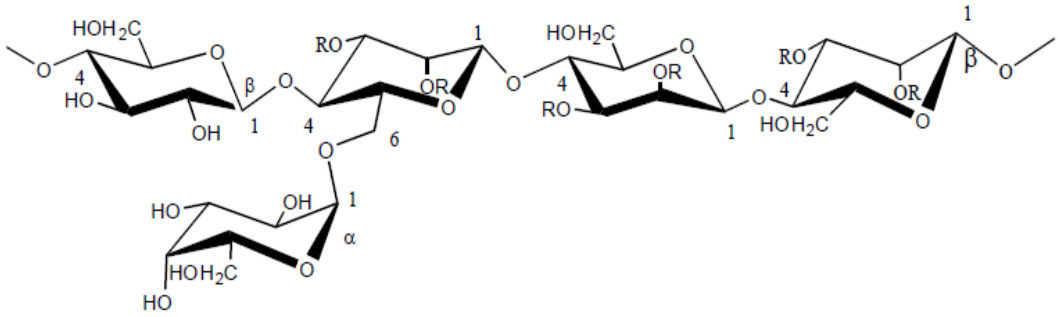

Figure 2.6 The chemical structure of hemicelluloses [25]

- **Lignin**

Lignin is a disorder phenolic structure of Phenylpropane which functions like cement between the fibres. Lignin improves stiffen of fibre and prevents cell wall to be degraded by enzymes. The chemical structure of lignin is illustrated in Figure 2.7

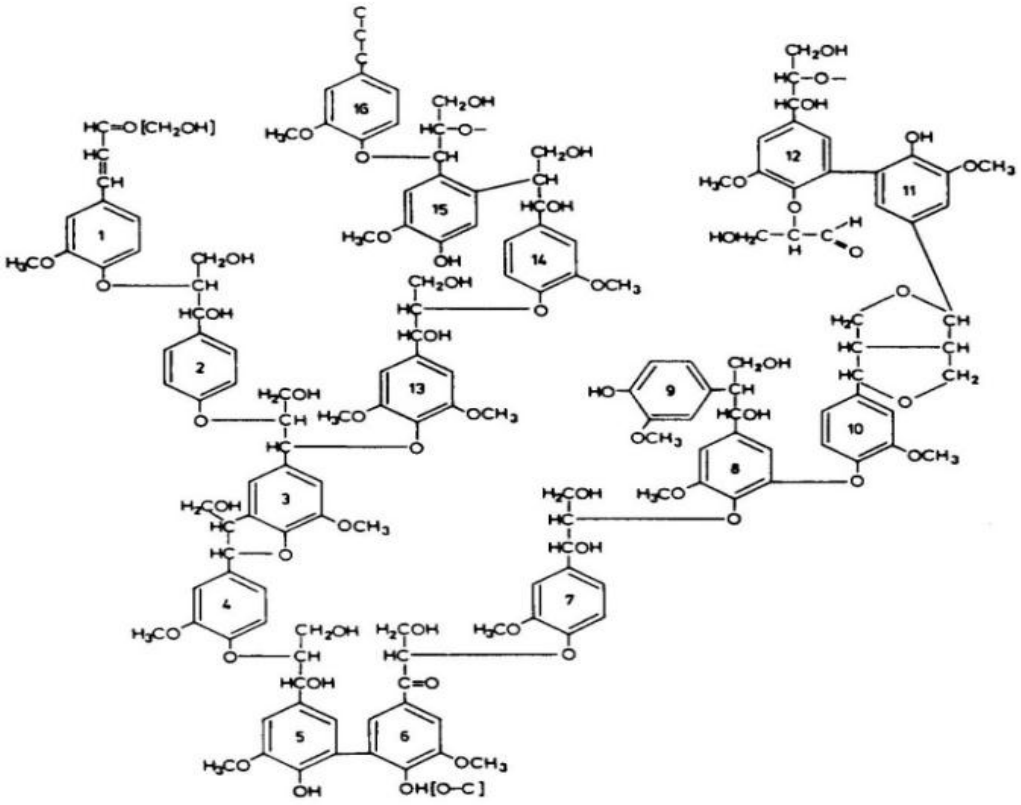

Figure 2.7 The chemical structure of Lignin [25]

Even though the wood/PLA composites have many advantages but the poor interfacial adhesion between wood and PLA surface is the majority problem because of the difference between a polarity of wood flour and PLA. Cellulose has the strong hydrogen bonds which make the wood to be more hydrophilic structure and influence the wood/PLA composites to decrease in their mechanical property. The system without compatibilizer or coupling agents treatment shows the poor compatibility between the PLA matrix and wood. The surfaces of wood particles are believed to be delaminated from the PLA matrix, and micro-size voids are formed during tensile test. The use of silane (as coupling agent) treatment significantly improved the compatibility, leading to less filler-matrix debonding and this can be confirmed by tensile testing.

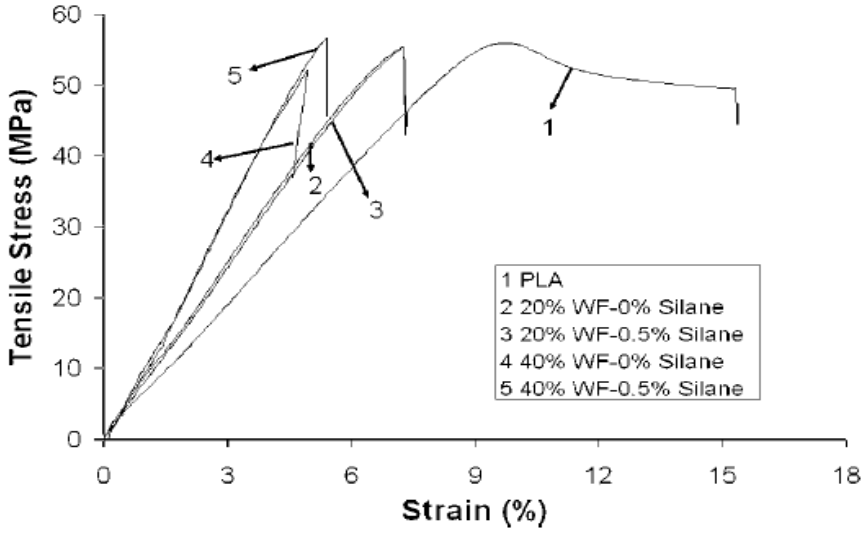

Figure 2.8 Tensile stress–strain curves of the PLA and WF/PLA composites [26]

An example of tensile stress–strain curves of the PLA and wood/PLA composites at the presence of 0 and 0.5% silane are given in Figure 2.8. Only neat PLA exhibited necking and had undergone stress-whitening before facture. The more wood was added, the more plastic deformation for the wood/PLA composites which became a brittle fracture mode of the wood/PLA composites. On the other hand, silane treatment was found to improve tensile strength. This can be attributed to the better interfacial adhesion between the wood and PLA. As the modulus showed the significant increase with the addition of wood content of 20 and 40% but toughness decreased. The adding of wood flour content controlled the movement of the polymer chains by the way of increasing stiffness. This can be attributed to that the wood has a much higher modulus compared to the PLA. The tensile strength of the wood/PLA composites were found generally to be declining when compared with the neat PLA. The addition of wood flour enhanced the crystallinity of PLA as shown in Table 2.1 The crystallinity of PLA improved from 13% to 38% and 44%, respectively for PLA-20% and PLA-40% wood (with no silane treatment) samples. Wood/PLA with silane treated could improve the percent of

crystallinity more than the un-treated. For instance, the crystallinity of treated PLA-20%wood composites was 12% higher than that of PLA-20%wood composites without silane treatment. This can be concluded that the addition of wood content increased the crystallinity by acting as a nucleating agent, nevertheless a treatment with a coupling agent can enhance the crystallinity because of the improvement on the interfacial adhesion.

Table 2.1 The relationship of wood content and percent crystallinity [27]

Sample	% Crystallinity
Neat PLA	13
PLA-20%WF	38
PLA-20%WF-0.5%Silane	50
PLA-40%WF	44
PLA-40%WF-0.5%silane	51

Organnoclay/poly(lactic acid) composites

The world of nanotechnology is one of the most popular areas for present researches. Even in nanocomposites field, there is a diversity of research topics exist, for examples, composite reinforcement, barrier properties, flame resistance, electro-optical properties, cosmetic applications, bactericidal properties. Polymer/clay nanocomposites have emerged as outstanding material for food packing due to its several benefits, such as, enhanced mechanical, thermal and barrier properties. Usually, the polymer/layered silicate (PLS) nanocomposites preparation belong to the same general family of 2:1 layered (Figure 2.9). The crystal structure consists of layers made up of two tetrahedrally coordinated silicon atoms fused to an edge-shared octahedral sheet of either aluminum or magnesium hydroxide. The layer thickness is about 1 nm. Stacking

of the layers is cause of a regular van der Waals gap between the layers called the interlayer or gallery. The clay is known as Montmorillonite (MMT), the most commonly used layered silicates, consists of two fused silica tetrahedral sheets sandwiched with octahedral sheet of either aluminum or magnesium hydroxide. The negative charge is located on the surface of silicate layers of tetrahedrally substituted layered silicates, thus polymer matrices can react interaction more readily with these than with octahedrally-substituted material.

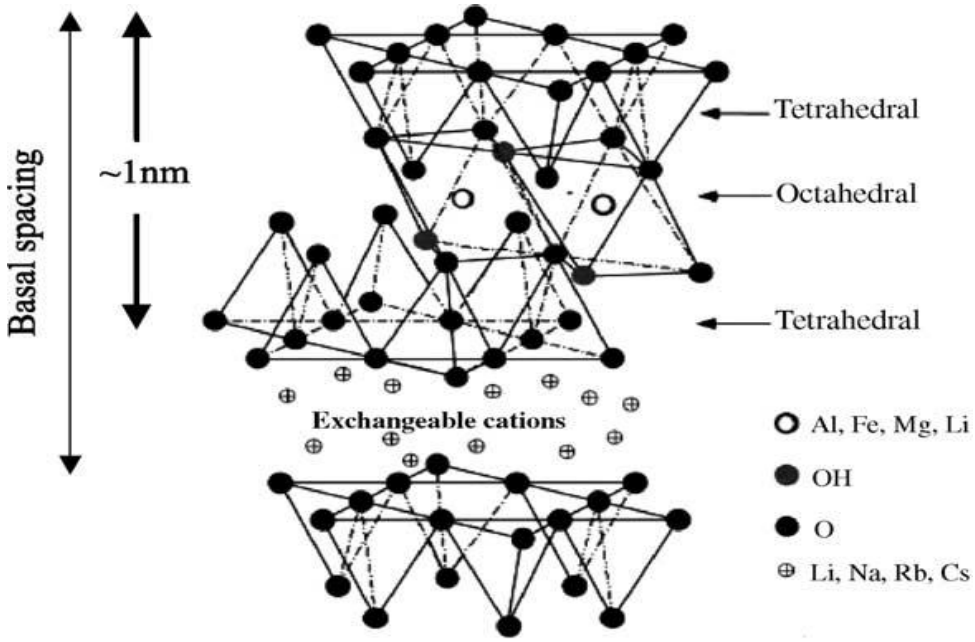

Figure 2.9 Structure of 2:1silicate layers [28]

Two characteristics of layered silicates those are generally considered for PLS nanocomposites consist of ability of the silicate particles to disperse into individual layers and the ability to adjust their surface chemistry through ion exchange reactions with organic and inorganic cations. These two characteristics are a cause of the degree of dispersion of layered silicates in a particular polymer matrix. But, normally MMT silicate surfaces are rather more hydrophilic than polymers. Thus, MMT must be

modified to be more compatible, which supports its dispersion in polymer matrix. Usually, cations exchange technique is selected to modify the compatibility of the clay and polymers by treating the clay with surfactants using primary, secondary, tertiary or quaternary alkylammonium or alkylphosphonium cations before MMT is being used [28].

- **Nanocomposite formation** [28-30]

There are various techniques to form nanocomposites, for examples, polymerization, solution, and latex methods. However, the melt processing is the most attractive because this is generally considered as more economical and flexible for the formulation. Complete exfoliation of the clay, i.e., separation of platelets from one another and dispersed individually in the polymer matrix, is the goal of the formation process. Normally, this exfoliation morphology is not achieved easily but only various degrees of dispersion are more common. Three conventional types of dispersion morphology are immiscible (conventional or microcomposite), intercalated, and miscible or exfoliated, respectively, The dispersion of clay can be examined by several techniques as shown in Figure 2.10 which illustrated the relationship of transmission electron microscopic of TEM images and the expected wide angle X-ray scans for nanocomposite materials. For the case called ‘‘immiscible”, this means no separation of clay platelets therefore, the wide angle X-ray of the polymer composite is expected to be the same as the obtained for the organoclay powder, i.e., no shifting of the X-ray d-spacing. For exfoliation, no wide angle X-ray peak is expected for the nanocomposte because there is no regular spacing of the platelets in any case, the distance between platelets is larger than what wide angle X-ray scattering can detect. However, X-ray scans of polymer nanocomposites often show an organoclay peak but shifted to lower

2θ or larger d-spacing. The peak shift indicates that the gallery has expanded and it is usually assumed that polymer chains have entered or have been intercalated in the gallery. Placing polymer chains in such a specific space would involve significant entropy that have to be driven by an energetic attraction presumably between the polymer and the organoclay.

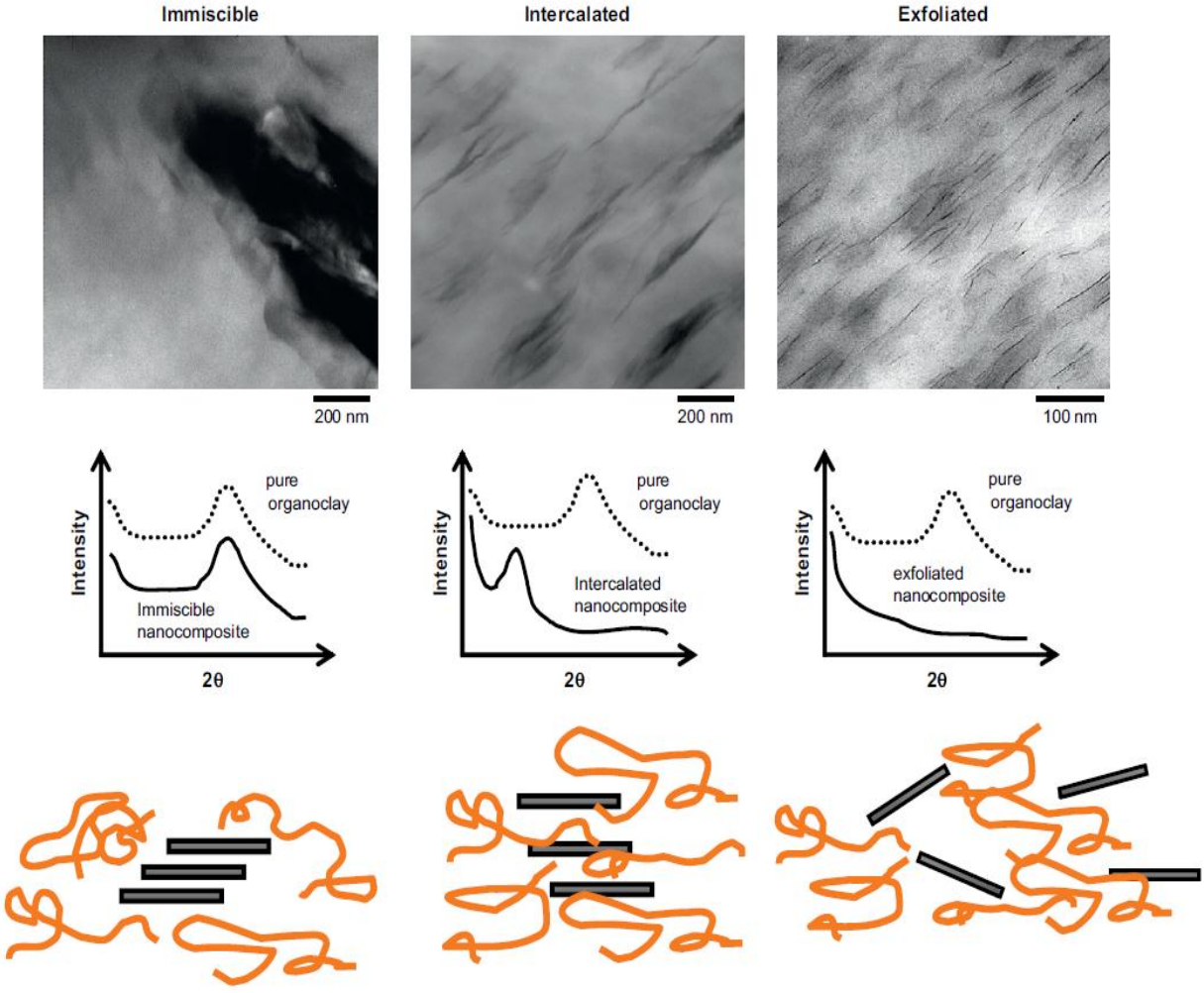

Figure 2.10 Relationship of transmission electron microscopic of TEM images and theexpected wide angle X-ray scans for nanocomposite materials [29]

The intercalation is also suggested to be a beginner of exfoliation. For food packaging application, good barrier property is very important because good barrier property can extend food quality and shelf life. Normally, the incorporation of nanoclay fillers in the polymer is often used and expected to improve the barrier property of packaging. The improvement of barrier property can be explained using the Figure 2.11.

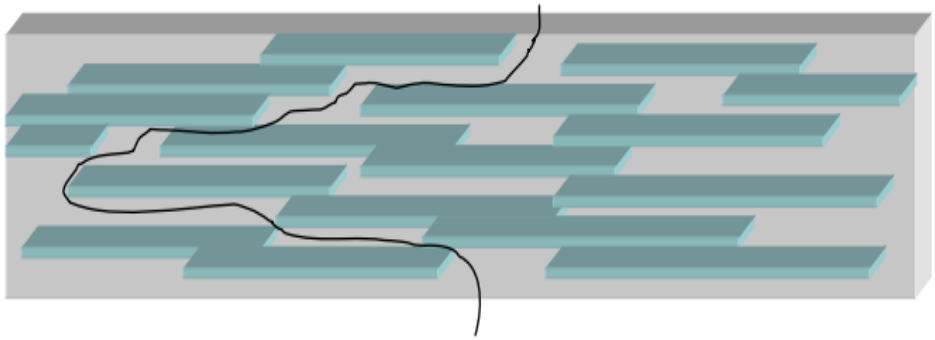

Figure 2.11 Schematic presentation of the formation of tortuous path in polymer/clay nanocomposite [29]

The layered clay sheets are essentially impermeable inorganic crystals that obstacles the path of the diffusion process, gas molecules have to permeate around them instead of permeation of a straight line path which takes longer mean path for gas absorption through these nanocomposites. In a well exfoliated and dispersed state, individual clay platelets are believed to increase the barrier properties by creating a maze or 'tortuous path'. Even though the clay can improve barrier properties, clay was also found to be a hydrolytic accelerator for the PLA. Paul *et al.* [30] investigated hydrolytic degradation of polymer layered silicate nanocomposites (unmodified montmorillonite-NaC (Cloisite®NaC)) based on PLA matrix with organo-modified montmorillonites Cloisite®25A and Cloisite®30B in phosphate buffer solution (Figure 2.12**)**.

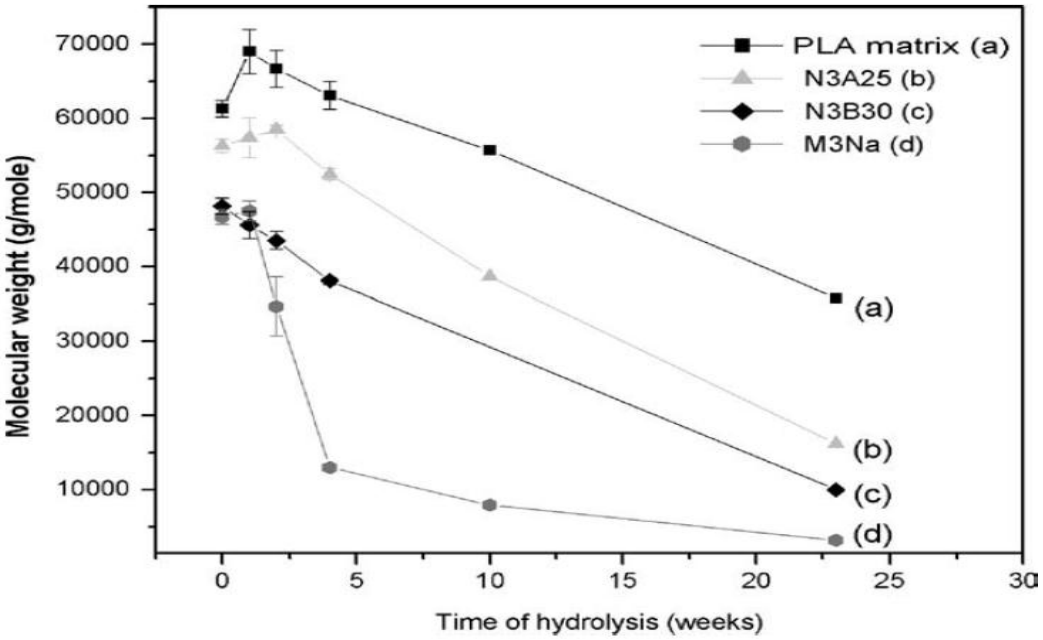

Figure 2.12 Relationship of Molecular weight and hydrolysis time of PLA and PLA/nano clay composites: (a) PLA; (b) PLA/ Cloisite®25A; (c) PLA/ Cloisite®30B; (d) PLA/Cloisite®NaC [30]

The study found that hydrolysis degradation of clay/PLA composites occurred quicker than that of pure PLA, the highest degradation was found to occur with naturaly unmodified montmorillonite -Na^+ blended PLA. This indicated that the hydrophilic clay initiated water molecules to penetrate into the PLA matrix and initiated the hydrolytic degradation.

2.4 Biodegradation

In general, the term of “biodegradable plastics” mentions the attack of microorganisms on non-water soluble polymer based. This indicates that biodegradation of plastics is usually a heterogeneous process. At the initial state, microorganisms cannot digest and transport the polymeric material into the cells directly because polymer is non-water solubility and the molecular weight is too high. Thus biochemical processes take place as follow; microorganisms excrete extracellular enzymes to depolymerize the polymers outside the cells (Figure 2.13).

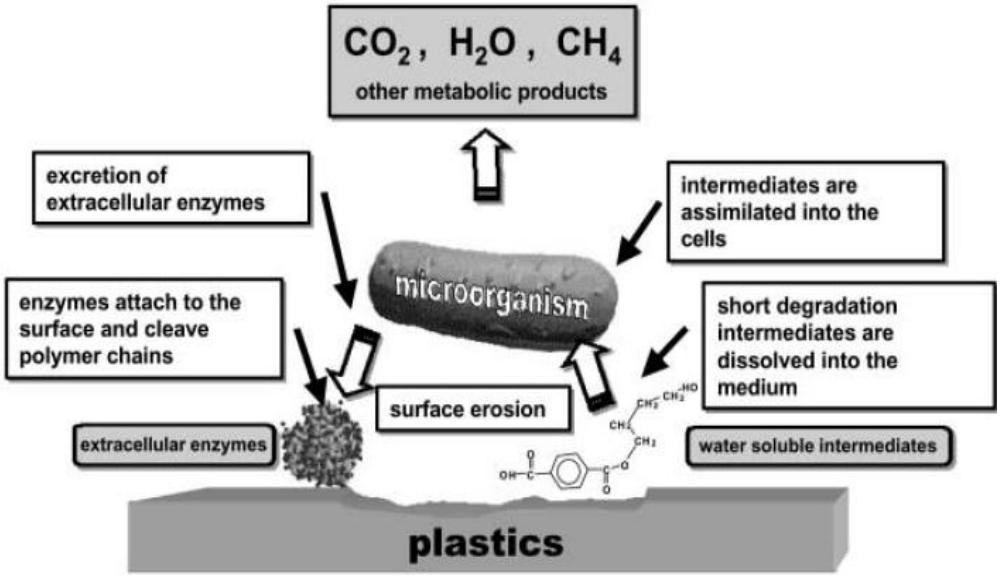

Figure 2.13 General mechanism of plastics biodegradation [31]

If the molar mass of the polymers is reduced enough to dissolve in water, these can be transported into the microorganism cell from which metabolism process starts. Then, water and carbon dioxide are created as a result of the metabolic process end-products. The extracellular enzymes cannot penetrate deeply into the polymer material because its size is too large, and the action occurs only at the polymer surface. This is considered as

a surface erosion process. The initial process of biodegradation, non-biotic chemical and physical processes can also occur on the polymer in parallel or as a first stage solely on the polymer. These non-biotic effects such as hydrolysis reaction, thermal degradation, and oxidation or scission of the polymer chains by irradiation induce in the biodegradation process. All mechanisms could also be referred to environmental degradation because of the coexistence of biotic and non-biotic processes. Not only environmental factors like humidity, temperature, the presence or absence of oxygen influences the polymer to be degraded but also the microbial population and the activity of the microorganism affect the biodegradation process. Thus these conditions must be considered before the biodegradability is tested [31].

- **Biodegradation of poly(lactic acid)**

The degradation of polymers generally occurs with the main chain scission of polymers. The chemical or biological are involved in the biodegradation of polyester. There are many factors which take the effect on biodegradation of PLA, such as, primary chemical structure (presence of functional groups), factors associated to surface conditions (surface area, hydrophilic, and hydrophobic properties) and degree of crystallinity [32]. But a major rate-determining factor for biodegradation of solid polymers is degree of crystallinity [33]. Usually, chain scission of PLA main chain occurs at the ester bonds, bringing to the oligomers formation. Therefore, a number of ester bonds of the PLA main chains are related to total amount of oligomers after chain scission. Biodegradation of PLA occurs in two different ways, enzymatic degradation, and non-enzymatic degradation, which includes chemical methods such as pH degradation. The principle mode of degradation of PLA is hydrolysis which takes place within three important steps[22].

1. Water diffuses into PLA material, then initiates random hydrolysis (coexist with surface erosion process).
2. PLA is fragmented to oligo-lactic acid
3. Finally, through a more extensive hydrolysis accompanied by phagocytosis, diffusion and metabolism.

Figure 2.14 illustrates the hydrolysis mechanism of PLA, starting by the absorbed water molecules attack at ester linkages, therefore, the PLA chain is cleaved into smaller molecular size and its molecular weight. The hydrolysis reaction depends on the size, crystallinity, hydrophilicity of polymer in addition to the involvement of environmental factors, such as, pH, temperature and humidity.

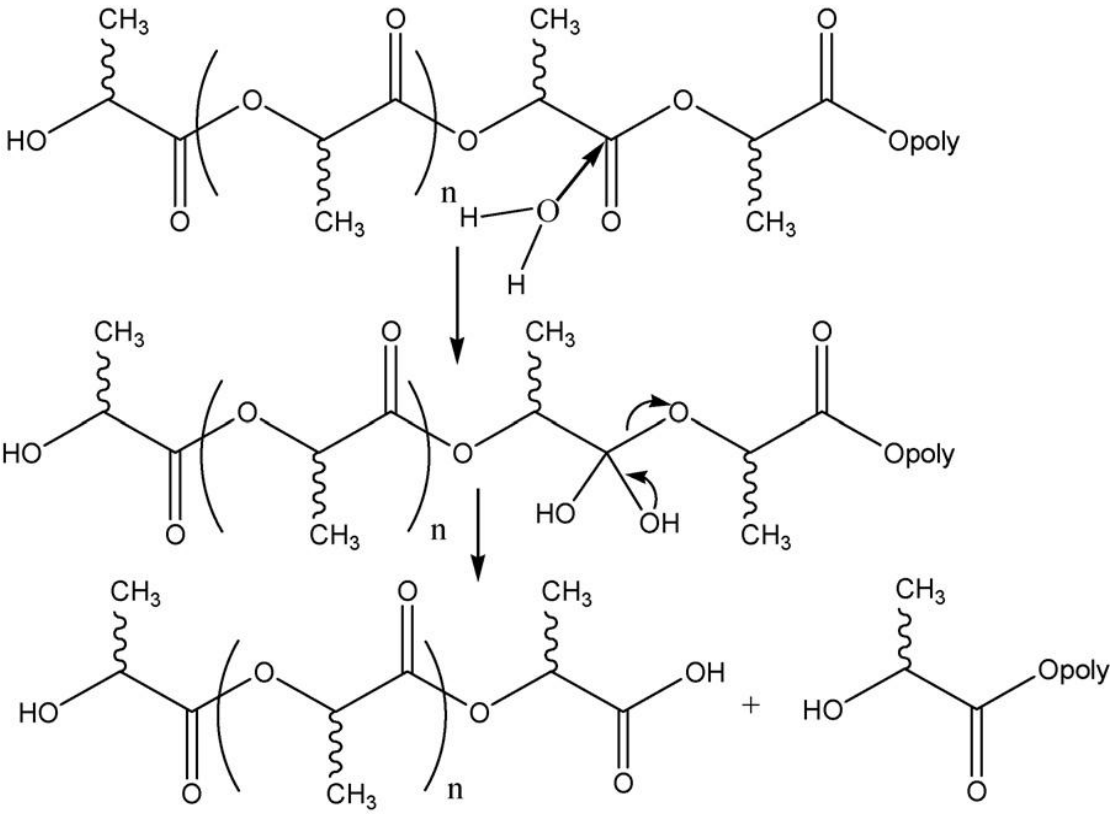

Figure 2.14 Mechanism of hydrolysis reaction of poly(lactic acid) [22]

Similar to the other bio-materials, biodegradation of PLA occurs via the non-biotic chemical degradation at the first step. These non-biotic chemical processes begin to induce the PLA to be degraded by hydrolysis. Besides the attack of water molecules, the enzymatic and non-enzymatic degradations are the two significant factors for the biodegradation of PLA that have to be considered.

- **Enzymatic degradation**

Enzymes play an important role for the degradation of bio-polymers. The degradation of aliphatic polyesters by enzyme, normally, has two steps. The first step is the adhesion of the enzyme onto the polymer surface then, hydrolysis occurs at the ester bond. PHB depolymerases and lipases are the most extensively studied enzymes. However, only a few information on L-PLA degrading enzymes such as proteinase K, lipase and polyester polyurethane-degrading enzymes have been reported until now [34]. The structures of extracellular PHB depolymerases are comprised of three important regions including catalytic region, substrate binding and a linker region. The function substrate binding is to bind the enzyme with the material surface. Catalytic domain is the active region which interacts with material. Linker region is used to combine the catalytic domain and substrate binding. The model of enzymatic polyester depolymerase is shown in Figure 2.15.

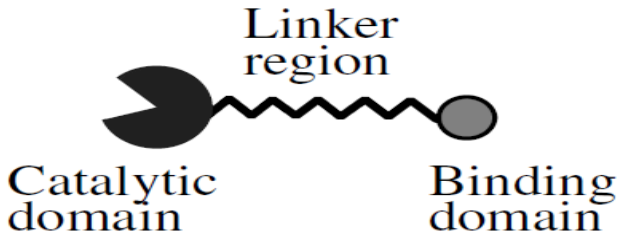

Figure 2.15 The model of enzymatic polyester depolymerase [35]

Enzymatic degradation process occurs only at the surface of substance, because enzymes cannot penetrate into the solid polymer substrate. Amorphous region is degraded before crystalline region because this region is loosely linked and easier than the crystalline region that needs enzyme to be diffused. Eventually, the crystalline region will be finally degraded. An example of enzymatic degradation is the use of three amino acid residues which consists of aspartate, histidine and serine as a common feature of hydrolases as shown in Figure 2.16. The mechanism starts by interaction of aspartate with the histidine ring to form a hydrogen bond. The ring of histidine interacts with hydrogen atom of serine. The deprotonating serine generates a highly nucleophilic alkoxide group and then attacks the ester bond of polymer. At last, water attacks at the acyl-enzyme bond to produce a carboxyl end group and the free enzyme.

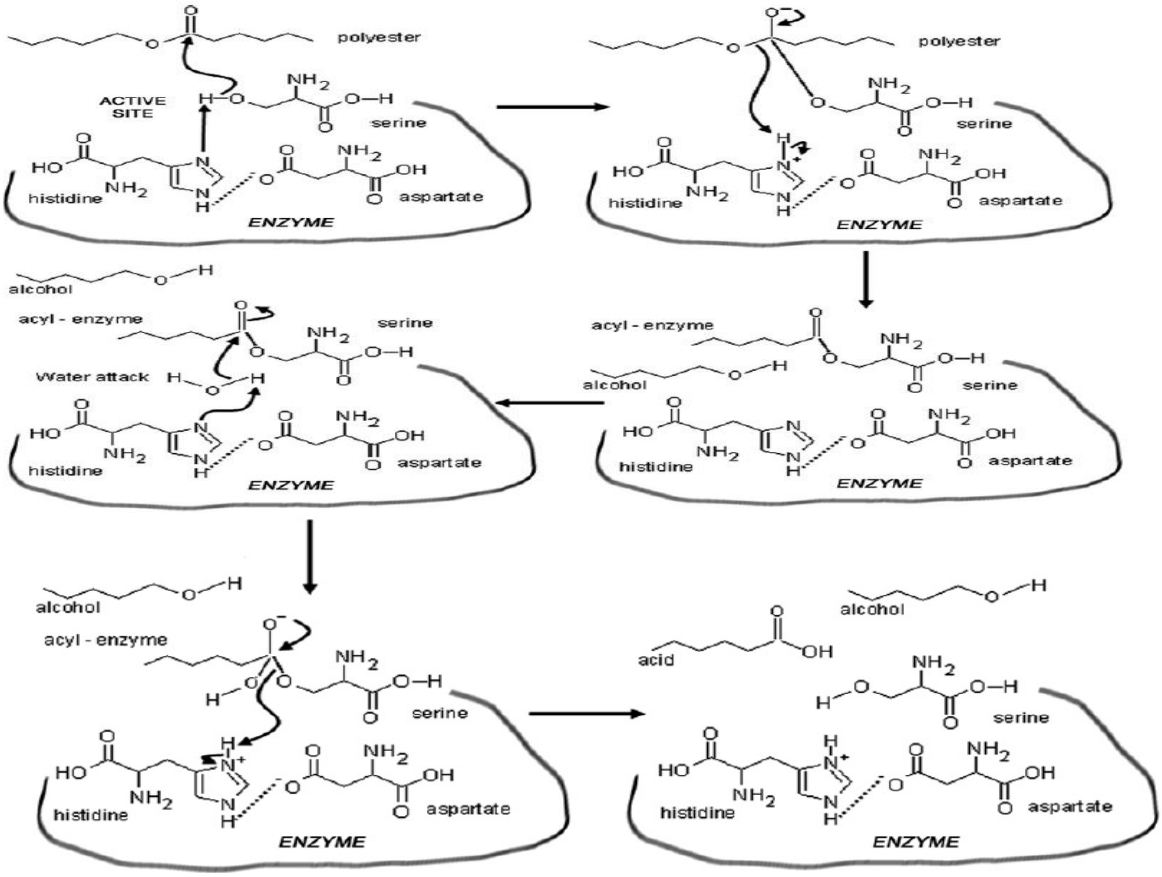

Figure 2.16 Mechanism of Enzymatic degradation [36]

- **Non enzymatic degradation**

One of a simple example of non-enzymatic degradation is a change of pH condition. Basic and acidic conditions are causes of hydrolysis reaction of polyester influence on losing its molecular weight. Tsuji and Ikarashi [37] revealed that hydronium and hydroxide ions took an effect on the hydrolysis of PLLA (Figure 2.17**)** that number-average molecular weights (Mn) of PLA in various pH solution were changed. For example, the Mn of PLA immersed in the solutions, having pHs of 0.9 (5 days), 0.2 (40 days), 7.4 (64 days), 11.7 (18 days) and 12.8 (2 days) were reduced to 46.6, 59.1, 89.5, 77.9, and 49.3%, respectively.

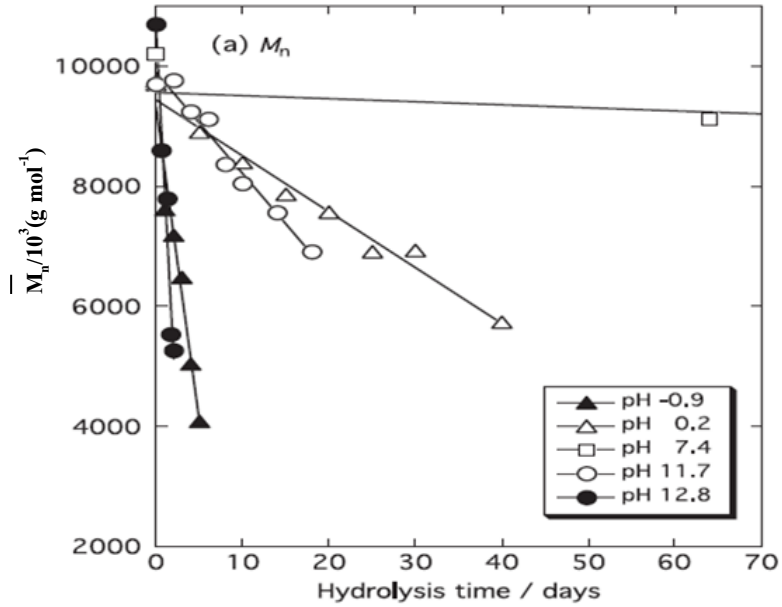

Figure 2.17 Effect of pH against hydrolysis reaction on poly(lactic acid) [37]

However, the degradation mechanisms of PLA in alkaline and acidic media are still unclear. De Jong *et al*.[38] proposed the possible mechanism of hydrolysis reaction for acidic and basic cases. In alkaline medium (Figure 2.18A), the degradation was described by intramolecular transesterification. The hydroxyl end group is attacked by

nuclephilic and the carbonyl group is formed to give a six-membered ring as intermediate. Because base interacts with hydroxyl end group, the nucleophilicity of oxygen atom increases by the cleavage of lactide molecule. Finally, free lactide is hydrolysed into two molecules of lactic acid. For the acidic condition (Figure 2.18 B), the degradation starts by the attack of hydrogen ion at the hydroxyl end group and intramolecular hydrogen bridge occurs. Intramolecular hydrogen bridge increases the electrophilicity of the carbonyl group. When water molecule attack at the carbonyl group, lactic acid splits off, thus the degree of polymerization of the PLA decreases.

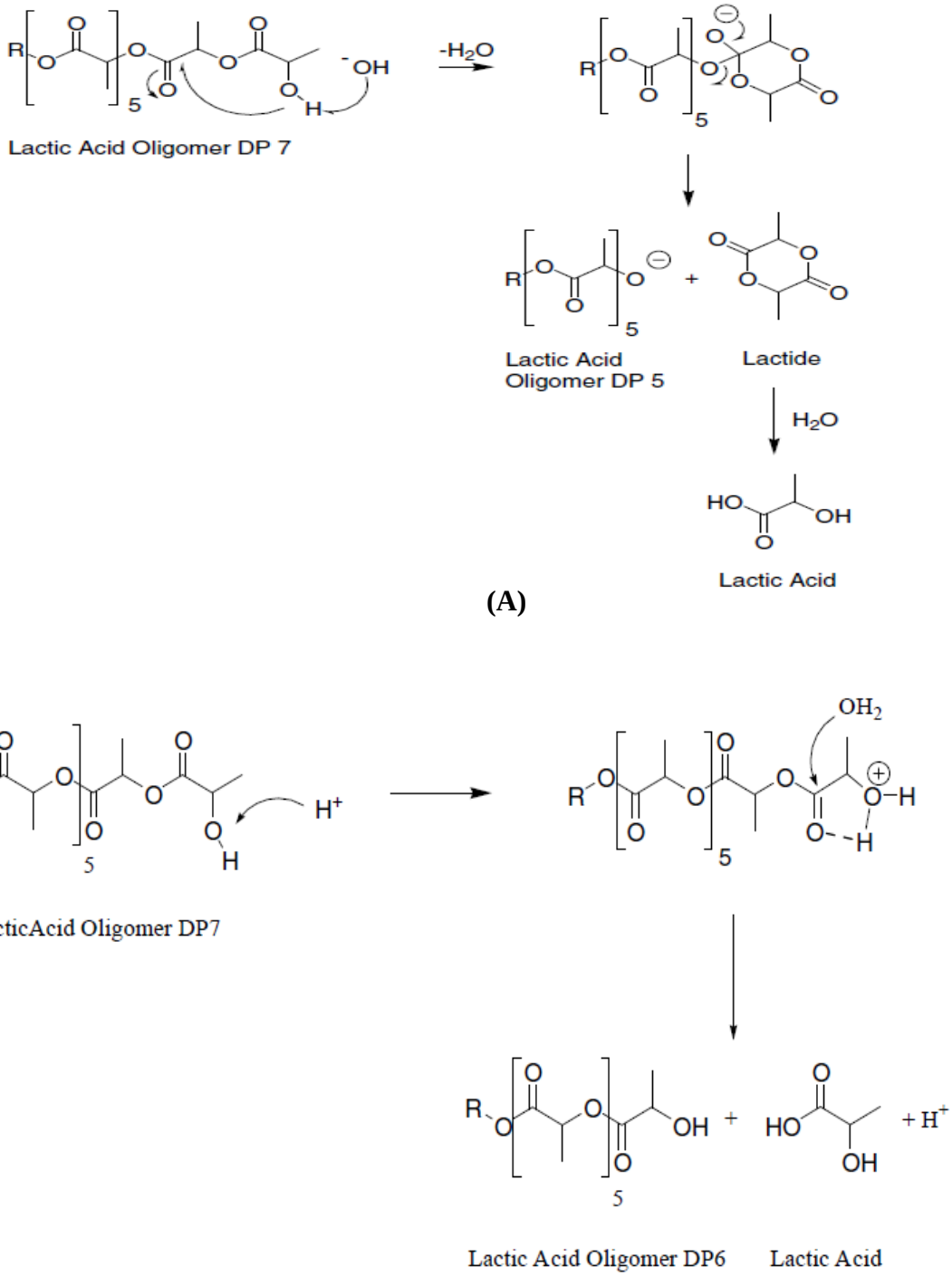

Figure 2.18 Possible mechanism of hydrolysis: (A) alkaline environment; (B) acidic environment [38]

2.5 Standard test methods for biodegradation of biopolymers

Standard test method for biodegradable polymers is used for two purposes: (i) separates biodegradable out of non-biodegradable polymers; (ii) determine how much the materials have been degraded during the test period. There are several techniques for measuring the biodegradation performance of biopolymers, including visual observation, weight loss measurement, changing in mechanical properties or molar mass and CO_2 detection [15]. Each technique has different accuracy depends on how significant is need in the work.

- **Visual observations**

The visible changes is a rough technique used to observe physical changes of plastic by observation of roughening on the surface, formation of holes or cracks, de-fragmentation, changes in color, or formation of bio-films on the surface. These transformations cannot prove the presence of biodegradation in terms of metabolism, but the parameter of visual changes can indicate the attack of microorganism by accompany with scanning electron microscopy (SEM). However, after the beginning of degradation, crystalline spherulites are always observed on the surface [14].

- **Weight loss measurements**

The weight loss of tested specimens is widely applied in degradation tests even though; it cannot prove the biodegradation. On the other hand, If the tested samples are not clean very well, the weight can be gained instead of loss [14].

- **Changes in mechanical properties and molar mass**

The minor changes of the tested specimens in many cases cannot be observed, the change in mechanical properties is often measured. Tensile strength is very sensitive with the chang in the molar mass of polymers, which is also indicated as an evidence of degradation. For abiotic degradation process, the mechanical properties may change significantly, though almost no loss of mass due to that solubilization of degradation intermediates occur at this stage. Thus, the measurement of changes in mechanical properties and molar mass is often used for materials that the abiotic processes occur at the first degradation step [14].

- **CO_2 evolution**

Under aerobic conditions, microorganism uses oxygen in the oxidation reaction and produces carbon dioxide as one of the metabolic end products. Thus, oxygen consumption or carbon dioxide formation is a good indicator for polymer degradation. This technique is the most popular method used for measuring the biodegradation and the accuracy of the test is usually good. A schematic diagram of carbon dioxide evolution measuring system is shown in Figure 2.19.

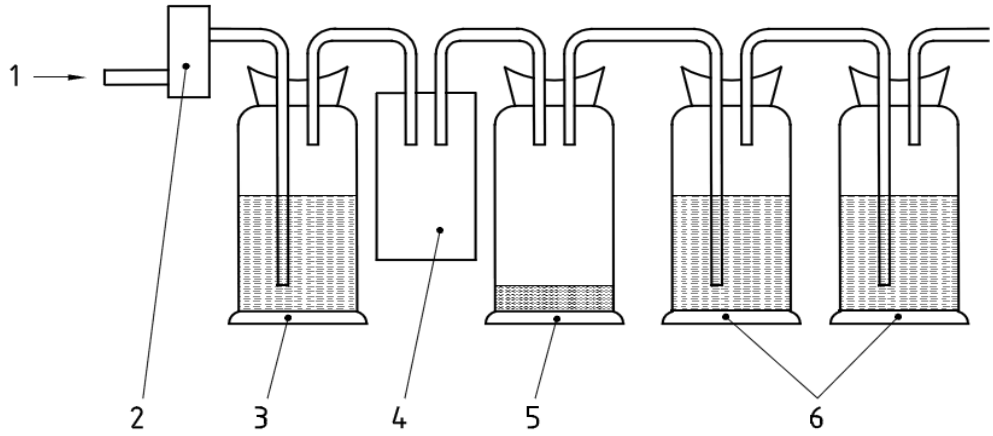

Key

1	air in
2	air-flow controller
3	CO_2 absorber
4	humidifier
5	test flask
6	CO_2-absorption bottles

Figure 2.19 Schematic diagram of carbon dioxide evolution measuring system [39]

The concept of this method is trapping CO_2 that occurs during the biodegradation process using $Ba(OH)_2$ solution and follows by the titration with HCl solution to determine total amount of $Ba(OH)_2$ remaining in the solution. The chemical reactions and equation of biodegradation percentage are given below [15, 39, 40].

$$Ba(OH)_2 + CO_2 \longrightarrow BaCO_3 + H_2O \qquad (2.1)$$

The $BaCO_3$ formed is insoluble and precipitates. Determines the amount of $Ba(OH)_2$ remaining in solution by end-point titration with HCl using phenolpthalein as an indicator according to the following equation:

$$Ba(OH)_2 + 2HCl \longrightarrow BaCl_2 + 2H_2O \qquad (2.2)$$

Then, the number of mmol of CO_2 produced is calculated using equation given below

$$\text{mmoles of } CO_2 = \text{mmoles of } Ba(OH)_2 \text{ at start} - \frac{\text{mmoles HCl}}{2} \qquad (2.3)$$

Calculate the percentage of biodegradation by dividing the average net gaseous-carbon production of the tested compound by the original average amount of carbon in the tested compound and multiplying by 100:

$$D_t = \frac{(CO_2)_T - (CO_2)_B}{ThCO_2} \times 100 \qquad (2.4)$$

where $(CO_2)_T$ = the amount of CO_2 trapped in the second and third $Ba(OH)_2$ solution flasks occurred from the reactor bottle with test specimens (mg)

$(CO_2)_B$ = the amount of CO_2 trapped in the second and third $Ba(OH)_2$ solution flasks occurred from the reactor bottle without test specimens (mg)

$ThCO_2$ = the theoretical amount of CO_2 from a specific specimen (mg)

2.6 Bacteria and biochemical target for drugs action

2.6.1 Bacterial cell structure

The bacteria are known as prokaryote microorganisms. Usually, bacteria are divided into gram positive and negative bacteria. Bacteria are typically a few micrometers in length, have a wide range of shapes, such as, coccus (spherical), bacillus (rod-like), spirillum (spiral) and filament. Bacteria are found in every habitat on Earth, growing in soil, water, and deep in the Earth's crust. Bacterial cell structure can be divided into 3 parts, external structure, cell wall, cell membrane and internal structure. Bacterial cell structure is illustrated in Figure 2.20.

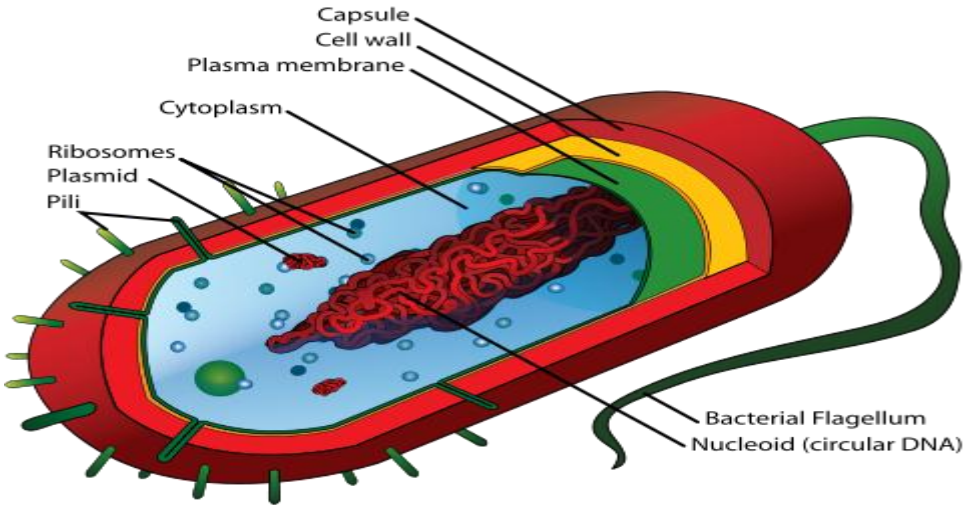

Figure 2.20 Bacterial cell structure [41]

External structure

- **Capsules:** Many bacteria secrete extracellular polymers outside their cell walls. These polymers are usually composed of polysaccharides and sometimes proteins. It helps bacteria from being killed by phagocytes; adhere to the surface and able to patient from the drought.

- **Flagella:** Flagella are responsible for the motility of pathogenic bacteria and can play a role in the production of disease.

- **Pili:** Bacterial pili are used in the exchange of genetic materials during bacterial conjugation, and short pilus called a fimbrium is used as a cell adhesion mechanism.

Cell wall & Cell membrane

- **Cell wall:** Cell wall is composed of one or more layers of a peptidoglycan. A peptidoglycan is a combination of peptides and sugar. It is located outside the cell membrane and provides these cells with structural support and protection, and also acts as a filter. A major function of the cell wall is to act as a pressure vessel, preventing over-expansion when water enters the cell.

- **Cell membrane:** The cell membrane or plasma membrane is one biological membrane separating the interior of a cell from the outside environment. The cell membrane surrounds all cells and it is a selectively permeable membrane, controlling the movement of substances in and out of cells. It contains a wide variety of biological molecules, primarily proteins and lipids.

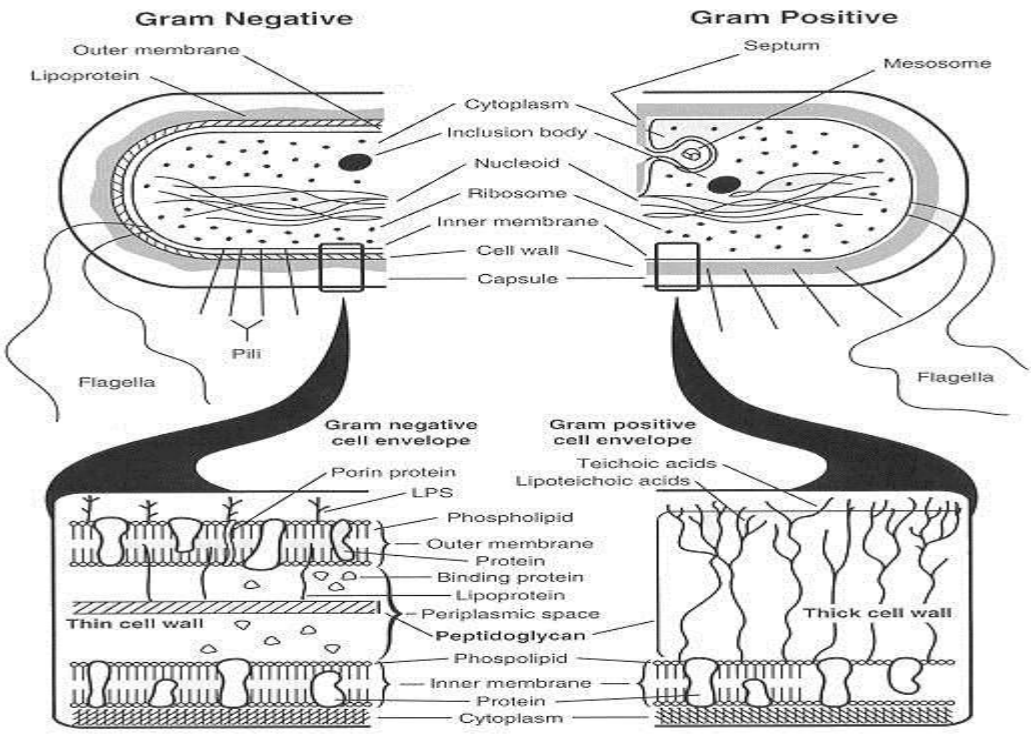

Figure 2.21 Comparison of cell wall of Gram positive and Gram negative bacteria [42]

Bacterial can be divided into two groups, gram positive and negative bacteria. The structure of cell wall and cell membrane of these two kinds are different. Figure 2.21 shows the comparison of cell wall of gram positive and gram negative bacteria. Gram positive bacteria have continuous 20 to 80 nm cell wall thick. The major part composes of peptidoglycan. In contrast, the peptidoglycan layers in Gram negative bacteria are thin (about 5 to 10 nm thick) but there is the outer membrane structure outside the peptidoglycan layers. The outer membrane of the gram-negative cell wall appears as a lipid bilayers composing of phospholipids, lipoproteins, lipopolysaccharides (LPS), and proteins. Phospholipids are located mainly in the inner layer of the outer membrane and lipoproteins that connect to outer membrane. The lipopolysaccharides are located in the outer layer of the outer membrane.

Internal structure

- **Ribosomes:** Ribosomes are the components of cells that make proteins from amino acids. Ribosomes read the information in this RNA and use it to create proteins. This process is known as translation (genetics), i.e. the ribosome "translates" the genetic information from RNA into proteins.

- **Cytoplasm**: Cytoplasm is the part of a cell that is enclosed within the cell membrane, surrounding the cytoplasmic organelles. It is a jelly-like material that is eighty percent water and usually clear in color. The cytoplasm is the site where most cellular activities occur, such as many metabolic pathways and processes such as cell division

- **Nucleoid:** The nucleoid is an irregularly-shaped region within the cell which has no nuclear membrane and where the genetic material is localized (60%DNA, 30%RNA and 10%protein).

- **Plasmids:** Plasmids are molecules of DNA that are found in bacteria, separated from the bacterial chromosome. They are small and circular, usually carry only one or a few genes and have a single origin of replication. Plasmids are replicated by the same machinery that replicates the bacterial chromosome. Some plasmids are copied at about the same rate as the chromosome. Genes on plasmids with high numbers of copies are usually expressed at high levels. In nature, these genes often encode proteins (e.g., enzymes) that protect the bacterium from one or more antibiotics. Plasmids enter the bacterial cell with relative ease. This occurs in nature and may account for the rapid spread of antibiotic resistance in hospitals and elsewhere.

2.6.2 Biochemical target for drugs action [43]

Drugs act by specifically interfering with cellular or biochemical processes, often called 'targets' as shown in Figure 2.22. The classic example of a drug target is an enzyme in bacteria which is inhibited by the drug. Effective drugs will exhibit a selective toxicity for the pathogen as compared to the host. Many factors contribute to this selective toxicity and these factors are not mutually exclusive. Rational drug design seeks to exploit these various factors to develop drugs which are highly toxic to the pathogen and at the same time exhibit minimal toxicity to the host.

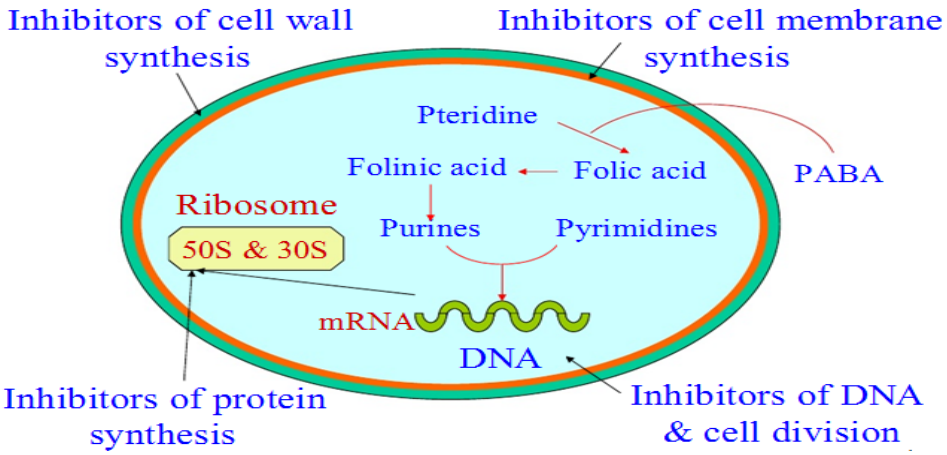

Figure 2.22 Targets for drug action [43]

- **Enzyme:** Enzymes play a major part role for all cells. The mobilization and transfer of energy, the transport of many substances into and out of the cells are under controlled and all processes are ultimately depended on enzymes. Every enzyme is protein and its action involves the formation of highly specific complex between the substrate and the enzyme protein. Complex formation arises by multiple points binding with weak bonds between the substrate and a small but highly organized part of the

protein, and such a complex formation leads to a chemical change in substrate or release of products. Enzyme molecules are usually two or three order of magnitude larger than their substrates, and two or three amino acids might suffice to form a binding site. Enzymes are obvious target for drug action and many attempts have been made to attack them. These would seem to be a number of possibilities, i.e.

- Direct action at the substrate binding side.
- Direct action at the cofactor binding side.
- Modification of the substrate (or cofactor) binding by false operation of the specific system that regulates enzyme/substrate interaction.
- Disorganization of the active centre by non-specific action elsewhere in the Enzyme

- **DNA:** DNA is a nucleic acid that contains the genetic instructions used in the development and functioning of all known living organisms. The main role of DNA molecules is the long-term storage of information. The information held in the DNA is first transcribed into messenger RNA which becomes attached to ribosome and is then translated into a specific sequence of amino acids peptide-bonded by the action of ribosome. Each of the processes of replication, transcription and translation involves, at least, an enzyme or enzymes and a macromolecule whose composition and conformation are essential to the transfer of information. These specific macromolecules offer further targets for drug action since alteration of their conformation, masking of their active groups and occlusion of their surfaces or stabilization of otherwise flexible section may well stop the accomplishment of their function.

- **Ribosome:** Ribosomes are the workhorses of protein biosynthesis, the process of translating mRNA into protein. The ribosome itself is a complex of proteins and RNA. The translation process involves several enzymes and several binding side of unknown composition; there would appear to be many possibilities for drug action here. Selective interference is certainly possible: prokaryotic and eukaryotic ribosome differ in sedimentation coefficient, protein content, and in their ability to bind antibiotic such as chloramphenicol, cycloheximide, and streptomycin. The ribosome presents a fertile field for further investigation and also a site for differentiation of species by drug-action.

- **Cell membrane:** The cytoplasmic membrane of the bacteria cell plays a dual role: it forms an osmotic barrier to free diffusion of small molecule, and controls the internal concentration of metabolite by specific transport mechanisms. The membrane totally encloses the cytoplasm. If the layers external to the cytoplasmic membrane are removed, as for example by antimicrobial lysozome, the membrane is exposed and, unless precautions are taken to balance the osmotic pressure of the cell contents, the membrane raptures and the cell lyses.

- **Cell wall:** The bacterial cell wall is a complex structure composed of a range of macromolecules. The cell wall polymers function as an envelope to protect the protoplast surrounded by its delicate cytoplasmic membrane, recognition and transport of certain substances and cell-cell recognition and interaction. Bacterial cell wall contains peptidoglycan strands. The peptidoglycan component plays a central dominant role in maintaining the integrity of the wall and shape of the cell and is found in all

groups of bacteria. Drug impairs the function or the synthesis of cell wall which is one example of drug action. Some other drug action are:

- Inhibitors of synthesis of peptidoglycan.
- Inhibitors of cross linking of peptidoglycan strands.

2.6.3 Mechanism of selected antibacterial action

Many types of antibacterial agents that exist may have the same target or not depending on the mechanism of each individual action. This thesis proposes mechanisms of three antibacterial agents, namely Nisin, triclosan, and silver nanoparticles.

Nisin

Nisin is a polycyclic antibacterial peptide with 34 amino acid residues which is used as a food preservative. The molecular structure of Nisin is given in Figure 2.23. Nisin is produced by fermentation with the bacterium *Lactococcus lactis*. Commercially, Nisin is obtained from the culturing of *Lactoccus lactis* on natural substrates, such as milk or dextrose, thus it is not chemically synthesized. It is used in processed cheese, meats, beverages, etc. during production to extend the product shelf life by suppressing Gram-positive spoilage and pathogenic bacteria. While most bacteriocins generally inhibit only closely related species, Nisin is a rare example of a "broad-spectrum" bacteriocin effective against many Gram-positive organisms. Nisin is soluble in water and can be effective at levels nearing the parts per billion ranges. In foods, it is common to use Nisin at levels ranging from ~1-25ppm, depending on the food type and regulatory

approval. Due to its naturally selective spectrum of activity [47], Nisin has been used with PLA under the expectation to be an alternative for antibacterial packaging.

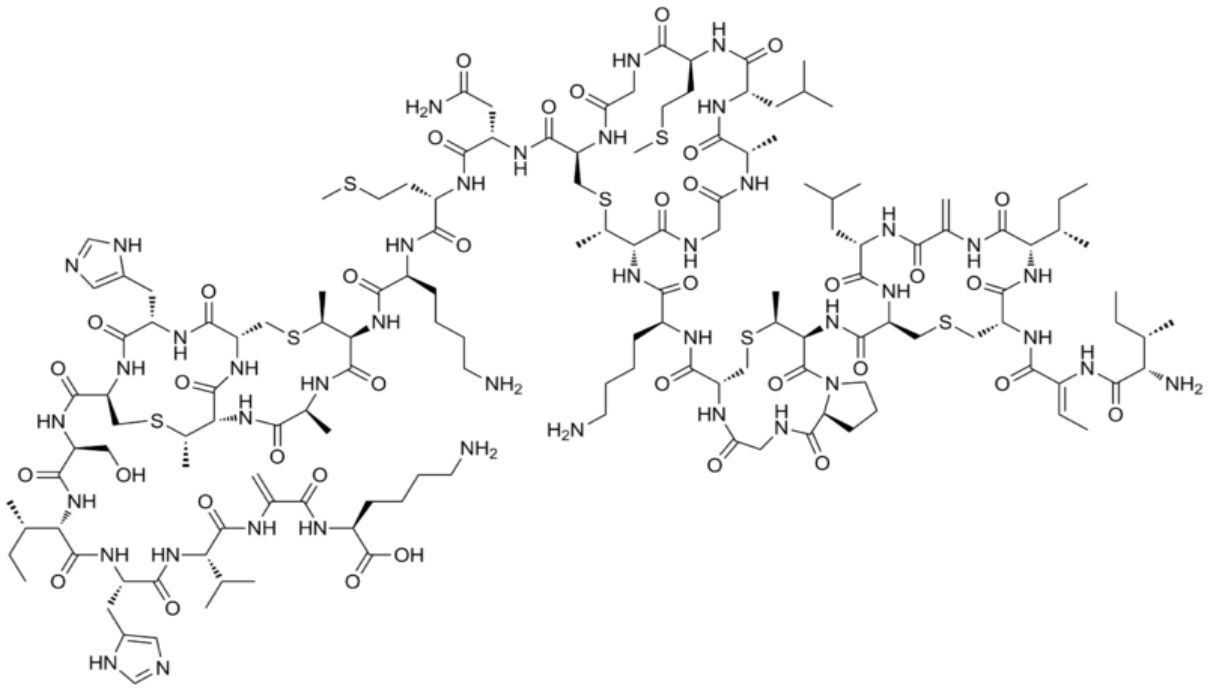

Figure 2.23 Molecular structure of Nisin [44]

- **Mechanism of Nisin action**

The general mechanism of action of cationic biocides Nisin is described as shown in Figure 2.24. Initially, cationic biocides must cross the cell wall; therefore, this compound is targeted at the cytoplasmic membrane. The outer most surface of the cytoplasmic membrane carries a net negative charge, often stabilized by the presence of divalent cations such as Mg^{2+} and Ca^{2+}. Cationic biocides display a high binding affinity for the cytoplasmic membrane. Then, the hydrophobic region of the agent penetrates into the hydrophobic core of the membrane. This leads to a progressive leakage of cytoplasmatic materials to the environment, disturbing membrane-located physiologies such as respiration, solute transport and cell wall biosynthesis. These effects are

sufficient to affect the cell growth (*i.e.* bacteriostatic effect) or even, to cause the cell die (*i.e.* bactericide effect) [45].

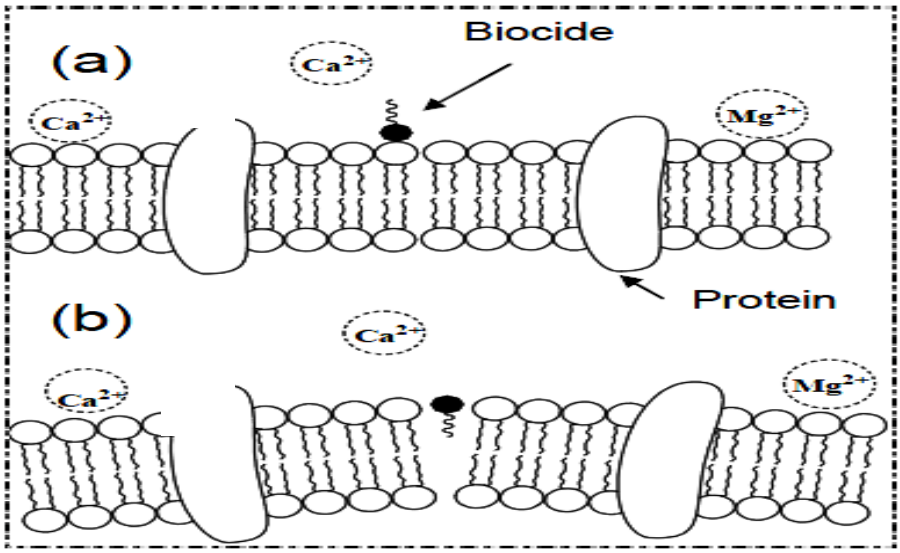

Figure 2.24 Mechanism of action for cationic biocides [46]

Triclosan

Triclosan (2,4,4´-trichloro-2´-hydroxydiphenyl ether) is a synthetic, broad-spectrum antimicrobial agent that has been used extensively in a variety of consumer products including toothpaste, mouthwash, deodorants, soaps, textiles (e.g., socks, underwear), toys, liquid dishwashing soap, and plastic kitchen ware [47]. The molecular structure of triclosan is shown in Figure 2.25. Triclosan has a board spectrum against gram positive and negative bacteria. Triclosan has been used with polymeric material and being used as active packaging under a trade name of Microban [48].

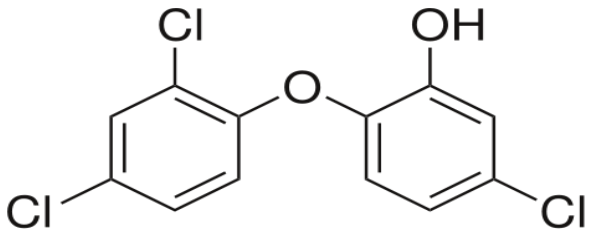

Figure 2.25 Molecular structure of triclosan [49]

- **Mechanism of triclosan action**

The target of triclosan is mainly inhibition of fatty acid synthesis. Triclosan inhibits bacterial fatty acid synthesis at the enoyl-acyl carrier protein reductase (FabI) step. Figure 2.26 depicts the structure of FabI-NAD1-Triclosan complexes. The hydroxychlorophenyl ring is close to the nicotinamide ring of the NAD1with the interplanar distance of 3.4 Å and contacts Tyr-146 and Tyr-156 on the protein. The hydroxyl group of the ligand forms hydrogen bonds with phenol of Tyr-156 and with the 2-hydroxyl of the NAD1. The 4-chloro substituent of triclosan accepts hydrogen at Ala-95. The formation of FabINAD1- triclosan complex is a stable complex, with the triclosan binding at the enoyl substrate site. This complex is unable to participate in fatty acid synthesis from fatty acids are necessary for reproducing and building cell membranes.[50]

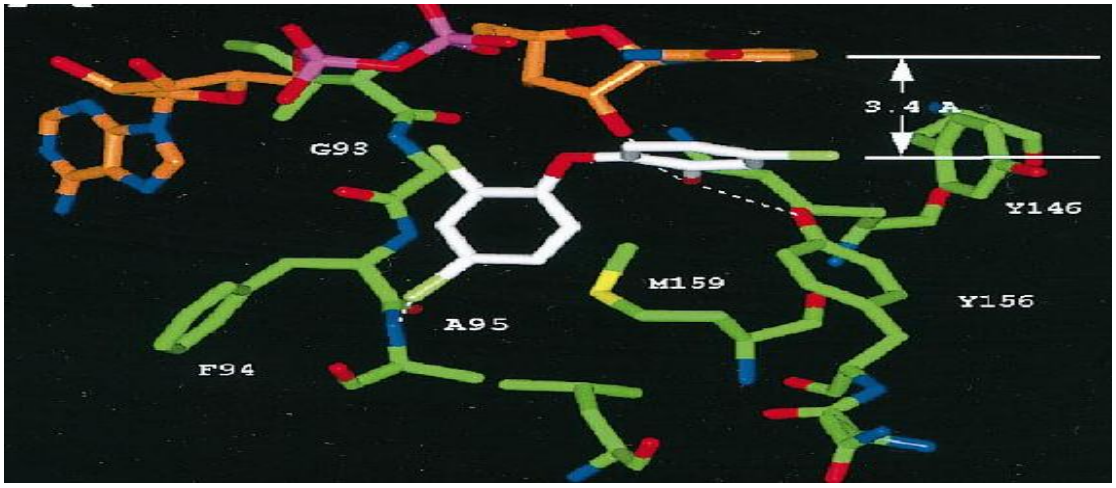

Figure 2.26 Structure of FabI-NAD1-triclosan complexes [50]

Silver nanoparticles

Silver nanoparticles are one of the most commonly utilized nanomaterials due to their anti-microbial properties, high electrical conductivity, and unique optical properties. Silver in different forms has been widely used in medicine for curing disease and help promote wound healing since early times. A common form of silver that is used to treat infections is silver nitrate. Silver nanoparticles have proved to be most effective as it has good antimicrobial efficacy against bacteria, viruses and other eukaryotic micro-organisms. Silver nanoparticles had been used with biodegradable polymer for packaging and medical applications like tissue engineer.

- **Mechanism of silver nanoparticles action**

The mechanism of the growth-inhibitory effects of silver nanoparticles on microorganisms has not been well understood. One possibility is that the growth inhibition may be related to the formation of free radicals from the surface of silver. Uncontrolled generation of free radicals can attack membrane lipids and then lead to a

breakdown of membrane function [51]. Sondi [52] demonstrated by TEM micrographs (Figure 2.27) that the treated *E. coli* cells with silver nanoparticles were damaged, showing formation of "pits" in the cell wall of the bacteria, while the silver nanoparticles were found to accumulate in the bacterial membrane. A membrane with such a morphology exhibits a significant increase in permeability, resulting in the death of the cell.

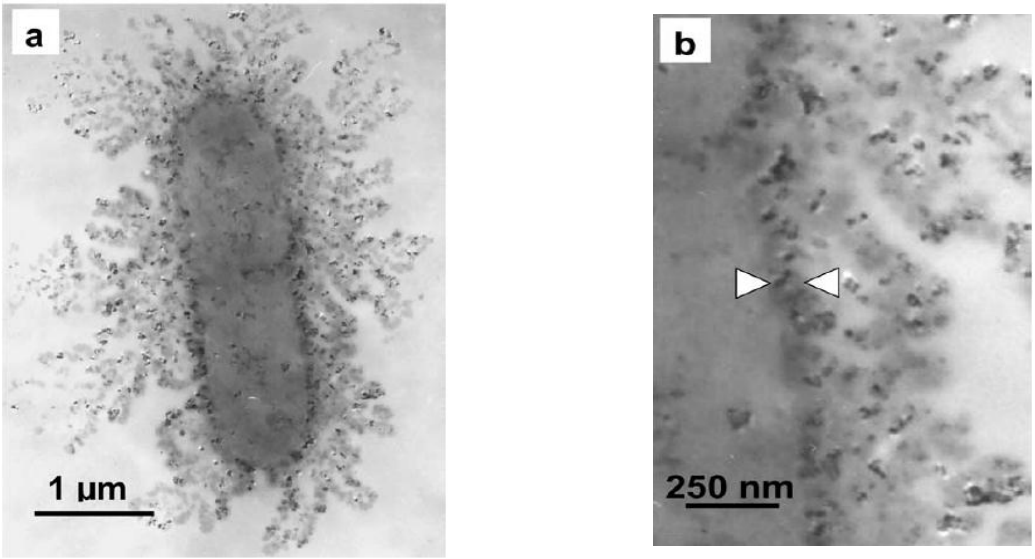

Figure 2.27 Transmission electron micrograph of *E. coli* cell treated with silver nanoparticles: (a) in liquid LB medium; (b) enlarged view of the membrane of this cell [52]

Yamanaka *et al*. [53] provided the mechanism of silver ions from which the silver ions were found to penetrate through ion channels without causing damage to the cell membranes; it denatured the ribosome and suppressed the expression of enzymes and proteins essential to ATP production. These processes imposed an effect on the membrane structures and resulted in the cell disruption.

2.7 Active polymeric materials

Active polymeric materials have been becoming more attractive because human being are more health conscious. In food packaging application, active packaging is not only to prevent human from the microbial attack but also to extend the quality and shelves life of the products. To produce active packaging, many techniques have been employed including [54] (1) using sachets or pads containing volatile antimicrobial agents into material packages; (2) directly incorporation of volatile and non-volatile antimicrobial agents into polymeric material; (3) inherently coating or absorption of antimicrobial agents on the polymer surfaces and; (4) immobilization of antimicrobial agent to polymers by ionic or covalent linkages

2.7.1 Using sachets or pads containing volatile antimicrobial agents into material packages

Ethanol vapor generator is achieved in commercial application**.** It consists of ethanol encapsulated in carrier materials and enclosed in polymer packets. The ethanol permeates the selective barrier and released into the headspace within the package. These systems have been used to extend the mold-free shelf-life of various bakery and dried fish products [54, 55].

2.7.2 Antimicrobial agents incorporated into polymer directly

The direct incorporation of antimicrobial agent additives in plastic films is a convenient means by which antimicrobial agent activities can be achieved. Many antimicrobial agents are incorporated at 0.1-5% w/w of the packaging material, especially films. Thermal polymer processing methods, such as, extrusion and injection molding can be used with thermally stable antimicrobial agents. Silver substituted zeolite (Ag-zeolite), for instance, can resist very high temperatures and hence have been incorporated as a thin co-extruded layer with other polymers. Antimicrobial packaging materials must contact the food surface if they are non-volatile, so the antimicrobial agent can diffuse to the surface as shown in Figure 2.28 [55]. To achieve optimal controlled release to the food surface, the use of multilayer films has been considered. The inner layer controls the rate of diffusion of the active substance while the matrix layer contains the active agent and the barrier layer prevents migration of the agent towards the outside of the package [54, 55].

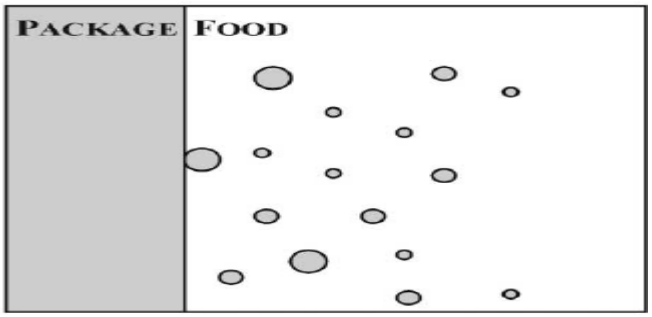

Figure 2.28 Antimicrobial agent incorporated for a packaging system [55]

2.7.3 Coating or adsorbing antimicrobial agents to polymer surface

In early developments in antimicrobial packaging, fungicides were incorporated into waxes to coat fruits, vegetables and cheeses. The fungicides (benomyl, imazalil, thiabendazole (TBZ) and iprodione) have been investigated for their efficacy as surface inhibitors of the molds. Antimicrobials are also used for coatings purpose to retard the growth of yeasts, molds and bacteria during storage and distribution. Organic acids and organic acid salts are common antimicrobial agents which are used for coating. However, some antimicrobial agents are too sensitive to the temperatures used for plastic film processing. An example of film coating is Nisin/cellulose ethers coated polyethylene (PE) film. Cellulose ethers are used as carriers for coating. This coated film was found to be effective in suppressing *Staphylococcus aureus* and *Listeria monocytogenes* [54, 55].

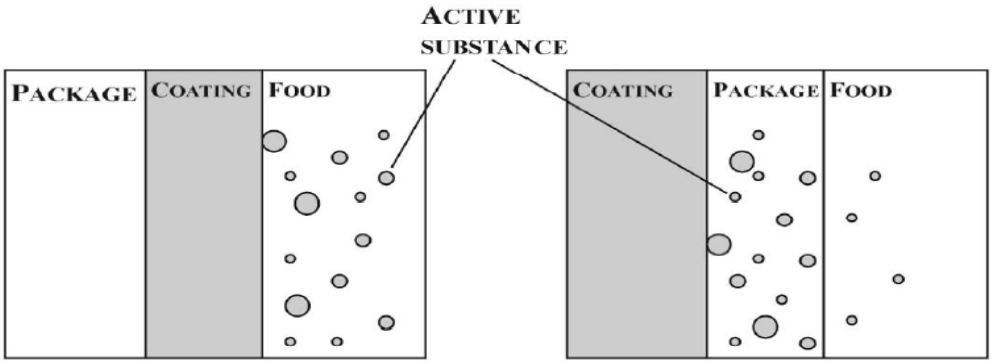

Figure 2.29 Antimicrobial agent coated for a packaging system [55]

Figure 2.29 shows how an antimicrobial agent could be released from a film which has the antimicrobial agent coated at the polymer surface. An adsorption of antimicrobial

agents on plastic films is an alternative to coating technique in order to facilitate heat-sensitive antimicrobial agents for film incorporation.

2.7.4 Immobilized antimicrobial agents to polymers by inorganic or covalent linkages

Besides diffusion and sorption, some active polymer systems utilize covalently or ionically immobilized active substances that suppress microbial growth. Thus, this immobilization requires the presence of functional groups on both the antimicrobial agents and the polymer. Instances of antimicrobial agents with functional groups are peptides, enzymes, polyamines and organic acids. Figure 2.30 shows the characteristic of antimicrobial immobilized packaging system. Besides the functional groups of antimicrobial agents and polymer supports, immobilization may need 'spacer' molecules that bind the polymer surface to the bioactive antimicrobial agent.

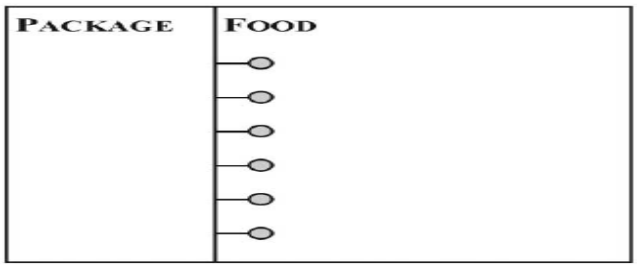

Figure 2.30 Antimicrobial agent immobilized for a packaging system [55]

These spacers allow sufficient motion freedom that the active antimicrobial site can contact microorganisms on the food surface. Spacers that could potentially be applied

for antimicrobial food packaging consist of polyethyleneglycol(PEG), ethylenediamine, polyethyleneimine and dextrans [54, 55].

2.7.5 Inherently antimicrobials polymer

Certain polymers are inherently antimicrobial activities which are usually used in film coating applications. Cationic polymers, for example, poly-L-lysine and chitosan, promote cell adhesion, causing leakage of intracellular constituents of microorganisms because amines could interact with negative charges on the cell membrane. Additionally, cationic polymer chitosan can be used together with other antimicrobials, such as, organic acids and plant extract to maximize the inhibition effect on the growth of microorganisms [54, 55].

2.8 Standard test methods for evaluation active of materials effectiveness

2.8.1 Inhibition zone test (Agar diffusion)

Agar diffusion is the molecules movement through the matrix which is formed by the gelling of agar under controlled conditions. The degree of the removed molecules can be related to the concentration of the molecule. This phenomenon forms the basis of the agar diffusion assay that is used to determine the susceptibility or resistance of a bacterial strain to an antibacterial agent. To determine the antibacterial efficacy of and active material, active material is placed on a solid agar medium containing the test microorganism. The agar plates are incubated until growth is visible. A clear zone

surrounding the material (Figure 2.31) indicates antimicrobial diffusion from the film and subsequent growth inhibition. A Lack of growth under a film may indicate inhibition, but appropriate controls must be included, this may be due to simple restriction to oxygen. The agar plate test method simulates wrapping of foods and may suggest what can happen when film contact contaminated surfaces and the antimicrobial agent migrates from the film to the food. The method can be quantitative if the diameter of the clear zones around the films is measured. Inhibition zone radius can be calculated by using equation below [54, 56, 57].

$$R_C = \frac{D_B - D_A}{2} \tag{2.5}$$

where D_A = diameter of the tested specimen (mm)

D_B = summation of the tested specimen and clear zone diameter (mm)

R_c = radius of the inhibition zone (mm)

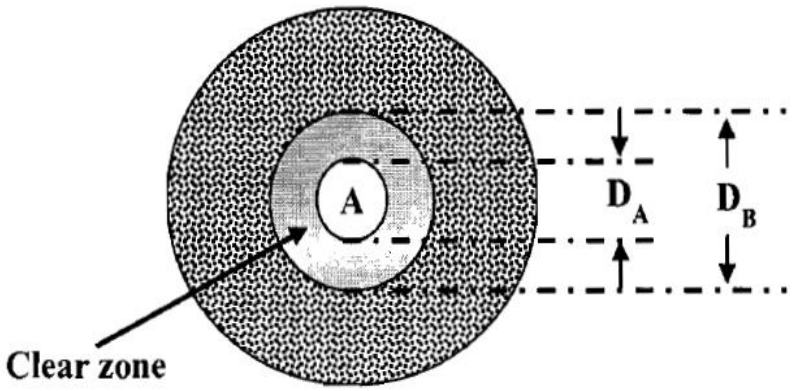

Figure 2.31 A model of inhibition zone [56]

2.8.2 Minimal inhibitory concentrations (MIC)

MIC is described as the lowest concentration of an antimicrobial activity that prevents the visible growth of a microorganism after a prolonged incubation and also can indicate the antimicrobial strength of the polymer that allows the comparison of the polymer's antimicrobial activity to that of the antimicrobial alone. The method consists of a series of tubes containing growth medium with the target microorganism and with polymers containing different concentrations of antimicrobial. The tubes are incubated for a certain period of time and visually inspected for microbial growth. As mention above, MIC is the lowest concentration of an antimicrobial in a polymer resulting the complete inhibition of growth of a test microorganism. Results should include polymer dimensions, composition and other relevant characteristics that vary from specimen to specimen [54, 56]

2.8.3 Shake flasks test or plate count agar (PCA)

Shake flasks tests provide more detailed information on antimicrobial kinetics. Liquid media (buffer, growth media, culture nutrients or foods) are seeded with the target microorganisms and the antimicrobial polymer. The flasks are incubated with mild agitation. Samples are taken over time and enumerated Unlike the MIC test, this method measures the reduction in bacterial growth rate even if, substantial grow occurs. Tests in broth provide information on microbial growth kinetics and the antimicrobial mode of action of the polymers. When testing antimicrobial films by the shake flask test, the ratio of film surface area to volume (of product or media) must be considered. Previous examples show that increasing the surface area/volume ratio increases the activity of

bioactive molecules incorporated into polymer films. From an antimicrobial standpoint, high surface volume/ratios may seem adequate. But in real packaging applications, surface area/volume ratios of 1 is considered optimal, and values higher than that may be impractical. By accounting the area/volume ratio, the feasibility of such films for practical applications may be assessed. As its name implies, the shake flask test includes agitation which enhances the contact between the antimicrobial polymer and the cells. The test may not be indicative of the degree of agitation that packaged foods receive and therefore studies should simulate agitation during storage and transportation. The percent reduction of bacteria colony forming units (CFU) can be calculated [54, 56].

$$\%R = \frac{A - B}{A} \times 100 \tag{2.6}$$

where R = the decrease of bacteria (%)

A = the average amount of bacterial colonies from composites without antibacterial agents for a given contact time (CFU/ml)

B = the average amount of bacterial colonies from composites with antibacterial agents for a given contact time (CFU/ml)

2.9 Literature review

Antimicrobial packaging or active packaging materials become a very interesting for industrial sector at present, especially for food packaging application. The active packaging can inhibit microbial growth which is a cause of illness while remain quality of the food. Various thermoplastics have been used for these applications, e.g. poly(vinyl chloride), polyethylene, polypropylene, polyurethane and polystyrene [1, 2]. To produce active packaging, many techniques have been employed, such as melt-mixing of antimicrobial agents with polymers, applying a coating on polymer surfaces, and immobilizing polymers by covalent bond linkages. But melt mixing is preferred for industrial applications because of cost effectiveness and compatibility with current processing techniques [3]. However, the use of biopolymers in food packaging has already received wide attention [58, 59]. Nisin is an antibacterial agent which is primarily active against Gram-positive bacteria, including *Clostridium*, *Bacillus*, *Staphylococcus* and *Listeria* species [60]. Nisin was discovered to bind the outer membrane receptors by conjugation with other cell components (i.e., phospholipids), or by aggregation with other proteins (i.e., glycoproteins) of bacteria cell [61]. Jin and Zhang [62] illustrated that Nisin/PLA films could inhibit growth of *Listeria monocytogenes* and *Escherichia coli* in culture media and liquid foods (orange juice and liquid egg white) but killing efficiency of each media was different. The greatest inhibition occurred at 24 h when the cell counts of L. monocytogenes in the Ninsin/PLA samples were 4.5 log CFU/mL less than the controls. The combination of a biopolymer and natural bacteriocin has potential for use in antimicrobial food packaging. Triclosan (2, 4, 4'-trichloro-2'-hydroxydiphenylether), a board spectrum antimicrobial substance, has been used effectively as toothpaste, mouthwash, deodorant and soap [47].

Silapasorn *et al* [2] revealed that the triclosan did not change the color of all thermoplastics used (LDPE, MDPE, HDPE, PP, PS, PVC). The differences in the antibacterial performances of the studied thermoplastics with triclosan were associated with their rigidities, abilities to crystallize, and free volume or molecular density. However, triclosan/PVC showed the worst antibacterial performance because of interaction of triclosan and PVC which was confirmed by FTIR. Cutter [63] indicated that the material containing 1500 ppm of triclosan inhibited the growth of bacterial strains, such as, *B. thermosphacta, S. aureus and S. typhimurium*. Biochemical target of triclosan is mainly inhibition of fatty acid synthesis [50]. Silver nanoparticles are a well-known antibacterial agent, which is widespread used for many applications especially, packaging application [64]. Only 1% of silver substitution zeolite in polyethylene was sufficient to reduce the microbial cell on the surface of polyethylene from 105 to 106 cells/ml to less than 10 cells/ml after 24 hours of contact [65]. The particles size of antibacterial agents also influences bacterial killing efficiency. Polypropylene filled with 0.1% of silver nanoparticles displayed an excellent antibacterial performance (above 99.9%), whereas micron-sized silver required silver content more than 0.5 % before exhibiting good antibacterial activity [66]. Fernadez *et al* [64] compared antimicrobial activity of Zeomic/PLA films prepared by a melt-mixing and solvent casting. The results were found that melt mixing films had greater crystallity but solvent casting films achieved antibacterial effectiveness. In that case, a higher water uptake due to that water diffusion through the filler induced voids has been more clearly associated to the higher silver ion release than the polyamide crystallinity. The antibacterial effectiveness is also dependent upon concentration of antibacterial agents, method and the testing conditions. Recently, Zeomic/Silicone rubber was studied, the results showed that the Zeomic was not beneficial to the antimicrobial activity of the

rubber against bacteria but improved the tensile strength, elongation at break and stored energy density at break of the rubber [67].

Wood flour, a biodegradable reinforcing material, is one of the most widely used materials for producing wood–polymer composites (WPC) because it possesses several advantages, e.g. high modulus, low density, reduced material use, and low cost [23]. Wood/PLA composites are of great interest because wood and PLA are not only environmentally friendly materials but they are also expected to degrade completely after disposal at the end of their service lives. The tensile strength of wood/PLA composite is almost independent of wood-flour content, suggesting only weak adhesion exists between the PLA matrix and the wood-flour particles [68, 69], usually overcomes by means of chemical modification [9, 10]. The addition of 1% silane treatment to the wood could improve the tensile modulus because silane enhances interfacial bonding of the wood and PLA [70]. The wood content was usually found to increase the Young's modulus while the tensile strength, elongation at break, and impact strength decreased [26]. Petinakis *et al* [71] demonstrated that the addition of wood-flour resulted in an increase of up to 95% in the tensile modulus, in comparison with pure PLA while the addition of a coupling agent, methylenediphenyl-diisocyanate (MDI) to the composition resulted in an increase in tensile strength and tensile modulus of the wood/PLA composites, of 10 and 135%, respectively, indicating enhanced matrix–particle interfacial adhesion. The T_g value of the wood/PLA was also found to decrease with the wood content because of the lower interfacial adhesion between the wood and PLA, consuming less power to move the PLA chain [72]. Shi *et al* [73] revealed that 1% Bamboo fiber incorporated with PLA could create double T_m values with double-melting behavior appeared as a result of the defects of BF structure promoted the melt-

recrystallization and promoted forming the small crystals. The addition of wood and wood type can influence the microbial killing efficiency. The wood/PVC composited filled with 3-iodopropinyl- N-butylcarbamate (IPBC) show better antifungal performance than the neat PVC while IPBC/PVC incorporated with Hevea brasiliensis Muell showed the best antifungal performance in comparison with Xylia kerrii Craib and Hutch [74]. Although PLA is an appropriate candidate for packaging end-use application, PLA has limitations in gas barrier property which should be overcome [8]. The filler incorporation, especially organoclay, is the most attentive method to improve the barrier property because of cost saving and good barrier property [9]. These nanocomposites have strong barrier property because the clay layers retard the diffusing molecule pathway due to tortuosity. Clays are essentially impermeable inorganic crystals, gas molecules have to permeate around them instead of permeation a straight line path which takes longer mean path for gas absorption though these nanocomposite [10]. Cloisite® 30B is an organo-modified montmorillonite having two hydroxyl groups. The reaction between hydroxyl groups of Cloisite® 30B and PLA makes this clay proper for producing PLA-clay nanocomposites [75]. The water vapor permeability of the nanocomposite films could decrease 6-33% through nanoclay compounding [13]. The oranoclay was also found to accelerate the hydrolysis reaction by initiation of water absorption [30].

Usually, the biodegradation occurs in two ways, enzymatic degradation, and non-enzymatic degradation. However, the hydrolysis reaction is the main reaction which initiates the biodegradation of the PLA [22]. The crystalline region is found to be rather hydrolysis resistant compared with those in the free amorphous region [33]. From a lab-scale, the biodegradation of neat PLA inoculated at 58°C for 60 days degraded slowly

only 13% compared to the pot type B (containing 5% poultry feather, 80% PLA, 15% starch), and C (containing 50% poultry feather, 25% urea, 25% glycerol) which were 53 and 39, respectively [76]. The PLA size distributions influence the biodegradation, there by the PLA powders with sizes of 60 and 120 mesh were found to be degraded by up to 91% after 35 days at 58 °C in the controlled compost [16]. Temperature and relative humidity (RH) were also found to affect biodegradation of PLA. Kai-Lai *et al* [77] disclosed that the degradation rate of PLA plastics was enhanced by the increase in temperature and relative humidity. The testing conditions were 28, 40, and 55°C at 100% RH which gave the average degradation rate of PLA of 28,931, 27,361, and 63,025 g mol^{-1}/week, respectively. However, enzymatic degradation by microorganism could occur when the molecular weight of the PLA is lower than 10,000 Da. A PLA-degrading actinomycete, *Kibdelosporangium aridum*, was found to degrad the PLA more than 97 mg out of 100 mg of the high molecular weight of PLA film within 14 days in a liquid culture [78]. However, biodegradation ability of PLA loaded with antimicrobial agents was still unclear and open for wide discussion.

CHAPTER 3 METHODOLOGY

3.1 Materials, chemicals and testing bacteria

All materials, chemicals and testing bacteria used in this work are given in Table 3.1

Table 3.1 Materials, chemicals and testing bacteria used in this work

Material	Grade/Type/Brand/Composition	Company
Poly(lactic acid)	2002D, 2003D	NatureWorks, USA
Triclosan	2,4,4'-trichloro-2'-hydroxydiphenylether, 24USP	Koventure Co. Ltd., Thailand
Silver substituted zeolite (Zeomic)	$MX_{2/n}O \cdot Al_2O_3 \cdot YSiO_2 \cdot ZH_2O$	Yamamoto Trading Co., Ltd., Thailand
Coupling agent	N-2(aminoethyl)-3-aminopropyltrimethoxysilane, KBM 603	Shin-Etsu Chemical Co. Ltd., Japan
Wood flour	average particle size of 100–300 μm	V.P. Wood Co., Ltd., Thailand
Nutrient broth	Standard formula ingredient (g/litre) Plurypeptone 5.00 Beef extract 3.00	Laboratorios Britania Co.,Ltd., Argentina
Plate count agar	Standard formula ingredient (g/litre) Casein enzymic hydrolysis 5.0 Yeast extract 2.50 Dextrose 1.00 Agar 15.00	Himedia Co.,Ltd., India
Peptone	RM 001-500G	Himedia Co.,Ltd., India
Organo-modified clay	Cloisite® 30B	Southern Clay Products Inc.,USA
Escherichia coli (E.coli)	Gram-negative bacteria, ATCC 25922	National Institute of Health of Thailand
Staphylococcus aureus (S.aureus)	Gram positive bacteria, ATCC 25923	National Institute of Health of Thailand

3.2 Research plans

The independent variables shown in Figure 3.1, were composed of wood flour (5 and 10%wt), and types and contents of antibacterial agents (triclosan and Zeomic) whereas the dependent variables (or testing methods) were antibacterial tests, mechanical properties test (tensile and impact), surface contact angle, ATR-FTIR, DSC, surface contact angle. For the work flowchart in Figure 3.2, a set of biodegradation test was arranged modified from ASTM D5538-1. Then the PLA and wood/PLA composites were selected to test biodegradation performance, including (i) PLA and wood/PLA; (ii) PLA and wood/PLA incorporating Zeomic and (iii) PLA and wood/PLA incorporating triclosan, respectively. The CO2 evolution occurred during 60 days of the test was measured every 2 days. In Figure 3.3, variables understudy were composed of wood flour, triclosan and organoclay Cloisite® 30B. Then antibacterial, mechanical, thermal properties and clay dispersion were investigated.

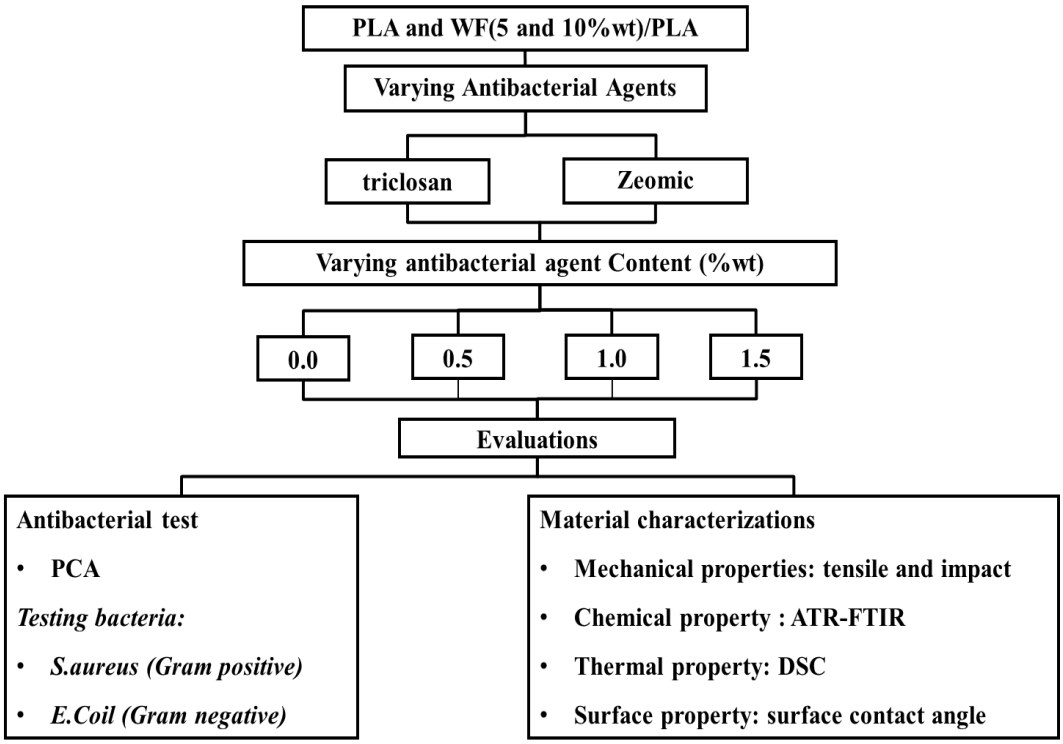

Figure 3.1 Work flowcharts for the studies of the effect of wood flour and antibacterial agents loading on PLA and wood/PLA composites properties

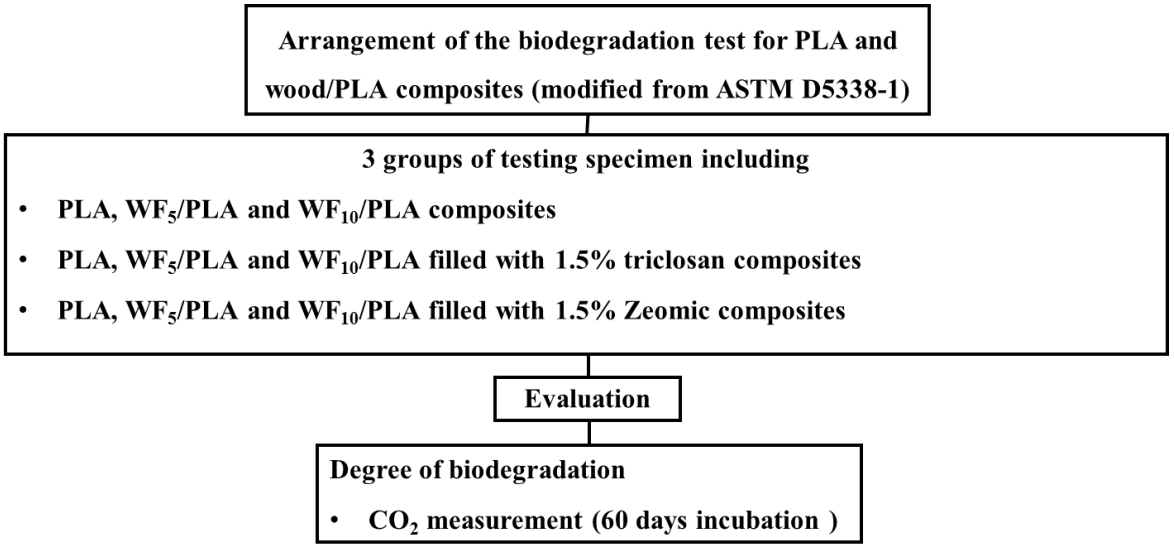

Figure 3.2 Work flowcharts for the studies of the effect of wood flour and antibacterial agents loading on biodegradable performance of PLA and wood/PLA composites

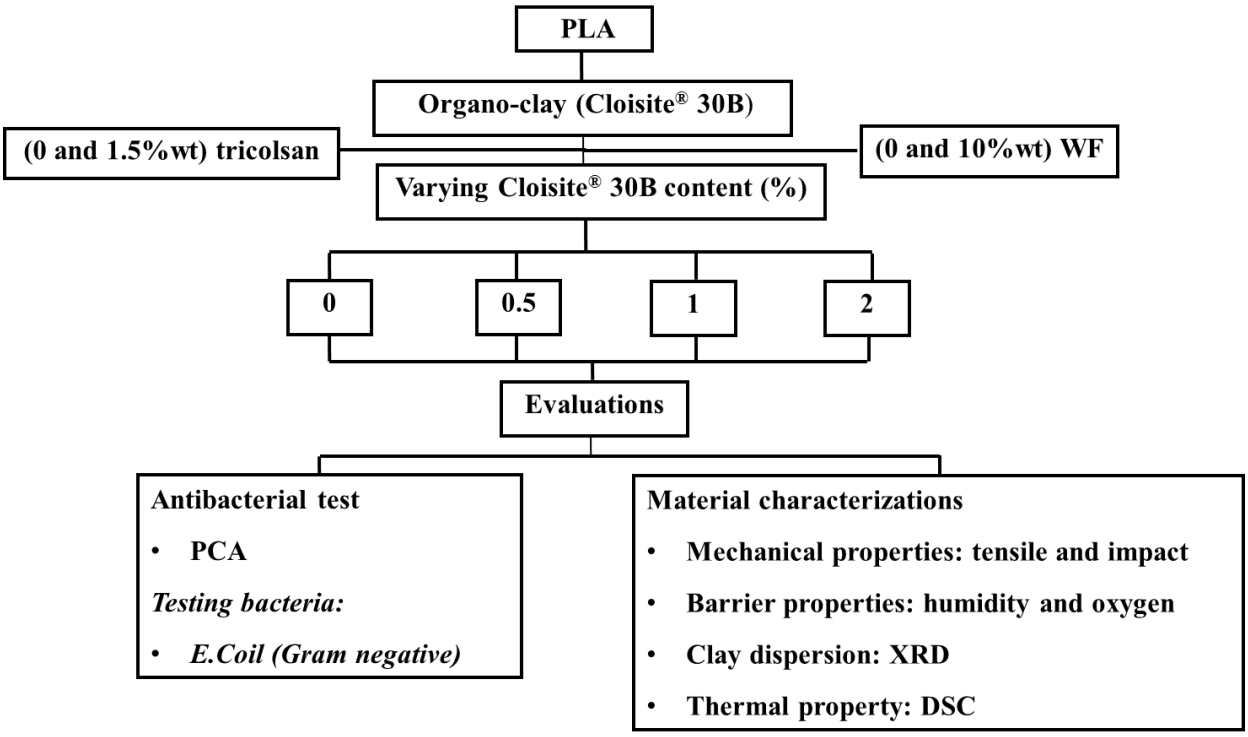

Figure 3.3 Work flowcharts for the studies of the effect of organoclay loading on mechanical, thermal, antibacterial properties and barrier properties of PLA and PLA based composites

3.3 Experiment

3.3.1 Specimen preparation

KBM 603 silane coupling agent (1%) was used for chemical surface treatment of wood flour by blending in a high-speed mixer. The treated wood flour was left in an oven at 80 ^{o}C for 3 days to remove all moisture content. Before the high-speed mixing process with antibacterial agents (triclosan or Zeomic) and Cloisite® 30B, the treated wood/PLA, Zeomic and Cloisite® 30B were dried in an oven at 80 ^{o}C for 24 hours. The lists of all composite formulations used are given in Tables 3.2 and 3.3. A twin-screw extruder (HAAKE™ Rheomex CTW 100P; Thermo Fisher Scientific, Waltham, MA, USA) was used to melt-blend all components, using temperature profiles from feed to die zone of 170, 180, 180, 180 and 170 ^{o}C, respectively, with 50 rpm screw rotating speed to produce pellets of PLA based composited. The extrudate was pelletized and then dried in an oven at 70 ^{o}C before compression-molded to give specimen films. The compression temperature and pressure used were 160 ^{o}C and 150 kg/cm^2, respectively, under 5 min preheating and 3 min holding times before cooling down to room temperature. For biodegradation and antibacterial testing, specimens with 1 mm thick were cut into rectangular pieces 2.5 × 5.0 cm^2. The thickness of 0.5 mm and 3 mm specimens were made for permeability and mechanical properties tests, respectively

Table 3.2 Composite formulations and sample codes used for the work flowcharts 1-2

Sample code	Ingredient and content			
	PLA (P, %wt)	**wood flour (W, %wt)**	**triclosan (T, %wt)**	**Zeomic (Z, %wt)**
PLA	100.0	-	-	-
0.5TP	99.5	-	0.5	-
0.5ZP	99.5	-	-	0.5
1TP	99.0	-	1.0	-
1ZP	99.0	-	-	1.0
1.5TP	98.5	-	1.5	-
1.5ZP	98.5	-	-	1.5
W_5P	95.0	5.0	-	-
$0.5TW_5P$	94.5	5.0	0.5	-
$0.5ZW_5P$	94.5	5.0	-	0.5
$1TW_5P$	94.0	5.0	1.0	-
$1ZW_5P$	94.0	5.0	-	1.0
$1.5TW_5P$	93.5	5.0	1.5	-
$1.5ZW_5P$	93.5	5.0	-	1.5
$W_{10}P$	90.0	10.0	-	-
$0.5TW_{10}P$	89.5	10.0	0.5	-
$0.5ZW_{10}P$	89.5	10.0	-	0.5
$1TW_{10}P$	89.0	10.0	1.0	-
$1ZW_{10}P$	89.0	10.0	-	1.0
$1.5TW_{10}P$	88.5	10.0	1.5	-
$1.5ZW_{10}P$	88.5	10.0	-	1.5

* W_5 and W_{10} represented the wood contents of 5 and 10 %wt, respectively

Table 3.3 Composite formulations and symbols used for work flowcharts 3

Sample code	Ingredient and content			
	PLA (P, wt%)	**Cloisite® 30B (C, wt%)**	**triclosan (T, wt%)**	**wood flour (W, wt%)**
PLA	100.0	-	-	-
0.5CP	99.5	0.5	-	-
1CP	99.0	1.0	-	-
2CP	98.0	2.0	-	-
TP	98.5	-	1.5	-
0.5CTP	98.0	0.5	1.5	-
1CTP	97.5	1.0	1.5	-
2CTP	96.5	2.0	1.5	-
WP	90.0	-	-	10.0
0.5CWP	89.5	0.5	-	10.0
1CWP	89.0	1	-	10.0
2CWP	88.0	2	-	10.0
TWP	88.5	-	1.5	10.0
0.5CTWP	88.0	0.5	1.5	10.0
1CTWP	87.5	1.0	1.5	10.0
2CTWP	86.5	2.0	1.5	10.0

3.3.2 Antibacterial activity evaluations

Antibacterial evaluation of PLA specimens was performed by plate count agar (PCA) method following ASTM E2149 (2001). An inoculum of *S. aureus* and/or *E.coli* was incubated at 37 ^{o}C overnight before measuring optical density (OD) values by UV-Vis spectroscopy (DR/4000; Hach, Loveland, CO, USA). Peptone solution (prepared with 1 g/L peptone in deionized water) was used to dilute each inoculum to OD 0.1. Two pieces of 2.5 × 5 cm^2 film specimens (1 mm in thickness) were placed in individual flasks filled with 50 ml peptone solution, OD 0.1. A reciprocal shaker was used to shake the flasks at a speed of 100–120 rpm at 37 ^{o}C ± 0.5 ^{o}C for 0, 60, 120, 180 and 240 min of contact time. In order to find a suitable range of colony-forming units (CFU) of *S. aureus* and *E.coli* [79], a tenfold serial dilution was applied. For each contact time, 100 μL of bacteria solution was placed on agar in sterilized Petri dishes. The inoculated plates were then incubated in an incubator for 24 h at 37 ^{o}C. The number of living cell bacterial colonies was counted to determine the antibacterial performance. The percentage reduction of bacterial CFU was calculated using Eq. (2.6)

3.3.3 The biodegradation test

Before the biodegradation test, the compost was fermented with fresh leaves for two months to enrich the microbial population. The properties of the fermented compost are given in Table 3.4. Figure 3.4 shows a diagram of the biodegradation test arrangement, which was modified from the standard test method ASTM D5338-11 (2003). One-mm-thick samples of PLA and PLA-based composites were cut into four rectangular pieces 2.5 × 5.0 cm^2 and placed inside a reactor bottle filled with 400 g of compost. Compost containing no specimens served as a blank, which was used to determine the CO_2 generated by bacterial activities. The test was controlled at 58 °C ± 2 in a water bath for 60 days. An air flow rate of 50 ml/min was fed into the system by an air pump (Figure 3.4, No. 1) during the test to ensure that aerobic conditions were maintained. $Ba(OH)_2$ solution used in the test was 250 ml of 0.0625 M. Silica gel columns (No. 2) and the first $Ba(OH)_2$ solution unit (No. 3) were used to remove moisture and CO_2 from the feed air, respectively. The CO_2 evolved from the reactor (No. 4) was trapped in $Ba(OH)_2$ solution at the second and third $Ba(OH)_2$ solution units (No. 5). The CO_2 reacted with the $Ba(OH)_2$ and precipitated as $BaCO_3$. The amount of CO_2 was measured every two days by titration with 0.05 M HCl, using a few drops of phenolphthalein as an indicator to determine the $Ba(OH)_2$ remaining in the solution.The CO_2 trapping reactions by the titration of $Ba(OH)_2$ and HCl are shown in Eqs. (2.1) and (2.2). The percentage of biodegradation (D_t) was calculated using Eq. (2.4).

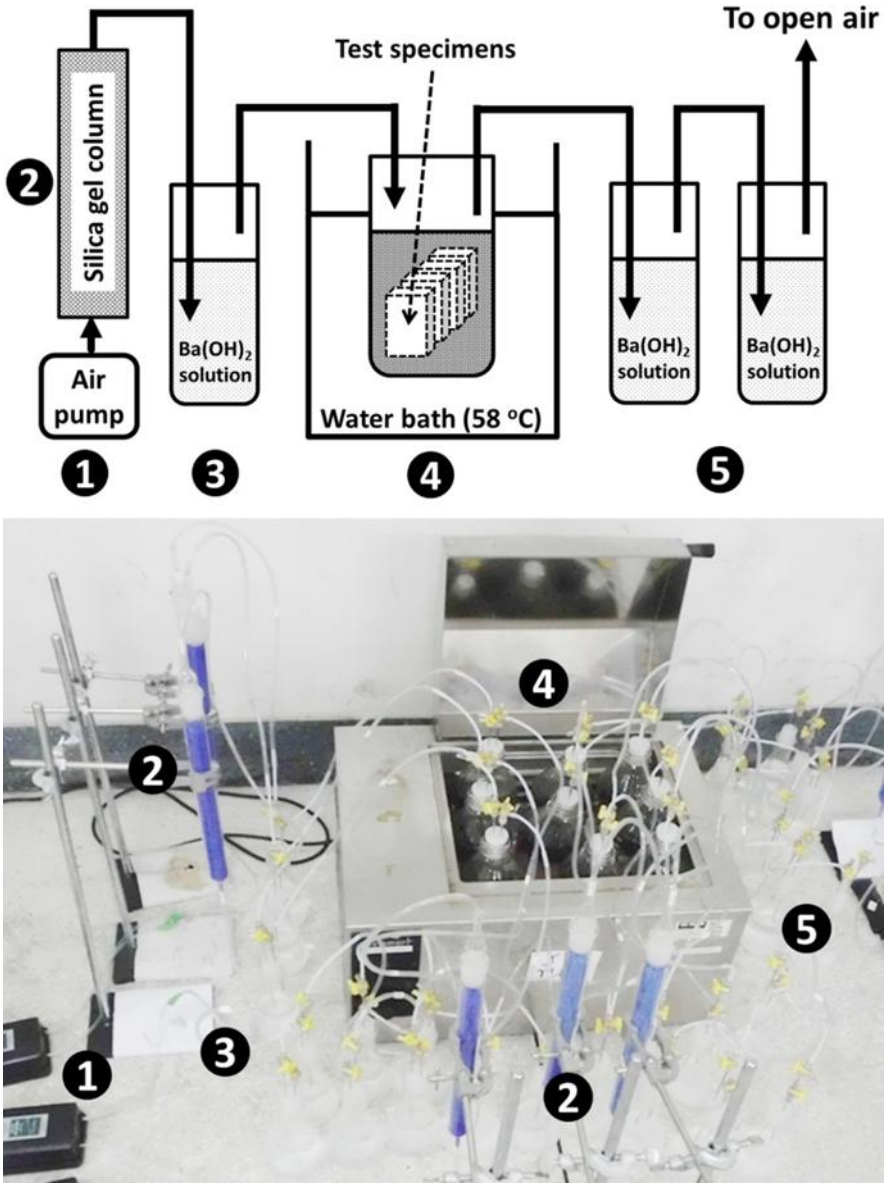

Figure 3.4 Arrangement of the biodegradation test for PLA and wood/PLA composites (modified from ASTM D5338-1)

Table 3.4 Properties of soil composed in this study

Item	Value
Total dry solid (%)[a]	40.32
Volatie solids (%)[b]	31.15
pH of compose	6.9
Total organic carbon amount (%)	8.22
Total nitrogen amount (%)	0.49
C/N ratio	17

[a] Total of solids gained by catching a know volume of compost dried at 105°C for 24 h.
[b] Total of solid gain by catching a know volume of compost burnt at 550°C 2h.

3.3.4 Barrier properties test

Water vapor permeability (WVP)

Water vapor permeability (WVP) was determined through ASTM E96/E96M-12. The film specimens were put on the cup filled 10g of silica gel. The cup (including film and silica gel was placed in an environmental chamber at 39°C and 90% RH. The silica gels were weighed after 1 week. WVP was calculated by using the standard water permeability Equation (3.5):

$$WVP = \frac{(permeance \times t)}{\Delta p} \tag{3.1}$$

where permeance = the rate of water vapor transmission (g/mm^2h)

t = the average film thickness (mm)

Δp = the vapor pressure difference between both sides of the film (Pa)

Oxygen permeability

To determine oxygen permeability of PLA composite films, an oxygen permeability test equipment OX-Tran model 2/10 (Mocon Co. Ltd., USA) was used. The experiment was performed in a stainless steel chamber. Oxygen and nitrogen were used as the test and purge gas. 0.5mm thick films were placed in the chamber which permeated oxygen was passed over each film for a certain period detected by the oxygen sensor. To ensure no leaked gas, O-ring and silicone grease were applied between the films and chamber wall. Each film was examined by two step procedures, the first step was to check the

leak between the film and chamber wall while then second step was to determine amount of oxygen passing the PLA film during the test (each step was done by 10 cycles with took 45 min each).

3.3.5 Characterizations

- Fourier transform infrared spectroscopy (FTIR; Spectrum Spotlight 300, PerkinElmer, USA) was utilized with an attenuated total reflectance mode to examine molecular interactions between PLA, triclosan and wood flour.

- Differential scanning calorimetry (DSC; DSC822, Mettler-Toledo, USA) was used to monitor the physical and thermal properties of PLA, PLA based composites. Each sample was first heated from 30 to 200 ^{o}C, cooled down to 30 ^{o}C and then re-heated to 200 ^{o}C. The heating and cooling rate were 10 ^{o}C/min under nitrogen atmosphere. The glass transition temperature (T_g) and melting temperature (T_m) were determined. Percentage of crystallinity (X_c) was also obtained via the DSC curves given by Equation (3.6):

$$X_C(\%) = \frac{\Delta H_m}{\Delta H_m^0} \times \frac{100}{w} \qquad (3.2)$$

where ΔH_m = the enthalpy of the sample

ΔH_m^0 = the enthalpy of fusion for 100% crystalline PLA (93.7 J/g)

w = the weight fraction of PLA in composites

- Water contact angle (WCA) studies were performed to quantify the change in surface energy, surface chemistry and roughness of PLA and PLA blended. Deionized water was dropped onto PLA blend and composite surfaces, and then the contact angle was measured using a contact angle goniometer (model 100-00, Ramé-hart Instrument Co., USA). In the developing step, 5 times/100 μL droplets were dropped on specimen surfaces using three independent samples, and the average contact angle values were then reported.

- X-ray diffraction (XRD) was used to determine distribution characteristic of organoclay in PLA matrix. The data of PLA composites has been collected with a Rigaku X-ray diffractometer, (CuK_{α} radiation, 30 kV, 10 mA) using step size of 0.02° and 4.0° min^{-1}. The basal spacing (d 0 0 1) was obtained from Bragg's equation ($n\lambda = 2d\sin\theta$)

3.4 Experimental problems and solutions during the work

3.4.1 Problems and solutions

Problem 1: PLA was over-melted during high speed mixing process (Figure 3.5) because PLA was very sensitivie to heat [80].

Figure 3.5 Over-melted PLA during the high speed mixing process

Solution 1: Reduced the mixing time of the high speed mixer from 5 to 2.5 min in order to reduce heat accumulation of the PLA. Finally, the PLA was extrudable.

Problem 2: The Extrudate of PLA loaded with 20 and 40 %wt wood flour were over-melted during the melt mixing process by the twin screw extruder (Figure 3.6**)** because the incompatibity of the PLA and wood flour and also moisture from the wood caused the hydrolysis reaction of the PLA.

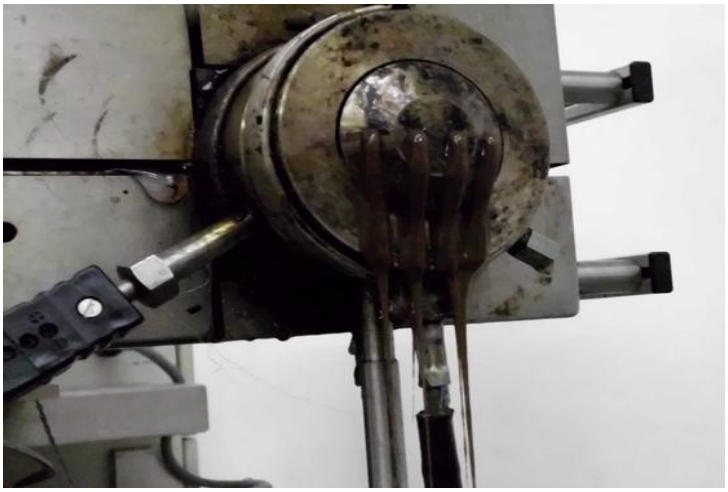

Figure 3.6 Over-melted PLA loaded with 20 and 40 %wt wood flour during the extrusion process

Solution 2: Used lower contentets of wood (5 and 10 %wt) and increased the drying time from 80°C for 12 hours to 80°C for 24 hours to minimize the effect of moisture from the wood and hydrolysis reaction.

Problem 3: Bubbles evolved within the wood/PLA sheets (Figure 3.7) during the hot press process when the upper heated plate moved down until touching the PLA, the PLA melted immeadiately then gas or moisture was trapped inside the PLA sheets.

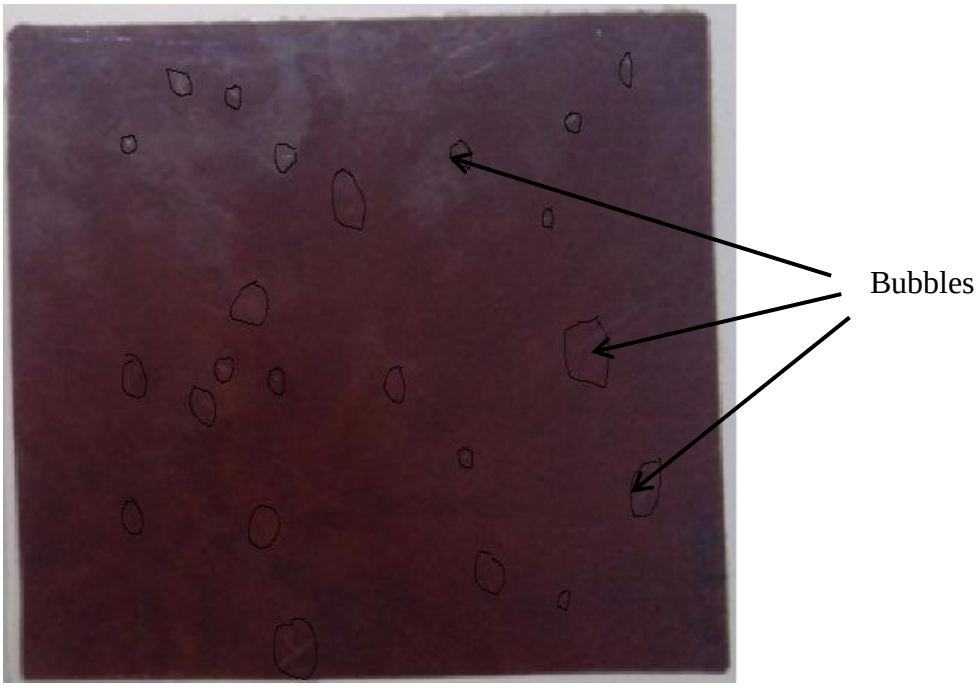

Figure 3.7 Bubbles evolved within the wood/PLA sheets

Solution 3: Reduced hot press temperatures form 170°C to 160°C to slow down the PLA melting in order to increase the time for gas or moisture to release.

Problem 4: Unable to cut the PLA and wood/PLA composite sheets to produce testing specimens by a cutting meachine because the PLA sheets melted and rejoined during the cutting process.

Solution 4: Using a cooling unit (Figure 3.8) during the cutting process to solve the PLA melting problem which was a cause of rejoining.

Figure 3.8 Cutting maching with a cooling unit

Problem 5: The PLA incorporated with Zeomic composite sheets is very brittleness and broken easily (Figure 3.9) because the incompatibility of PLA and Zeomic and also moisture from the Zeomic caused the hydrolysis reaction of the PLA to take place.

Figure 3.9 Broken Zeomic/PLA composite sheets

Solution 6: Dried the Zeomic at 80°C for 12 hours to release the moisure content.

Problem 6: Failed to extrude wood/PLA filled with Zeomic loading of 1.5 %wt (Figure 3.10) because of the incompatibility of wood and PLA, together with mositure contents in Zeomic absorbed by Si–OH bonding as a function of zeolite initiating the hydrolysis reaction.

Figure 3.10 Over-melted wood/PLA loaded with 1.5%wt Zeomic composites during the extrusion process

Solution 7: Changed the drying time of Zeomic from 80°C for 12 hours to 80°C for 24 hours to release all the absorbed moisture content.

Problem 7: The biodegradations of the PLA and PLA based composite specimens proceed very slowly during the test because the microbial populations were insufficient.

Solution 7: Fermented the tested soil with fresh leaves for two months to enrich and ensure the microbial population (Figure 3.11) in order to digest the PLA and PLA based composited during the test.

Figure 3.11 Fermented soil for biodegradation test

CHAPTER 4 RESULT AND DISCUSSION

4.1 Effect of wood flour and antibacterial agents loading on the mechanical, antibacterial and biodegradable properties of PLA and PLA based composites

4.1.1 Mechanical properties

4.1.1.1 Effect of wood flour loading

The mechanical properties of the poly(lactic acid) (PLA) filled with different concentrations of wood flour are given in Figures 4.1a-b in terms of Young's modulus, tensile strength, elongation at break and impact strength. The Young's modulus of neat PLA was 0.9 ± 0.04 GPa. As the wood content increased, the Young's modulus of the wood/PLA composites also increased to 0.91± 0.03 and 0.98 ± 0.025 GPa for 5 and 10% wood , respectively. The increase in the modulus was due to the fact that the wood had greater rigidities than the PLA. This effect was usually found with the thermoplastics that had lower rigidities than the wood [81-83]. However, the tensile strength, elongation at break, and impact strength decreased with the wood content. The decreases in these properties were caused by incompatibilities between the wood and PLA [69-71], the effect was more pronounced for higher wood contents.

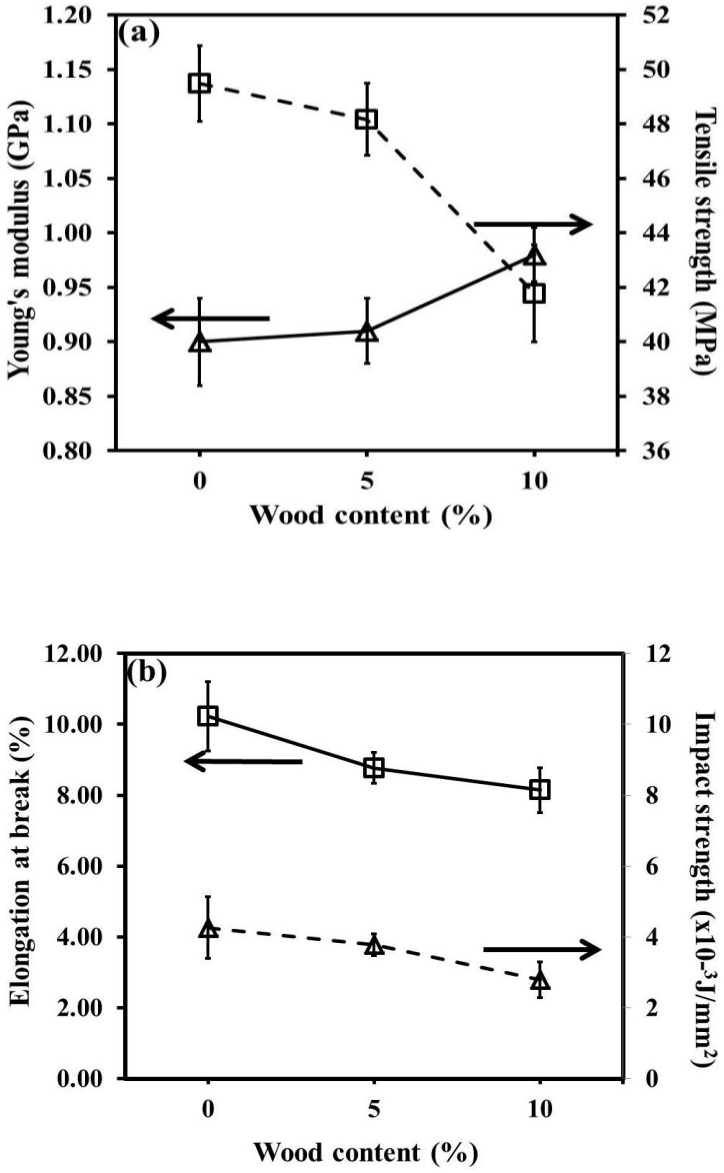

Figure 4.1 Mechanical properties of PLA and wood flour/PLA composites in terms of: (a) Young's modulus and tensile strength; (b) elongation at break and impact strength

4.1.1.2 Effect of antibacterial agents loading

Mechanical properties of PLA and wood/PLA composites (5% and 10% wood content) with different types and contents of antibacterial agents are given in Figures 4.2-4.5 It was observed that, compared with neat PLA, the Young's modulus tended to increase with the presence of wood and Zeomic (Figure 4.2). This was due to the greater rigidity of wood and zeolite particles (in Zeomic) in comparison with neat PLA. Low rigid thermoplastics were usually found to be increased in the Young's modulus when the higher rigidity particles were added [82-84].

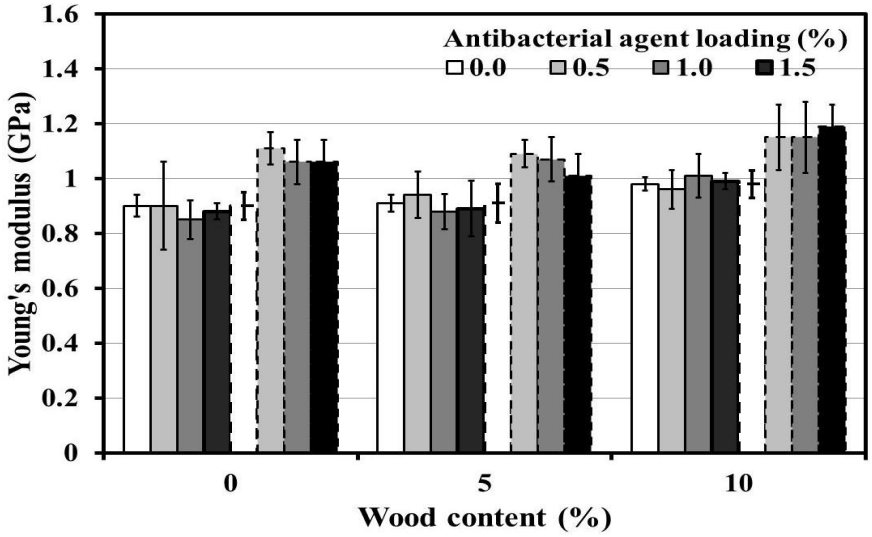

Figure 4.2 Young's modulus of PLA and wood/PLA composites with different wood contents, different types and amounts of antibacterial agents (solid and dashed lines are triclosan and Zeomic systems, respectively)

The tensile strength, elongation at break, and impact strength (Figures 4.3-4.5) of PLA decreased with increasing wood content. The reduction in these mechanical properties was due to the incompatibility of the wood and PLA [70, 71, 85, 86]. Similar to the effect of wood, the mechanical properties of the specimens declined with the addition of

Zeomic, especially in the case of PLA with 10% wood content. For example, the tensile strength of PLA, 5% wood/PLA (W_5P) and 10% wood/PLA ($W_{10}P$) decreased from 49.48, 48.16 and 41.77 MPa to 48.61, 43.8 and 11.01 MPa, respectively, when 1.5% Zeomic was loaded. This was likely caused by degradation of the PLA matrix as a result of a hydrolysis reaction between PLA and water molecules in the zeolite structure, and also because water molecules were absorbed by Si–OH bonding of zeolite and the hydroxyl groups in the wood. This was reported by Kaali et al. [87], who revealed that Ag^+-loaded zeolite could initiate a hydrolysis reaction for both polyester polyurethane and silicone rubber because the Si–OH bonding as a function of zeolite induced the adsorption of water molecules. The effect of triclosan on the mechanical properties of PLA and wood/PLA did not show a clear trend under the given experimental errors. In order to facilitate the understanding of the effect of triclosan, the mechanical property results were reported in range as given in Table 4.1, showing the ranges of mechanical property changes after adding triclosan at 0.5–1.5%wt. It was found that the changes in Young's modulus (ΔE), tensile strength (ΔTS), elongation at break (ΔB), and impact strength (ΔIS) of the PLA and wood/PLA composites ranged 0.02–0.06 GPa, 3.35–4.54 MPa, 1.25–2.44%, and 0.21–0.54 x 10^{-2} J/mm^2), respectively, for the addition of wood contents of 5–10%wt and triclosan loadings of 0.5–1.5%wt. This implies that the addition of triclosan did not involve in the hydrolysis reaction. Another possible reason is that the dosage of triclosan used was relatively small.

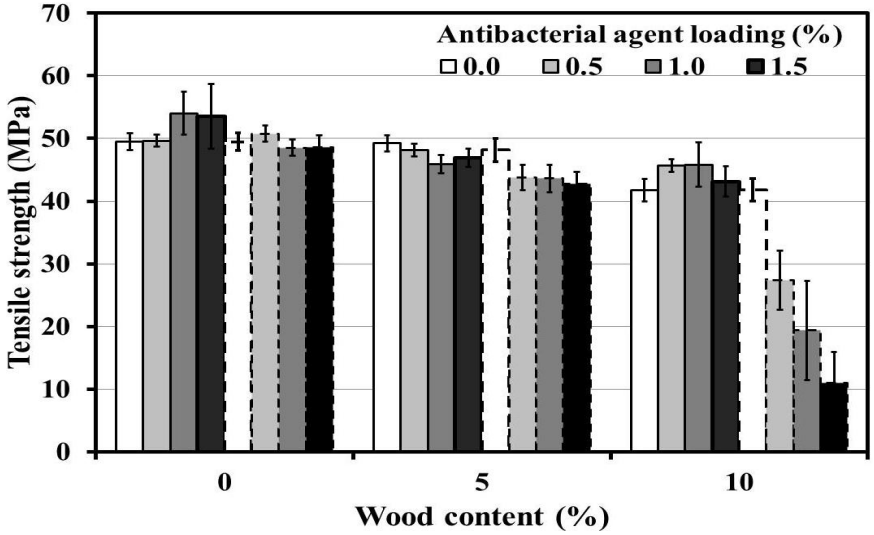

Figure 4.3 Tensile strength of PLA and wood/PLA composites with different wood contents, different types and amounts of antibacterial agents (solid and dashed lines are triclosan and Zeomic systems, respectively)

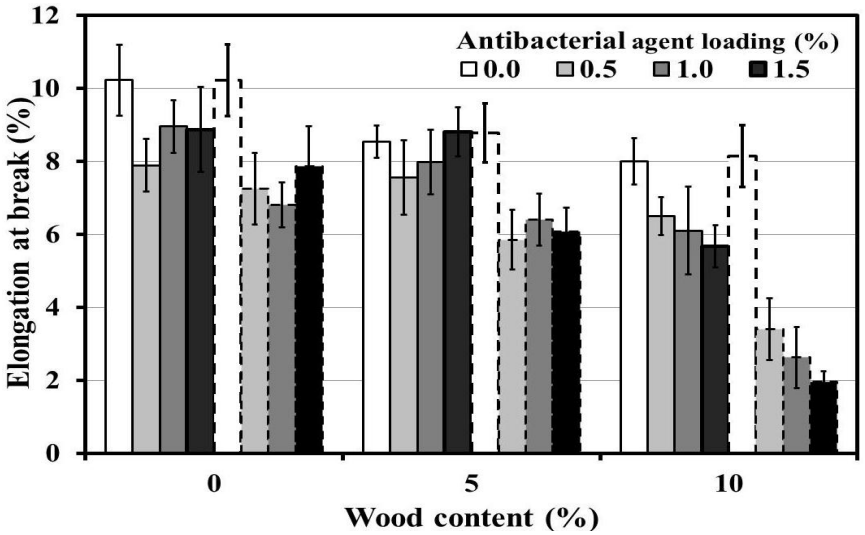

Figure 4.4 Elongation at break of PLA and wood/PLA composites with different wood contents, different types and amounts of antibacterial agents (solid and dashed lines are triclosan and Zeomic systems, respectively)

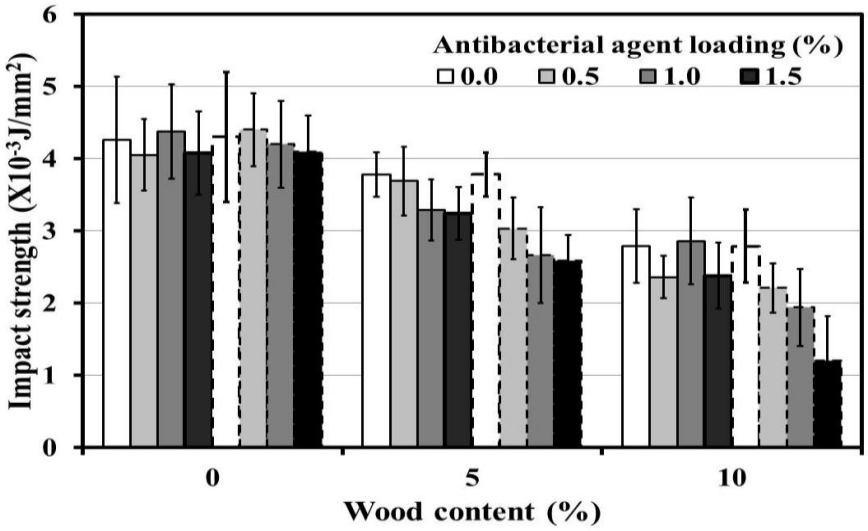

Figure 4.5 Impact strength of PLA and wood/PLA composites with different wood contents, different types and amounts of antibacterial agents (solid and dashed lines are triclosan and Zeomic systems, respectively)

Table 4.1 Effect of triclosan content on the changes in mechanical properties of PLA and wood/PLA composites

Materials	Young's modulus (E, GPa) for triclosan loadings of 0.5-1.5%wt		Tensile strength (ST, MPa) for triclosan loadings of 0.5-1.5%wt		Elongation at break (E, %) for triclosan loadings of 0.5-1.5%wt		Impact strength (IS, x10^{-3}J/mm^2) for triclosan loadings of 0.5-1.5%wt	
	Max-Min	**ΔE**	**Max-Min**	**ΔST**	**Max-Min**	**ΔB**	**Max-Min**	**ΔIS**
PLA	0.90 - 0.88	0.02	54.02 - 49.48	4.54	10.22 - 7.78	2.44	4.26 - 4.05	0.21
W_5PLA	0.94 - 0.88	0.06	49.23 - 45.88	3.35	8.81 - 7.56	1.25	3.78 - 3.24	0.54
W_{10}PLA	1.01 – 0.96	0.05	45.84 - 41.77	4.07	8.00 - 5.67	2.33	2.86- 2.36	0.5

4.1.2 Antibacterial properties

4.1.2.1 Qualitative antibacterial test

In this section, agar diffusion was used as a method to observation the diffusion efficiency of antibacterial agents against *E. coli* as the testing bacteria. Usually, the inhibition zone appears when the antibacterial agent is able to migrate out of polymer surface to kill or inhibit the bacteria. It was observed in Figure 4.6 that control samples (filter paper soaked with pure triclosan) appeared the largest clear zone suggesting that triclosan could migrate and kill *E.coli*.

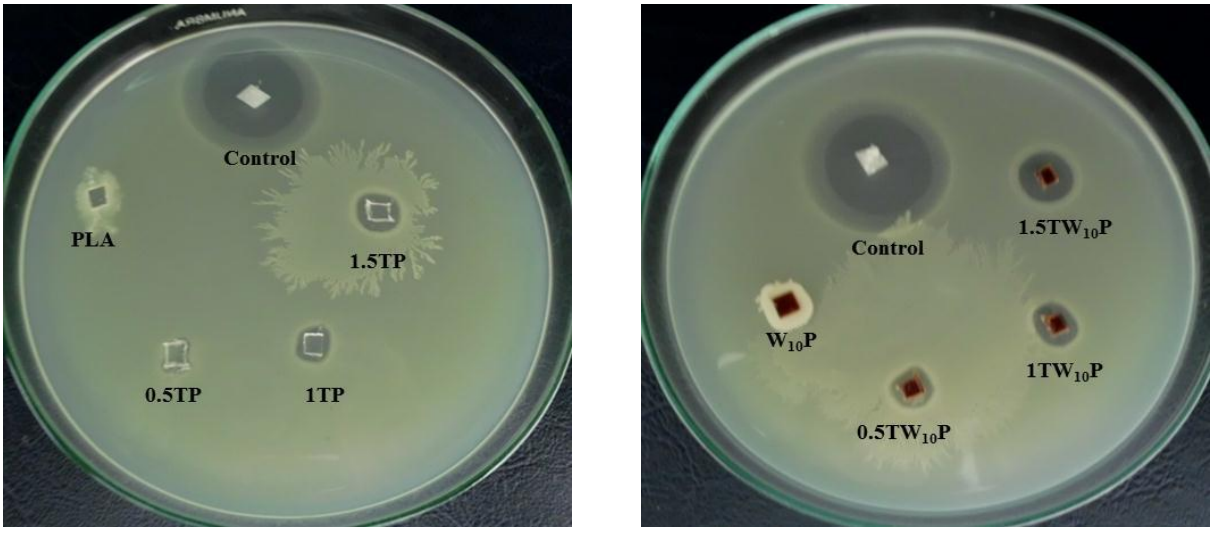

(a) **(b)**

Figure 4.6 Inhibition zone test against *E.coli* : (a) PLA; (b) 10% wood/PLA composites

The inhibition zone did not occur with neat PLA and $W_{10}P$ showing that the neat PLA and wood fiber did not have an effect on killing *E. coli*. But, when increasing the triclosan dosages, the clear zones were formed more apparently. In comparison between

PLA and wood/PLA composites, it was obviously found that the greater inhibition zone was seen with $W_{10}P$ with for all triclosan contents (0.5, 1 and 1.5%) suggesting that the wood facilitated the triclocan to migrate out of the PLA matrix to kill the *E.coli*. While the inhibition zone did not occur with the PLA and wood/PLA with Zeomic loading even when Zeomic was added at the maximum dosage of 1.5% (Figure is not shown).

4.1.2.2 Quantitative antibacterial test

Quantitative test was carried out using a Plate Count Agar (PCA) technique. All PLA specimens including PLA, 5% wood/PLA and 10% wood/PLA blended with triclosan and Zeomic were tested against *E.coli* and *S.aureus.*

- **Effect of antibacterial agents loading on antibacterial property against *S.aureus***

The antibacterial performances against *S. aureus* of PLA and wood/PLA composites incorporated with triclosan or Zeomic at different concentrations and for varying contact times are given in Figures 4.7 and 4.8, respectively. For triclosan systems, the viable cell counts of triclosan-loaded PLA and wood/PLA (Figures 4.7a–c) for all contact times were lower than those of specimens without triclosan. Nevertheless, *S. aureus* bacteria still grew at a slower rate when the contact time was increased. This suggested that triclosan could kill or inhibit *S. aureus* bacterial growth for PLA and wood/PLA composites. For Zeomic systems, an increase in contact time and/or Zeomic content did not affect the reduction of *S. aureus* colony-forming units (Figures 4.8a–c). With longer contact time, more colony-forming units occurred, even when Zeomic was added at the maximum dosage of 1.5%. This suggested that Zeomic did not have ability

to retard bacterial growth. In order to further illustrate antibacterial effectiveness, the percentage of bacterial reduction was calculated.

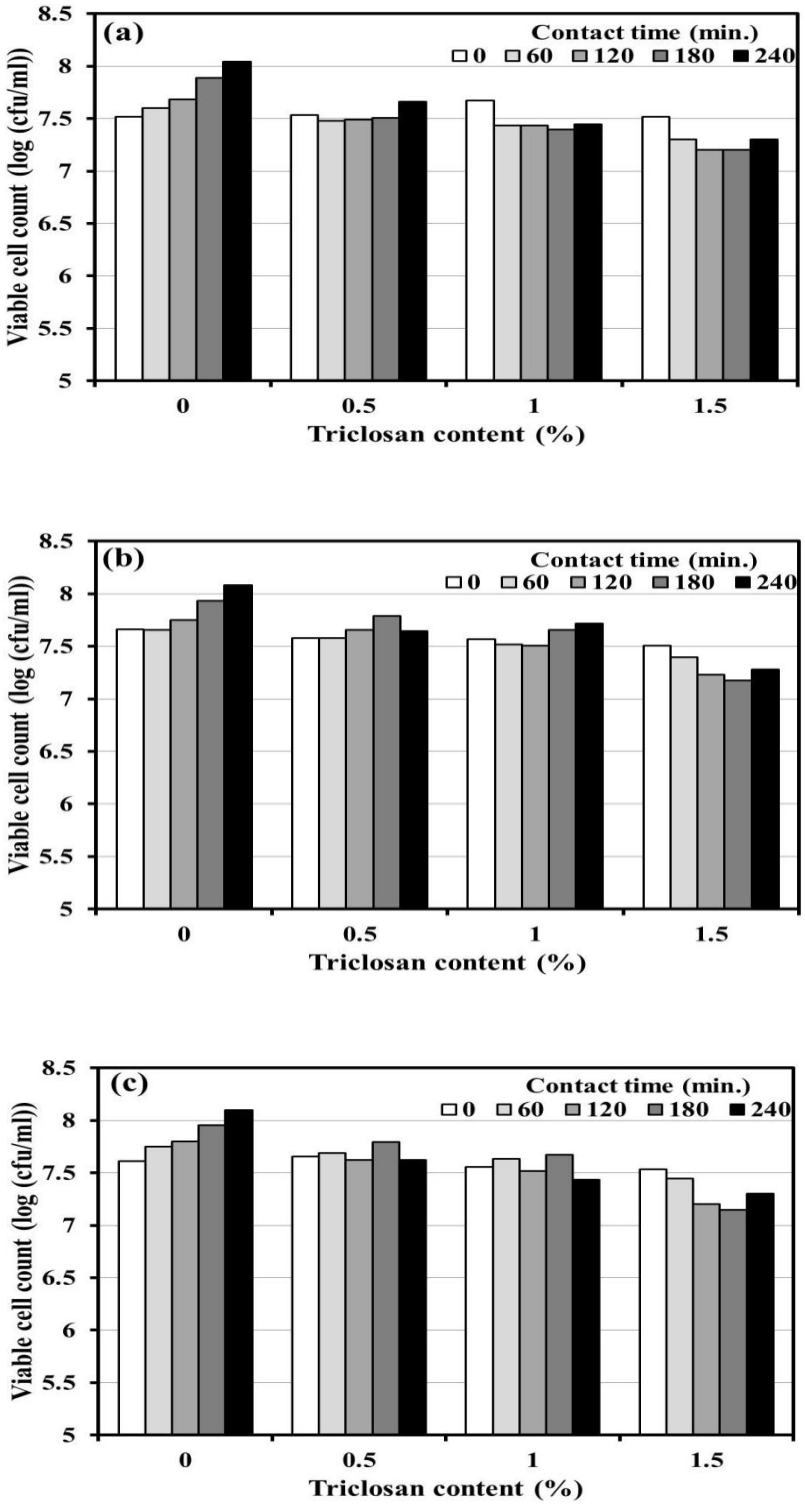

Figure 4.7 Viable cell count of *S. aureus* with triclosan loadings of 0.5–1.5 %wt for different contact times: (a) PLA; (b) W_5P composites; (c) $W_{10}P$ composites

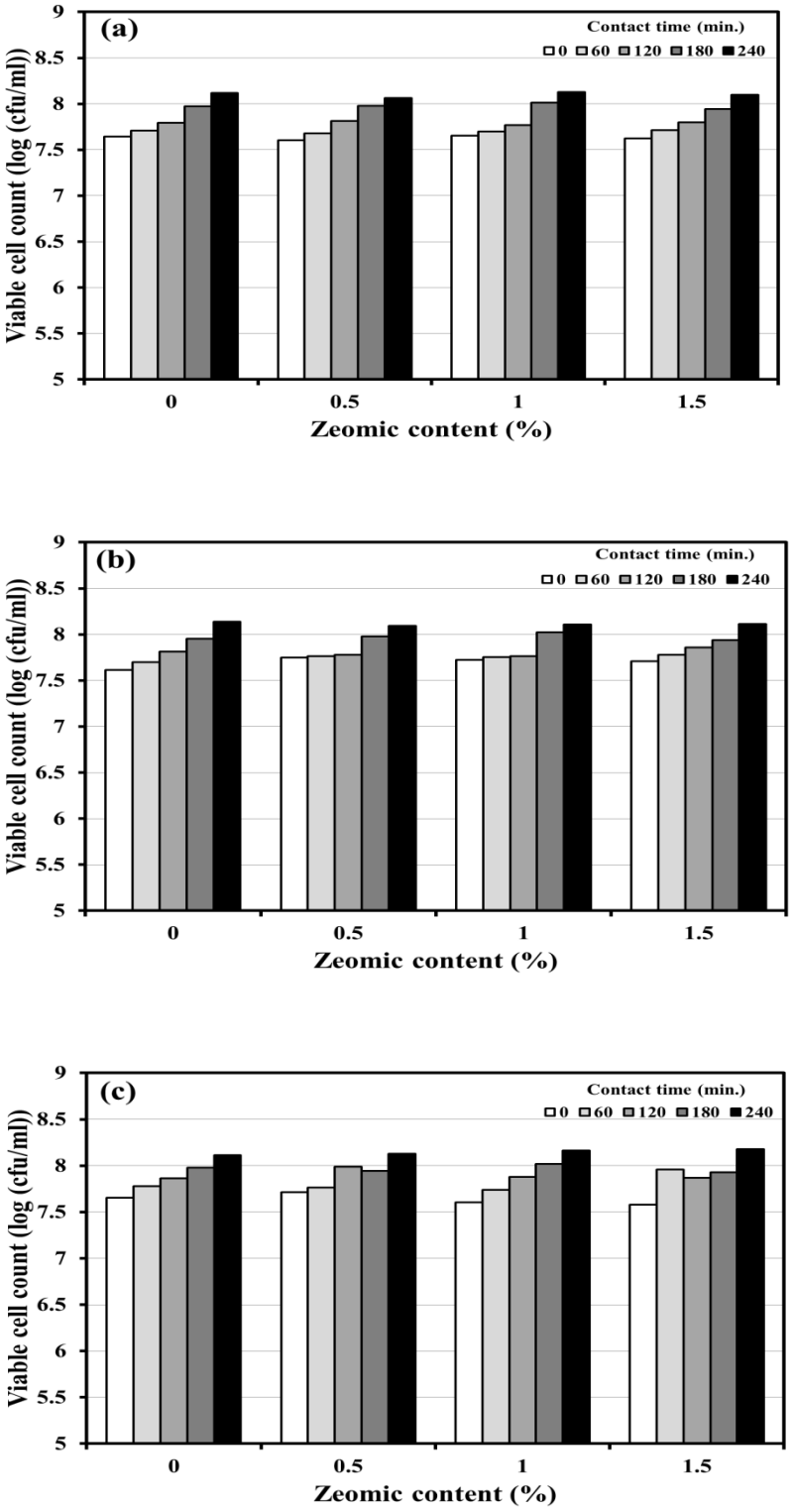

Figure 4.8 Viable cell count of *S. aureus* with Zeomic loadings of 0.5–1.5 %wt for different contact times: (a) PLA; (b) W_5P composites; (c) $W_{10}P$ composites

Table 4.2 shows the percentage of bacterial reduction of *S. aureus* for PLA and wood/PLA composites containing triclosan or Zeomic loadings of 0.5–1.5 wt% at different contact times. With one exception ($0.5TW_{10}P$ at 180 min), the higher the triclosan concentration and/or the longer the contact time, the greater the percentage of bacterial reduction. For example, at 60 min contact time, the antibacterial performance of PLA containing 0.5% triclosan was enhanced from 25.00% to 50.00% when the triclosan content was raised to 1.5%; the percentage reduction also increased up to 58.18% when the contact time was extended to 240 min. The optimum antibacterial performance of PLA, W_5P and $W_{10}P$ (81.82, 84.17 and 84.80%, respectively) occurred with 1.5% triclosan loading and 240 min contact time. On the other hand, Zeomic did not show any antibacterial property. Higher Zeomic dosages and longer contact times did not affect the antibacterial activity of the composites.

Table 4.2 Percentage of *S.aureus* bacterial reductions at different contact times for PLA and wood/PLA composites with triclosan and Zeomic loadings of 0.5 - 1.5%wt

Specimens	Contact time (min.)	Percentage bacterial reduction (%)					
		0.5%		1.0%		1.5%	
		triclosan	Zeomic	tricolsan	Zeomic	tricolsan	Zeomic
PLA	60	25.00	5.88	32.50	1.96	50.00	0.00
	120	35.42	0.00	43.75	4.84	66.67	0.00
	180	58.44	0.00	67.53	0.00	79.00	6.39
	240	58.18	12.12	74.55	0.00	81.82	5.30
W_5P	60	15.56	0.00	26.67	0.00	44.44	0.00
	120	19.64	7.69	42.86	10.80	69.65	0.00
	180	28.23	0.00	47.06	0.00	82.35	3.33
	240	63.33	9.50	56.67	5.84	84.17	5.11
$W_{10}P$	60	12.50	3.33	23.21	8.33	50.00	0.00
	120	33.33	0.00	47.61	0.00	74.60	0.00
	180	24.39	7.37	47.78	0.00	84.44	10.53
	240	66.40	0.00	78.40	0.00	84.80	0.00

- **Effect of antibacterial agents loading on antibacterial property against *E.coli***

The quantitative results for antibacterial performances of PLA and wood/PLA composites incorporated with triclosan and Zeomic are given in Figures 4.9 and 4.10, which shows a viable colony count for *E. coli* under different antibacterial agents concentrations and contact times. It was observed that for neat PLA (Figure 4.9a), as the triclosan content increased the viable cell count decreased for all contact times, suggesting that triclosan had the ability to retard bacterial growth. However, when the contact time was increased the bacteria continued to grow, but at a slower rate in the case of PLA with the presence of triclosan. For wood/PLA composites (Figures 4.9b and 4.9c), increasing the triclosan content reduced the viable cell count. This effect was more pronounced when compared with the neat PLA, as mentioned earlier. The effect of contact time on the changes in viable cell count for wood/PLA composites did not exhibit the same trend as observed for the neat PLA; with increased contact time, the viable cell count for wood/PLA composites tended to decrease. This phenomenon was clearly seen for high triclosan loadings of 1.0–1.5%wt. For Zeomic system (Figure 4.10 a-c), the antibacterial performances of PLA and wood/PLA composites against *E.coli* were found to be similar to those of the specimens against *S.aureus.* The *E.coli* kept growing when the contact time increased for every dosage of Zeomic added, suggesting that the Zeomic did not achieve on killing *E.coli* under the tested condition. The antibacterial performance could also be viewed in terms of percent bacteria reduction. Table 4.3 shows bacterial reduction percentages of *E.coli* for PLA and wood/PLA composites with different antibacterial agent contents and contact times.

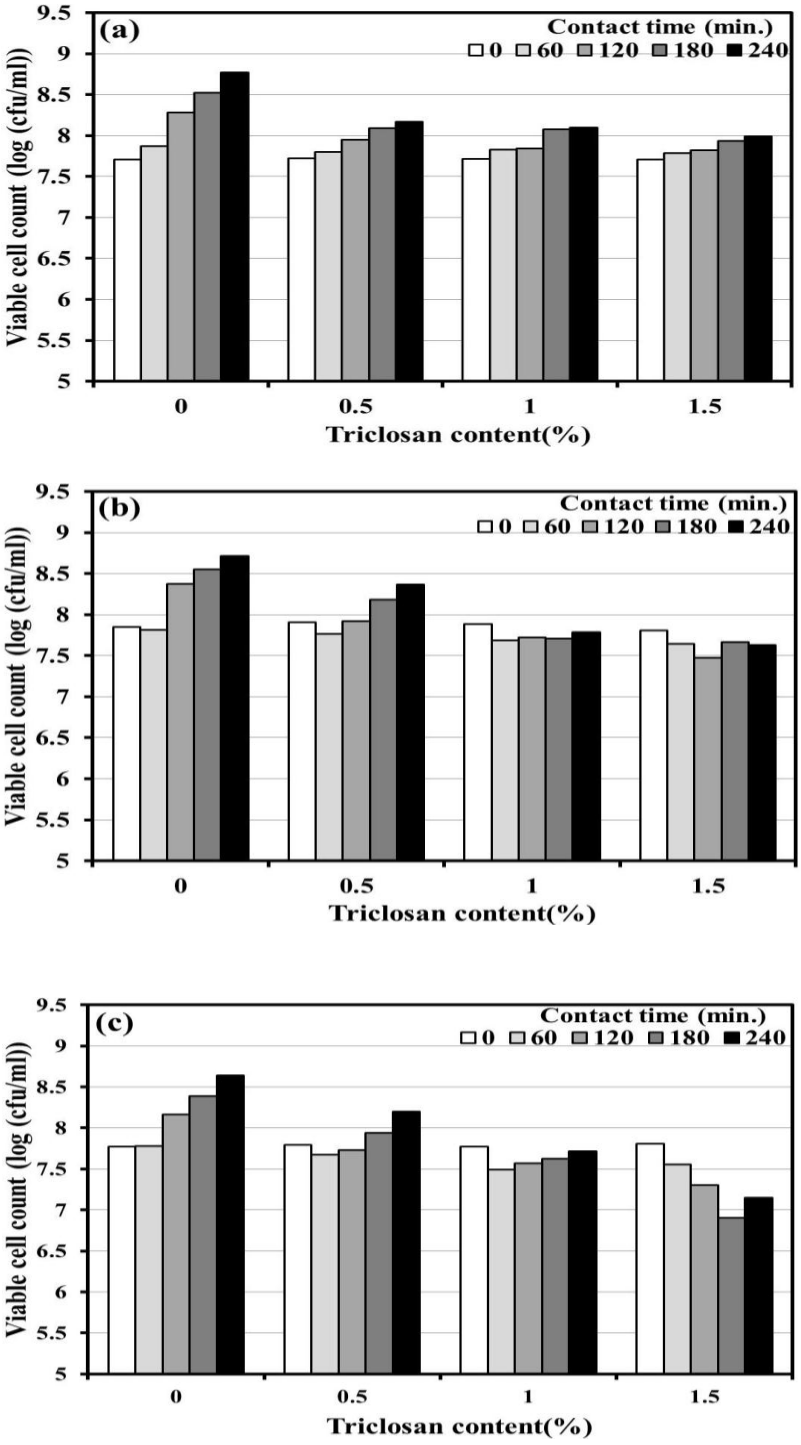

Figure 4.9 Viable cell count of *E.coli* with triclosan loadings of 0.5–1.5 %wt for different contact times: (a) PLA; (b) W_5P composites; (c) $W_{10}P$ composites

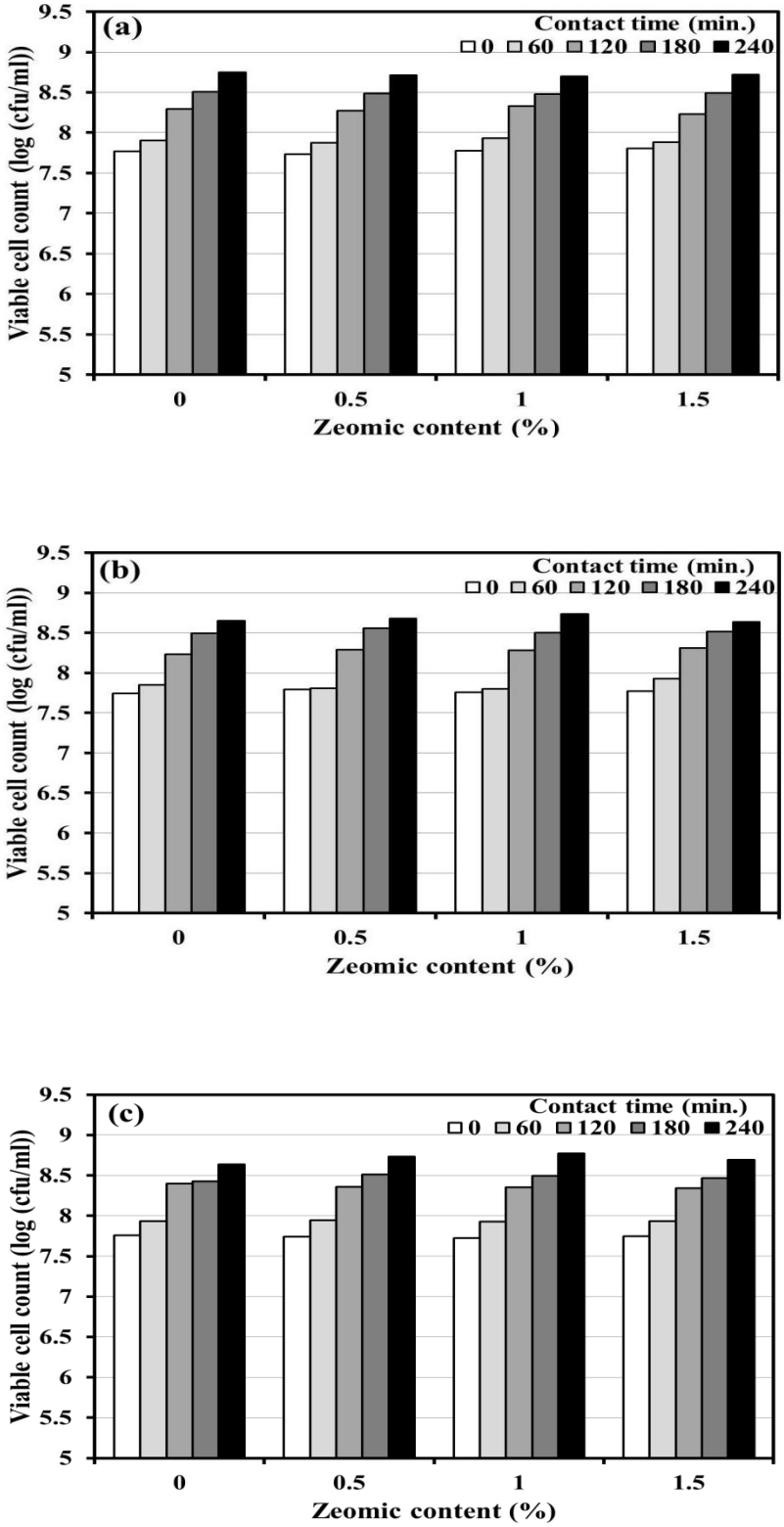

Figure 4.10 Viable cell count of *E.coli* with Zeomic loadings of 0.5–1.5 %wt for different contact times: (a) PLA; (b) W_5P composites; (c) $W_{10}P$ composites

Similar to the results in Figures 4.9 and 4.10, percent bacterial reduction did not increase with Zeomic content or contact time. However, the higher the triclosan concentration and contact time, the greater the percent of bacterial reduction. Evidently the wood particles acted as an antibacterial promoter for triclosan-based wood/PLA composites.

Table 4.3 Percentage of *E.coli* bacterial reductions at different contact times for PLA and wood/PLA composites with Triclosan and Zeomic loadings of 0.5 - 1.5%wt

Specimens	Contact time (min.)	Percentage bacterial reduction (%)					
		0.5%		1.0%		1.5%	
		triclosan	Zeomic	tricolsan	Zeomic	tricolsan	Zeomic
PLA	60	14.86	6.25	9.46	0.00	17.57	5.00
	120	53.16	4.55	63.16	0.00	65.26	14.14
	180	62.95	4.38	63.86	5.63	74.11	2.81
	240	74.92	6.98	78.81	10.38	83.40	6.80
W_5P	60	10.77	9.86	24.62	11.27	32.31	0.00
	120	49.58	0.00	77.73	0.00	87.39	0.00
	180	45.74	0.00	81.91	0.00	83.69	0.00
	240	54.95	0.00	88.16	0.00	91.65	4.44
$W_{10}P$	60	21.67	0.00	48.33	1.16	40.00	0.00
	120	63.27	8.73	74.83	10.71	86.39	13.09
	180	64.20	0.00	82.72	0.00	96.71	0.00
	240	63.68	0.00	88.05	0.00	96.78	0.00

4.1.2.3 Assumption proofs

There are two different assumptions to answer the question why the PLA and wood/PLA filled with Zeomic and triclosan showed the different results of antibacterial performances. For Zeomic system: the Zeomic created crystalline regions in PLA that could interrupt the generation of silver ions which affected the killing efficiency of silver ions. For triclosan system, the highly hydrophilic wood particles [88, 89], would interrupt the interaction between the triclosan and PLA and also absorbed water molecules which facilitated the triclosan to migrate onto the PLA surface to kill the bacteria. To prove these two assumptions, differential scanning calorimetry (DSC) water contact angle and Fourier transform infrared spectroscopy (FTIR) had been performed.

- **Assumption proofs for Zeomic system**

Because the assumption for Zeomic system is that the Zeomic could create the crystalline region which disturbed the killing efficiency of silver ion against testing bacteria, thus silver ion releasing mechanism has to be considered. Figure 4.11 shows silver ion releasing mechanism of Zeomic. To kill the bacteria, the immobilized silver particles in the zeolite carrier exchange their ions with the positive ions, such as sodium ions from moisture or environment then release silver ions to kill the bacteria [90]. If the Zeomic could improve crystallinity level of the PLA, the ions exchange process would be interrupted which affected the bacterial killing efficiency of the Zeomic.

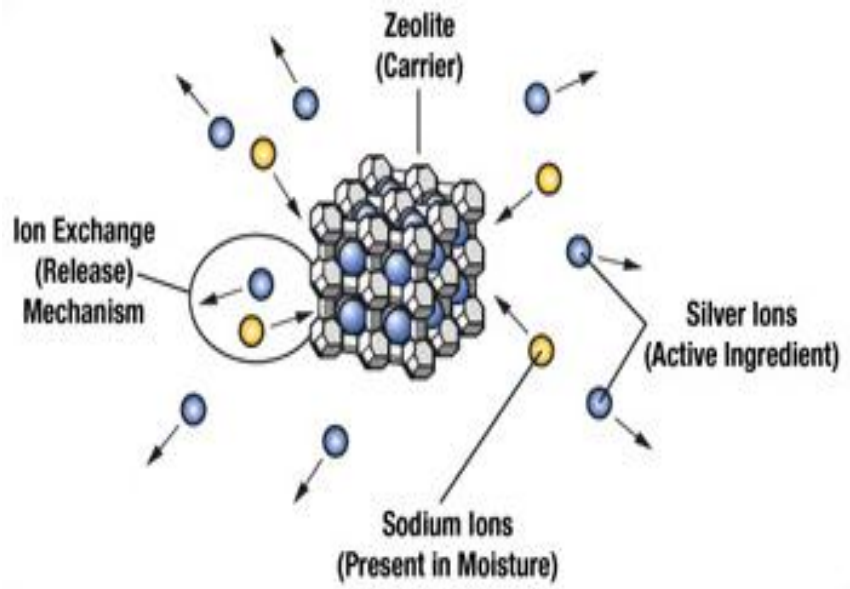

Figure 4.11 Silver ions releasing mechanism of Zeomic [91]

The DSC patterns for PLA, W_5P and $W_{10}P$ with and without triclosan or Zeomic loadings are given in Figure 4.12, showing the glass transition (T_g) and melting (T_m) temperatures and the degree of crystallinity (X_c). The T_g of neat PLA was 63 ^oC, whereas the T_g values of all other PLA composites were lower. The reduction in the T_g value is thought to be connected with the hydrolysis reaction initiated by additives used (especially in the case of wood/PLA systems), which causes the PLA to have a lower molecular weight. A reduction in the T_g of the PLA matrix with the presence of fibers was also observed by Mohamed et al. [72]. With the incorporation of wood and Zeomic, the T_m value for neat PLA was around 153 °C whereas the T_m values for the wood/PLA composite displayed a double melting peaks, the first melting peak being at around 140–152 °C and the second melting peak exhibiting at around 151–159 °C. It is possible that wood and Zeomic may perform as rigid foreign particles that create crystalline regions, whereas the second one could be associated with imperfect PLA crystals occurring as a result of the addition of wood and Zeomic. The double-melting-

peak behavior of PLA composites was also found by Shi et al. [73]. These double melting peaks indicate that Zeomic was responsible for raising PLA crystallinity levels from 7.9% for the neat PLA to 31.9%, 34.4% and 36.3% when 1.5 wt% Zeomic was loaded into PLA (1.5ZP), 5% wood/PLA ($1.5ZW_5P$) and 10% wood/PLA ($1.5ZW_{10}P$), respectively. The increases in crystallinity level due to the presence of wood particles were also suggested in the case of wood/PP composites, as a result of transcrystalline structures formed on the wood surfaces [92]. The DSC results are consistent with the assumption; Zeomic increased the crystallinity level of the PLA.

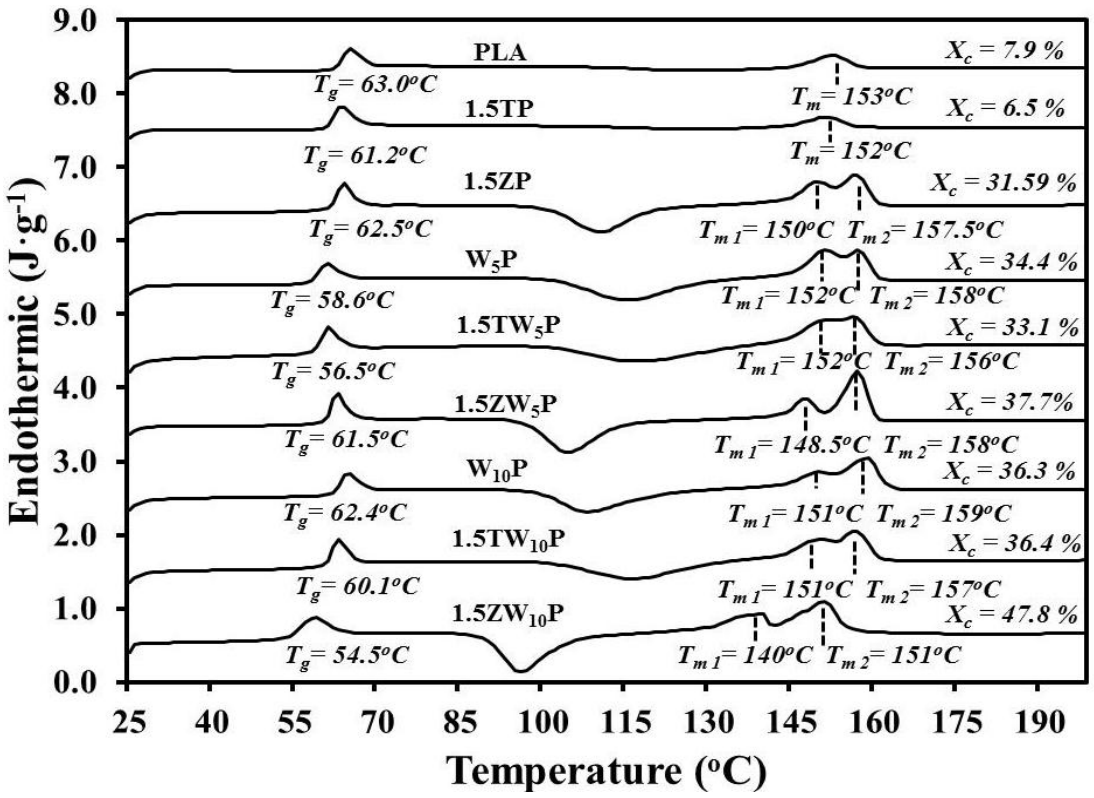

Figure 4.12 DSC thermograms of PLA, W_5P and $W_{10}P$ composites with and without the addition of 1.5 wt% triclosan or Zeomic

Fast and slow cooling are well known techniques used to control crystallinity level of semi-crystalline polymers; fast and rapid cooling (quenching) usually reduces relaxation time of semicrystalline polymer which increases amorphous region of the polymers. To prove the effect of crystalline structure against the antibacterial performance of PLA and wood/PLA composites incorporated with Zeomic, the quenching process was set up. After heating process of a hot press; Zeomic/PLA sheet was immediately immersed in cold water and left until the temperature was reduced to room temperature.

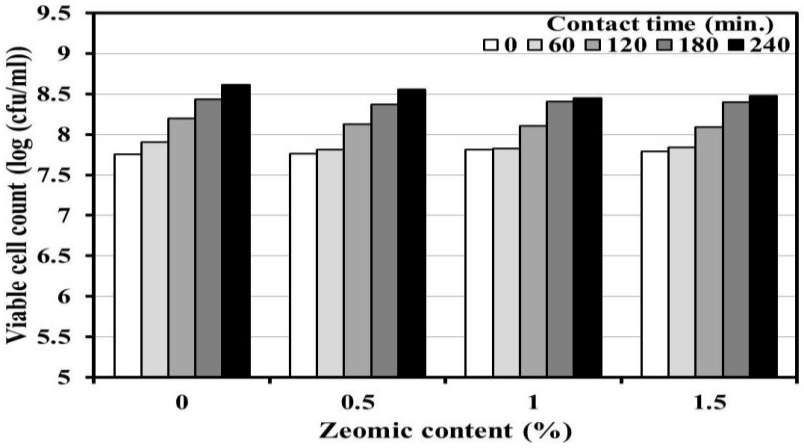

Figure 4.13 Viable cell count of *E.coli* for PLA sample with Zeomic loadings of 0.5–1.5 %wt at different contact times prepared by the quenching process

Table 4.4 Percentage of *E.coli* bacterial reductions at different contact times for PLA with Zeomic loadings of 0.5 - 1.5 %wt prepared by the quenching process

specimen	Contact time (min.)	Percentage bacterial reduction (%)		
		0.5%Zeomic	1.0% Zeomic	1.5% Zeomic
PLA	60	18.75	16.25	13.75
	120	14.56	19.62	22.15
	180	12.59	5.19	7.41
	240	12.20	31.71	26.83

Figuer 4.13 and Table 4.4 present the viable cell count and percentage of *E.coli* bacteria reductions with Zeomic loadings of 0.5–1.5%wt prepared by the quenching process. Similar to the previous result, the more contact time, the more *E.coli* colony forming units occurred. However, greater percentage bacteria were observed in comparison with non-quenching specimens. None of zero percentage bacterial reduction was found for all contact time, suggesting Zeomic had slightly better ability to inhibit *E.coli* population. Fernandez *et al* [64] also discovered that the degree of crystallinity of PLA was the cause of the drop in antibacterial performance of Zeomic/PLA composites. Thus, it can be considered that the crystallinty of the PLA has an effect on the killing efficiency of the Zeomic.

- **Assumption proofs for triclosan system**

It is essential to prove the proposed mechanism for explanation of the role of wood flour as an antibacterial promoter in a triclosan system, as discussed earlier, through independent physical and structural characterizations. If triclosan migration on the PLA surface by the assistance of wood flour had occurred, one would expect to observe chemical and physical changes on the wood/PLA composite surfaces. In this respect, water contact angle (WCA) measurement and Fourier transform infrared spectroscopy were performed. Table 4.5 shows the contact angle values for PLA and PLA with triclosan, Zeomic or wood additive. The addition of Zeomic for the neat PLA and wood/PLA composites changed water contact angle value from 58.6° to 60.55°, 69.3° to 70.37° and 70.8° to 70.51° for PLA, W_5P and $W_{10}P$ respectively. The increase in water contact angle suggesting that the PLA and wood/PLA composites became more hydrophobicity when Zeomic was added. For triclosan system, the addition of triclosan or 10%wood on PLA had significant effects on its hydrophilicity: the contact angles of

PLA appeared to increase from 58.6^{o} to 68.8^{o} and from 58.6^{o} to 70.8^{o}, respectively. This indicates that the PLA became less hydrophilic due to the presence of triclosan. The changes in the hydrophilicity of PLA by the addition of triclosan are related to molecular interactions between the two substances, as illustrated in Figure 4.14. Intermolecular hydrogen bonds are presumed to exist between PLA and triclosan. If these interactions occur, the initial hydrophilicity of PLA would be expected to decrease. A similar phenomenon probably applies for the composite of PLA and wood. However, when 1.5% triclosan was added into the wood/PLA composites (5 and 10% wood contents), the contact angle value for the wood/PLA was found to decrease from 70.8^{o} to 64.8^{o}. This can be explained using a proposed interactive model, as given in Figure 4.15.

Table 4.5 Water contact angle of PLA and wood/PLA incorporated with triclosan and Zeomic loadings of 0 and 1.5 %wt

Materials	Contact angle values	photos
PLA	59	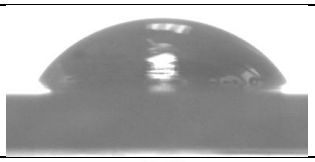
1.5TP	69	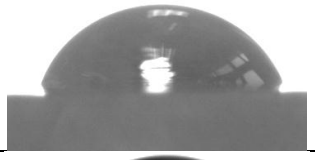
1.5ZP	61	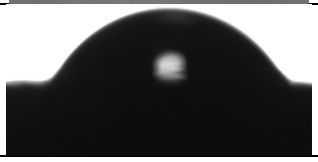
W_5P	69	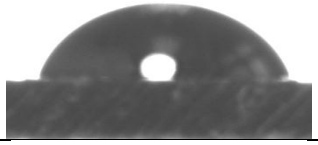
$1.5TW_5P$	62	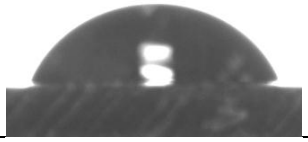
$1.5ZW_5P$	70	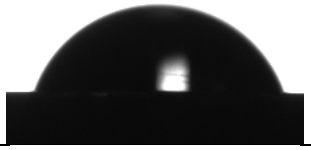
$W_{10}P$	71	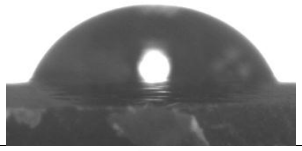
$1.5TW_{10}P$	65	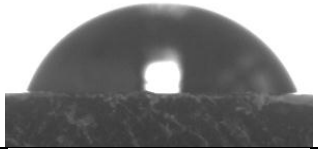
$1.5ZW_{10}P$	71	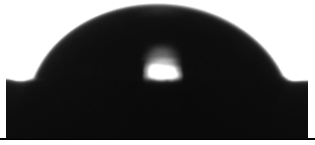

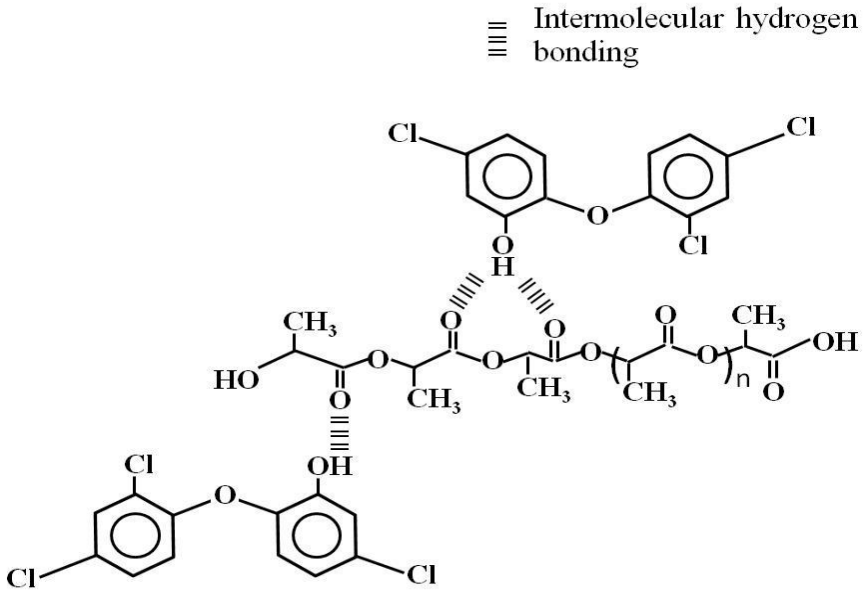

Figure 4.14 Intermolecular hydrogen bonds of PLA with triclosan

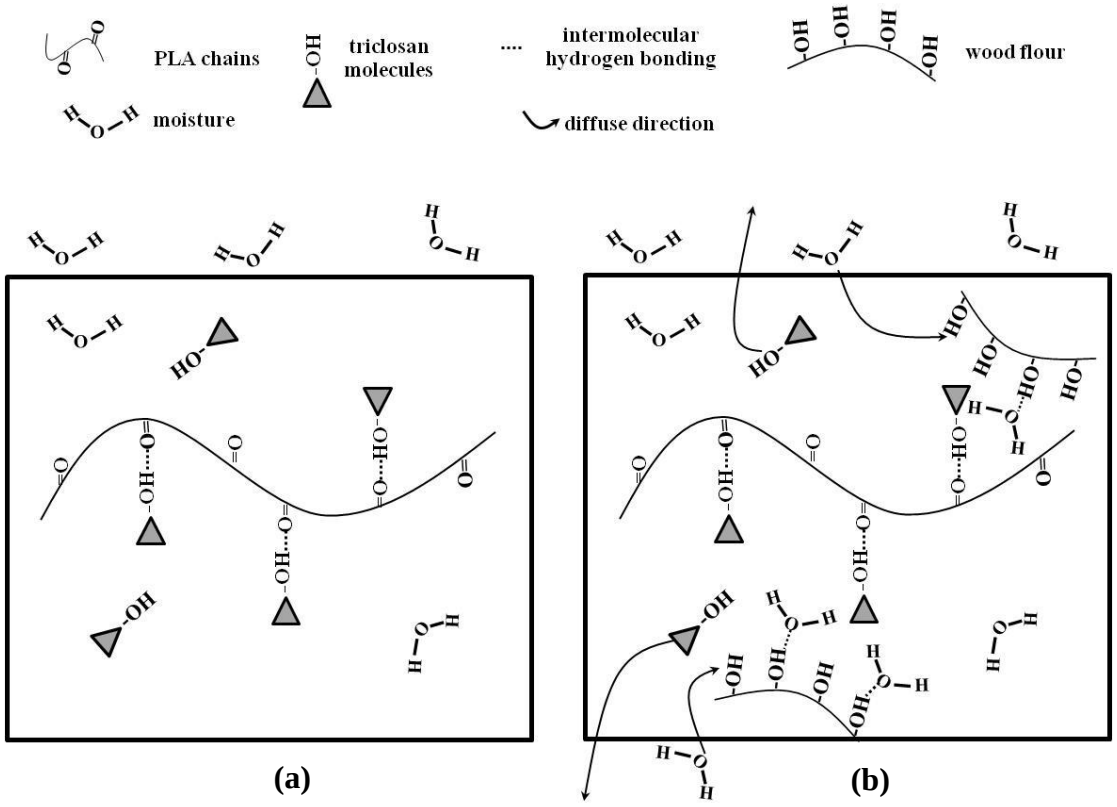

Figure 4.15 A possible model of moisture regain by the presence of wood in triclosan/PLA blends: (a) without wood; (b) with wood.

It is thought that triclosan is likely to have a preference with PLA via hydrogen bonding. The wood particles in the triclosan/PLA system would interrupt the bonding and enable the wood/PLA composites to absorb more water molecules onto the triclosan/wood/PLA surfaces; this absorbed moisture would allow triclosan migration onto the PLA specimen surfaces due to a diffusion process, and eventually resulted in the decreases in contact angle value. The diffusibility of triclosan to kill bacteria has been found by Silapasorn et al. [2] and Chung et al. [56], who suggested that the efficiency of triclosan for killing bacteria incorporated in vinyl thermoplastics was dependent on its diffusion ability in the media. The results shown in Figures 4.14 and 4.15 can be used to support the viable cell count results for triclosan/wood/PLA composites as compared with triclosan/PLA. Table 4.5 shows the effect of triclosan content on hydrophilicity (water contact angle) for PLA and wood/PLA composites. It can be seen that although the presence of triclosan decreased the hydrophilicity of the PLA and wood/PLA composites, its varying content had very little effect on the change in hydrophilicity. This may be because the increased triclosan content was probably distributed and/or dispersed within the bulk PLA and wood/PLA composites, rather than on the sample surfaces where the contact angles were being measured. The interactions among PLA, triclosan and wood, as seen in the contact angle results, can be substantiated by the FTIR analysis results in Figure 4.16a**,** showing FTIR spectra for PLA, triclosan, and PLA with 1.5%wt triclosan. It can be seen that the FTIR spectrum for triclosan/PLA was very similar to that for the neat PLA. This was to be expected, since the triclosan content added was very small compared to the bulk PLA. However, a slight change could be observed in the carbonyl functional (C=O) peak of PLA at a wavenumber of 1753 cm^{-1}. The carbonyl peak became broadened and split into two small peaks (at wavenumbers of 1753 and 1746 cm^{-1}).

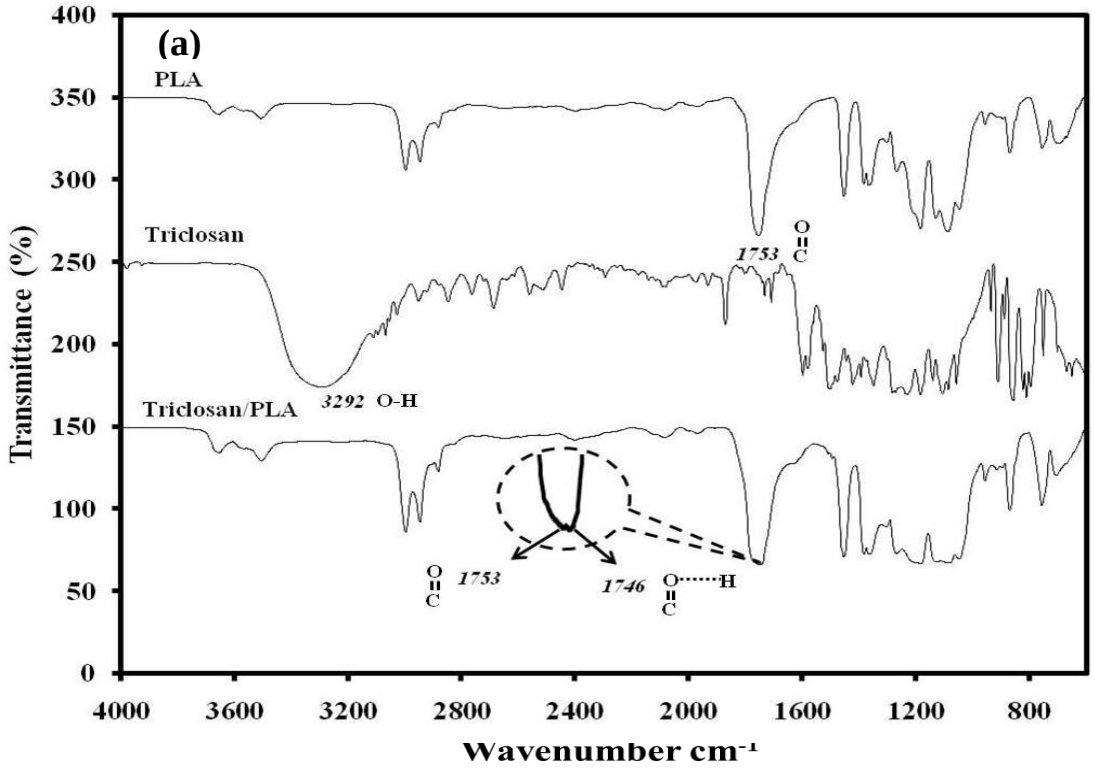
(a)
PLA
Triclosan
Triclosan/PLA
1753
3292 O-H
1746
Transmittance (%)
Wavenumber cm⁻¹

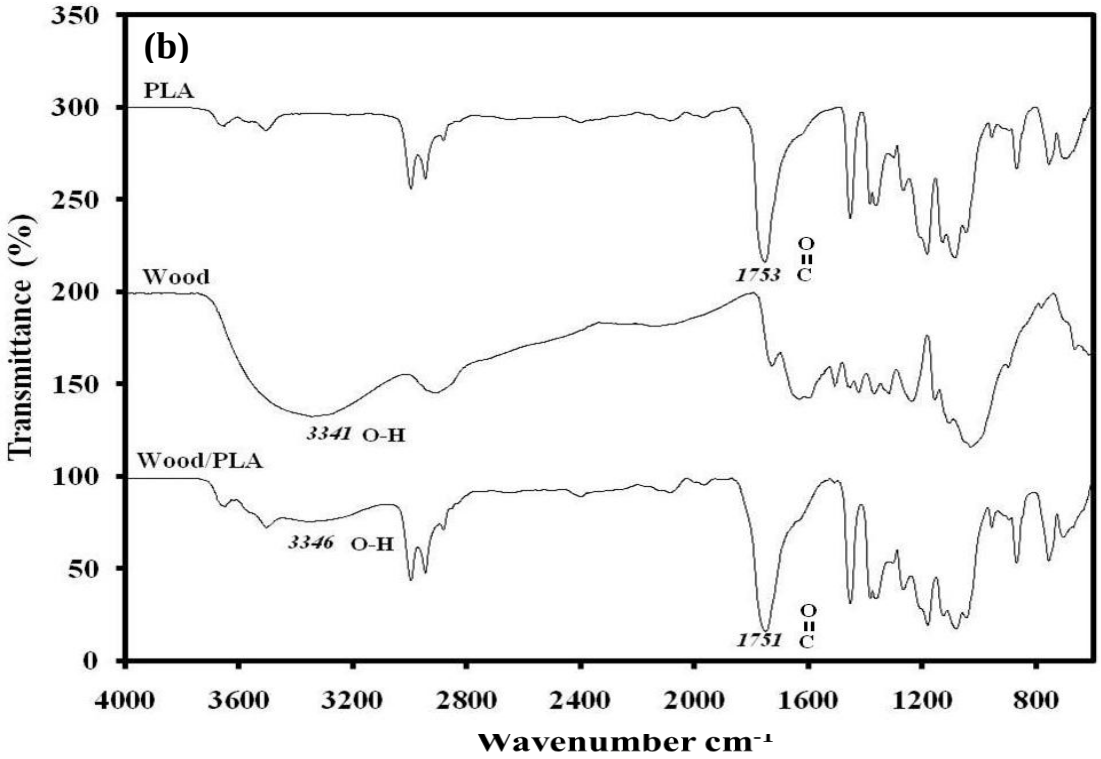
(b)
PLA
Wood
Wood/PLA
1753
3341 O-H
3346 O-H
1751
Transmittance (%)
Wavenumber cm⁻¹

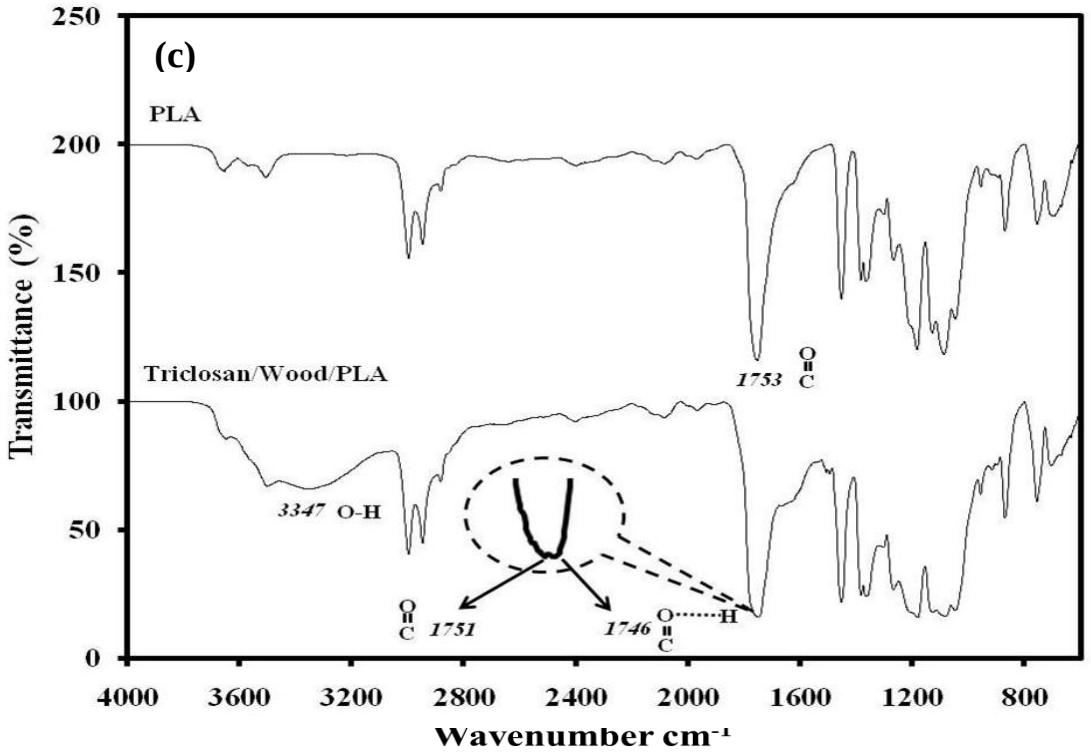

Figure 4.16 FTIR spectra for PLA and wood/PLA composites filled with triclosan: (a) PLA, triclosan, and triclosan/PLA; (b) PLA, wood, and wood/PLA composites; (c) PLA and triclosan/wood/PLA composites

These changes in the FTIR spectra indicated the intermolecular interaction between PLA and triclosan (Figure 4.15). Figure 4.16b shows FTIR spectra for PLA, wood, and PLA with 10%wt wood content. It can be seen that the FTIR spectrum for wood/PLA was similar to that for neat PLA, with the presence of a hydroxyl group (-OH) at a wavenumber of 3341 cm^{-1}. Unlike triclosan in PLA, the additional hydroxyl peak occurred due to the reasonable amount of wood flour added to the PLA. Finally, it was interesting to note that the FTIR spectrum for the triclosan/wood/PLA sample in Figure 4.16c exhibited a mixture of the triclosan/PLA and wood/PLA spectra. This represents the broadening and splitting of the carbonyl peak at wavenumbers of 1753 and 1746 cm^{-1} from the triclosan/PLA interaction, and the hydroxyl peak at a wavenumber of

3341 cm^{-1} from the wood part. It appears that the contact angle results in Table 4.5, the molecular interactions in Figure 4.14, and the FTIR results in Figure 4.16 correspond well to the antibacterial activity results in Figures 4.7 and 4.9, in accordance with the proposed concept of the role of wood flour as an antibacterial promoter. More evidence highlighting the role of wood flour as an antibacterial promoter was the data from DSC analysis. It was essential to relate the thermal behavior with the antibacterial performance of PLA by the addition of triclosan and wood. Park et al. [57] documented that thermoplastics with a higher degree of crystallinity would have lower antibacterial activities due to the difficulty of the antibacterial agent in penetrating through the crystalline phase as compared with the amorphous structure. However, this characteristic was not the case in wood/PLA composites. The increases in the degree of crystallinity due to the addition of wood obtained in this work did not increase the rigidities of the triclosan/PLA to that extent. This was clear evidence that the increase in the tensile modulus with increasing wood flour content was relatively small (see Figure 4.1). In other words, the increasing effect on the rigidity of triclosan/PLA is probably suppressed by the increasing hydrophilic effect when wood flour is added to the triclosan/PLA blend (Table 4.5 and Figure 4.15). This was why the antibacterial performance still improved, although the crystallinity and rigidity of the triclosan/PLA had slightly increased with the added wood flour. It can therefore be concluded that the hydrophilic effect played a more important role than the physical and thermal properties in the antibacterial activity of triclosan in the PLA and wood/PLA composites.

4.1.3 Biodegradable property

In this part, biodegradation test of PLA and wood/PLA composites filled with triclosan and Zeomic were performed. Figure 4.17 shows the total CO_2 evolution of all tested specimens including blank. Blank was reactor bottle filled with 400 g of compost without PLA samples added. It can be seen that CO_2 evolved for all samples when the incubation time was increased. The graphs of all materials tested and the blank increased and were in a similar trend. CO_2 was generated as a result of metabolic process [32] throughout 60 days of the test, suggesting that microbial could consume the compost or PLA and PLA composites as carbon sources.

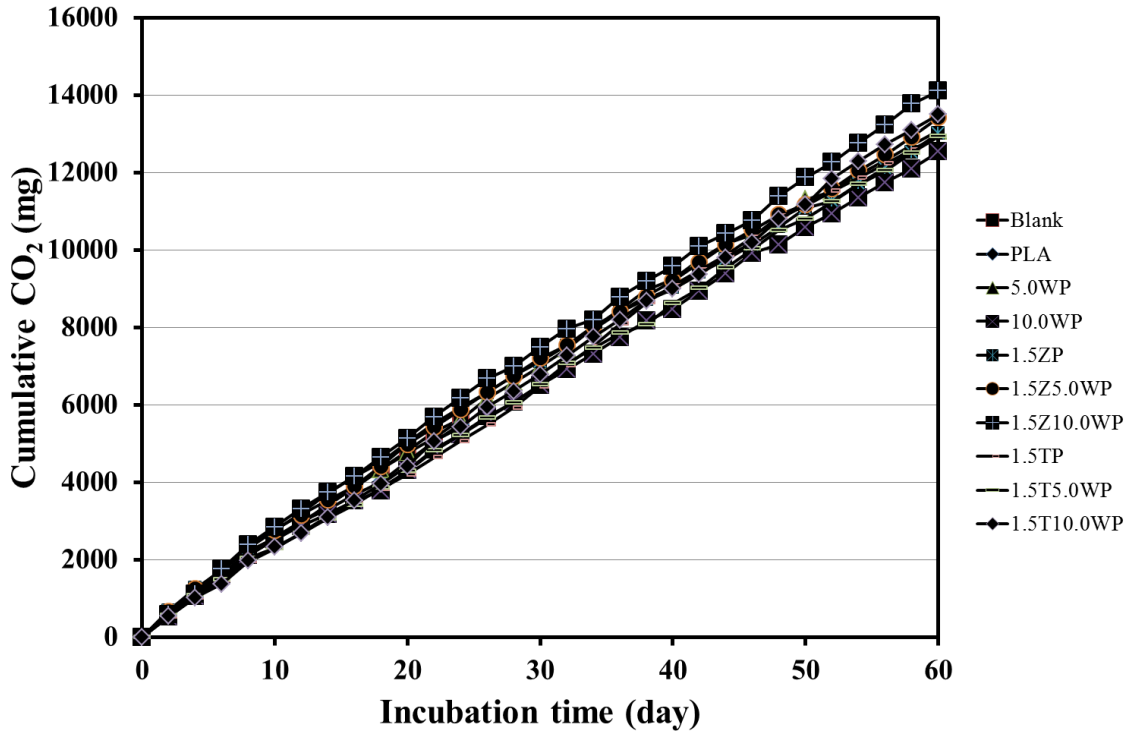

Figure 4.17 Cumulative CO_2 evolutions during biodegradation test

Table 4.6 Appearance of PLA and PLA based composites before and after biodegradation test

Specimens	Before biodegradation test	After biodegradation test (60 days)
PLA		
W_5P	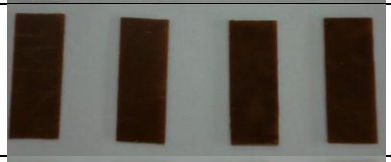	
$W_{10}P$		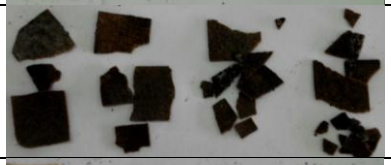
1.5ZP		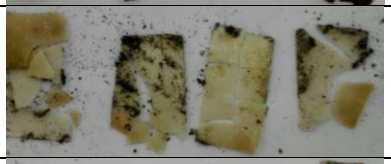
$1.5ZW_5P$		
$1.5ZW_{10}P$		
1.5TP		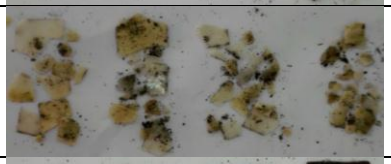
$1.5TW_5P$		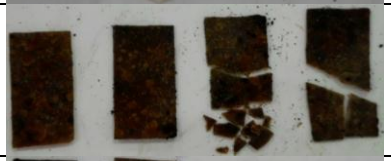
$1.5TW_{10}P$	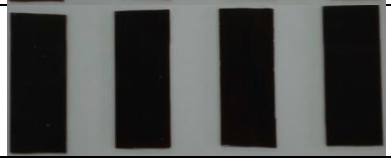	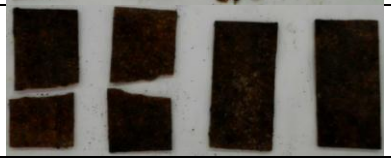

Appearances of all specimens before and after biodegradation tests are given in Table 4.6 which shows that all composite formulations tested was attacked by the microorganism during the test period. Biodegradation test results for PLA and PLA composites are shown in Figures 4.18-4.20. The results were divided into three categories: (i) PLA and wood/PLA (Figure 4.18); (ii) PLA and wood/PLA incorporating Zeomic (Figure 4.19); and (iii) PLA and wood/PLA incorporating triclosan (Figure 4.20), respectively. Each category was further subdivided into three different periods of incubation time: zone 1 (1–20 days); zone 2 (21–40 days); and zone 3 (41–60 days). In order to obtain a better understanding of the biodegradation behavior of PLA and PLA composites, the biodegradation rates for different time periods were calculated and are given in Table 4.7.

Table 4.7 Biodegradation rates for PLA and wood/PLA composites with and without the addition of Zeomic or triclosan (1.5 wt%)

Specimens	**Biodegradation rate in fixed period (%/day)**		
	1-20 days	**21-40 days**	**41-60 days**
PLA	0.12	0.39	0.32
W_5P	0.08	0.50	0.43
$W_{10}P$	0.08	0.33	0.54
1.5ZP	0.18	0.24	0.45
1.5ZW_5P	0.16	0.34	0.58
1.5$ZW_{10}P$	0.19	0.52	0.72
1.5TP	0.00	0.58	0.39
1.5TW_5P	0.00	0.37	0.54
1.5$TW_{10}P$	0.00	0.43	0.63

For PLA and wood/PLA (Figure 4.18), the graphs showed a slow increase in biodegradation levels for the first 20 days (zone 1), especially for PLA containing 5% and 10% wood. After 20 days (at the beginning of zone 2), the degradation rates of

wood/PLA became faster. Finally, after 60 days of incubation (at the end of zone 3), the wood/PLA systems exhibited better degradation performances than neat PLA, with degradation levels of 19.97%, 18.99% and 16.59% for W_5P, $W_{10}P$ and PLA, respectively. Table 4.7 shows that the degradation rates of wood/PLA started at 0.8%/day, which was lower than the rate of 0.12%/day for PLA. As indicated in the DSC thermogram (Figure 4.12), wood enhanced the crystallization of PLA; this plays an important role in retarding the hydrolysis reaction, which is the main chemical reaction in the biodegradation process. The crystalline structure of PLA takes a longer time to hydrolyze at the ester linkages and become lower in molecular weight [22], when it can be more easily digested by microorganisms. The degradation rates increased after 20 days, to 0.39, 0.50 and 0.33%/day (for W_5P, $W_{10}P$ and PLA, respectively) for the second period (zone 2; 21–40 days) of the test. Finally, during the third test period (zone 3; 41–60 days), the degradation rates of PLA, W_5P and $W_{10}P$ rose to 0.32, 0.43 and 0.54%/day, respectively. It can be observed that the biodegradation rate of W_5P became higher than that of neat PLA in zone 2, and that both W_5P and $W_{10}P$ had higher rates than PLA in zone 3. Although wood created crystalline regions in PLA (as indicated by the DSC thermogram, Figure 4.12), wood particles are also known to be highly hydrophilic, containing hydroxyl groups (–OH) that can absorb water molecules. The absorption of moisture initiated the hydrolysis reaction, which influenced the comparatively higher biodegradation rates of wood/PLA during zones 2 and 3. Therefore, it could be said that wood particles can be considered to be a “biodegradation promoter” for PLA.

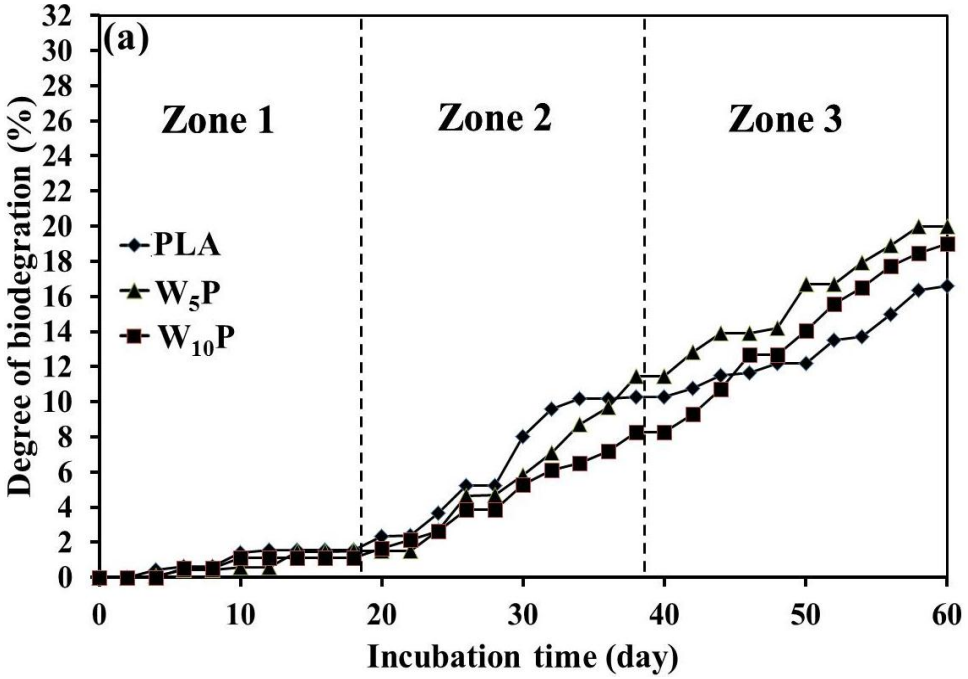

Figure 4.18 Degree of biodegradation for PLA and wood/PLA composites

For Zeomic systems (Figure 4.19), biodegradation occurred rapidly, beginning in the first zone. The similar patterns of biodegradation occurred in zones 2 and 3 but to an increased degree, especially for $1.5ZW_{10}P$. Ultimately, the biodegradation levels of 1.5ZP, $1.5ZW_5P$ and $1.5ZW_{10}P$ after 60 days of incubation were 17.32, 21.50 and 28.61%, respectively. Table 4.7 shows that the biodegradation rates increased sharply throughout the 60-day testing period, particularly with the presence of 10% wood. As discussed earlier, the Si–OH bonding as a function of zeolite, together with the hydrophilic wood particles, could absorb water molecules from the environment, thereby initiating the hydrolysis reaction. Therefore, the biodegradation rates of 1.5ZP, $1.5ZW_5P$ and $1.5ZW_{10}P$ after 60 days of incubation were 0.45, 0.58 and 0.72%/day, respectively, which were the highest degradation rates compared with the other systems. These results clearly suggested that Zeomic could also act as a biodegradation promoter for PLA.

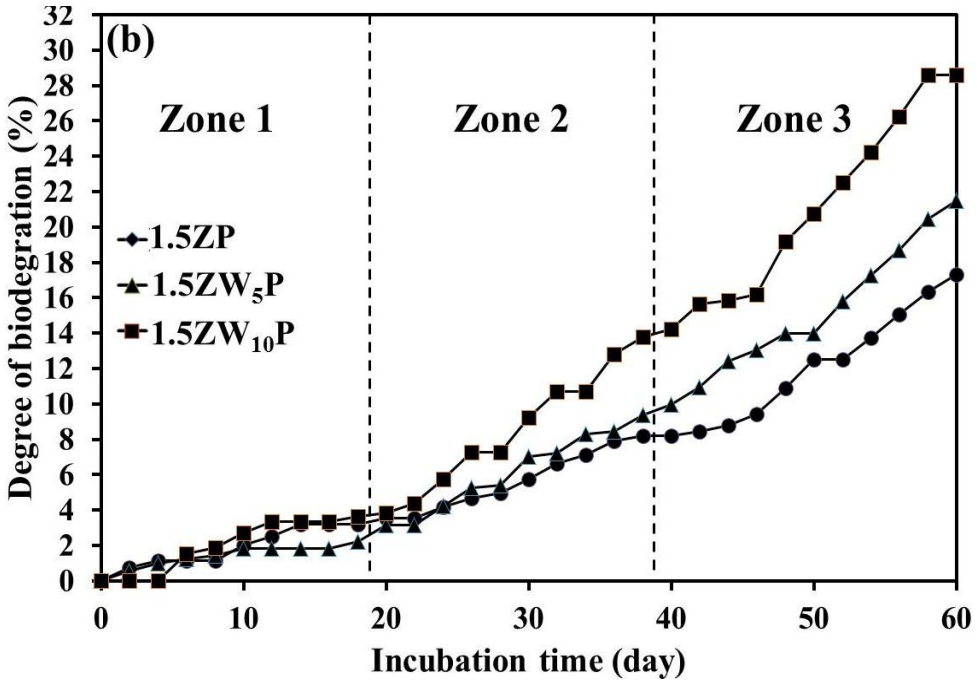

Figure 4.19 Degree of biodegradation for PLA and wood/PLA composites with Zeomic

For triclosan systems (Figure 4.20), the degree of biodegradation of all specimens was zero during the first 20 days. However, substantial degradation began to occur in zone 2. In zone 3, the biodegradation levels continued to steadily increase until day 60 of the test, when the biodegradation levels of 1.5TP, 1.5TW$_5$P and 1.5TW$_{10}$P reached 19.45, 18.12 and 21.20%, respectively. Table 4.7 shows that the biodegradation rates were 0%/day during the first 20 days because none of the microorganisms could attack the specimens. Triclosan can kill or inhibit bacterial growth above 80%. Triclosan is released from the PLA surface and prevents the surrounding microorganisms from attacking the PLA. This suggests that triclosan acted as a biodegradation retarder for PLA. However, the degradation rates in zone 2 increased dramatically, from 0 to 0.58, 0.37 and 0.43%/day for 1.5TP, 1.5TW$_5$P and 1.5TW$_{10}$P, respectively. Although triclosan could protect the PLA from microbial attack, the hydrolysis reaction also

occurred simultaneously. Therefore, over time the concentration of triclosan may not be sufficient to protect PLA from attack by microorganisms, the biodegradation rate took place abruptly. During days 41–60 of the test, the biodegradation rates were 0.39, 0.54 and 0.63%/day for 1.5TP, 1.5TW$_5$P and 1.5TW$_{10}$P, respectively, showing an increase only for the samples containing wood.

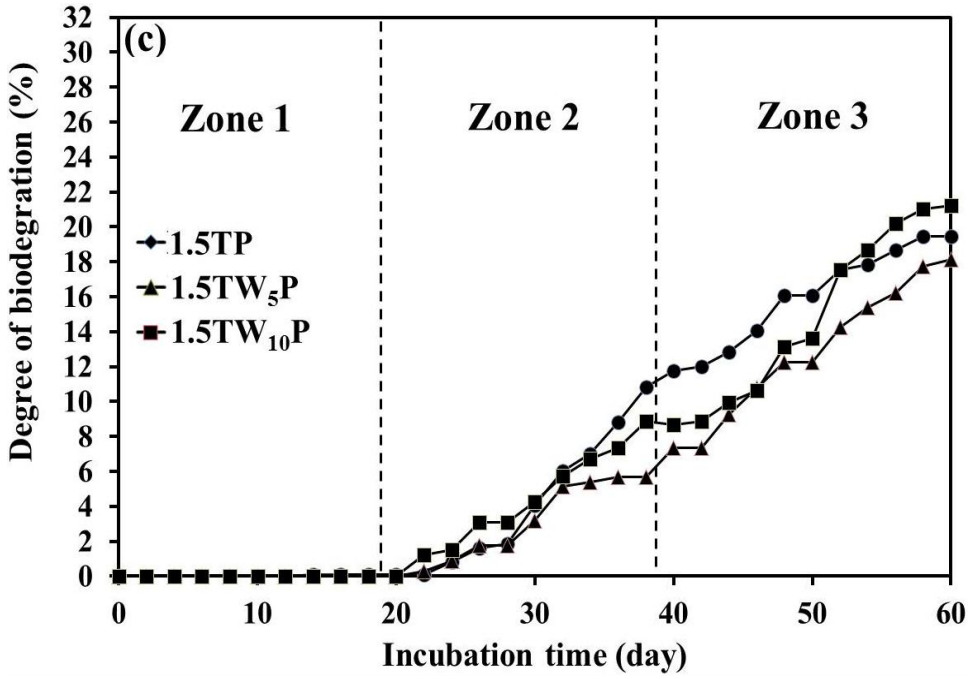

Figure 4.20 Degree of biodegradation for PLA and wood/PLA composites with triclosan

4.2 Effect of Organoclay Incorporation on Mechanical, Barrier and Thermal Properties and Anti-bacterial Performance of PLA and PLA composites with triclosan and Wood Flour

In this section, the effect of organoclay incorporation on mechanical, barrier and thermal properties and anti-bacterial performance of PLA and PLA composites with triclosan and wood Flour were studied

4.2.1 Mechanical properties

Figures 4.21-4.24 show the mechanical properties of PLA and 10% wood/PLA composites with and without 1.5% triclosan filled with different concentrations of Cloisite® 30B. It was observed that the mechanical properties (Young's modulus, Elongation at break and impact strength) of PLA and PLA based composite as a function of Cloisite® 30B did not change significantly with clay content. For example, the modulus of the neat PLA changed from 3.80 GPa to 3.89, 3.88 and 3.93GPa (Figure 4.21) whereas elongation at break changed from 2.87% to 2.32, 2.71 and 2.51% when 0.5, 1 and 2% clay were added (Figure 4.23), respectively. However, tensile strength was found to drop (Figure 4.22). Tensile strength of neat PLA decreased from 62.36 MPa to 56.13, 55.16 and 52.55MPa with 0.5, 1 and 2% clay loaded (Figure 4.22), respectively. In general, tensile strength of organoclay/polymer composites has been found to increase with clay content, however, a drop in tensile strength property of the clay/polymer composites was also found by some authors [93, 94]. The reason of this difference is still unclear. However, Zaidi *et.al.* suggested that the decreasing

phenomena could be considered as a result of the delamination between the polymer matrix and silicate interlayer [93].

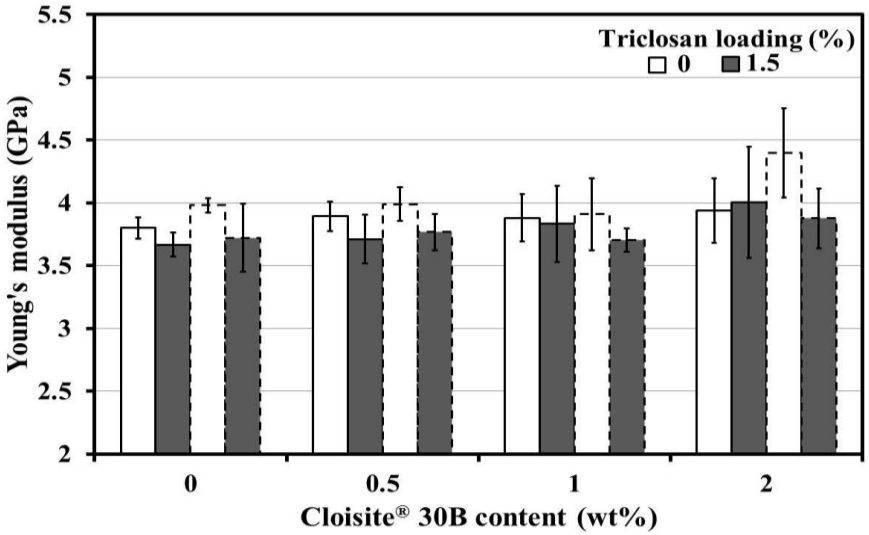

Figure 4.21 Young's modulus of PLA and PLA based composites with different concentration of triclosan and Cloisite® 30B (solid and dashed lines are PLA and wood/PLA systems, respectively)

For the wood/PLA specimens, the higher rigidity of 10% wood was found to increase the modulus of the PLA. The lesser rigidities thermoplastics often underwent this effect [82, 83]. On the other hand, tensile strength, elongation at break and impact strength decreased with the addition of 10% wood (Figures 4.22-4.24). For example, tensile strength, elongation at break and impact strength of the neat PLA decreased from 60.36 MPa, 2.87% and 31.76J/M to 49.23MPa, 1.54% and 29.64J/M, respectively . The drop in the mechanical properties was due to weak compatibility between the wood and PLA [69, 70] while the effect of triclosan compounding did not show definite trend because of small amount of the triclosan loaded.

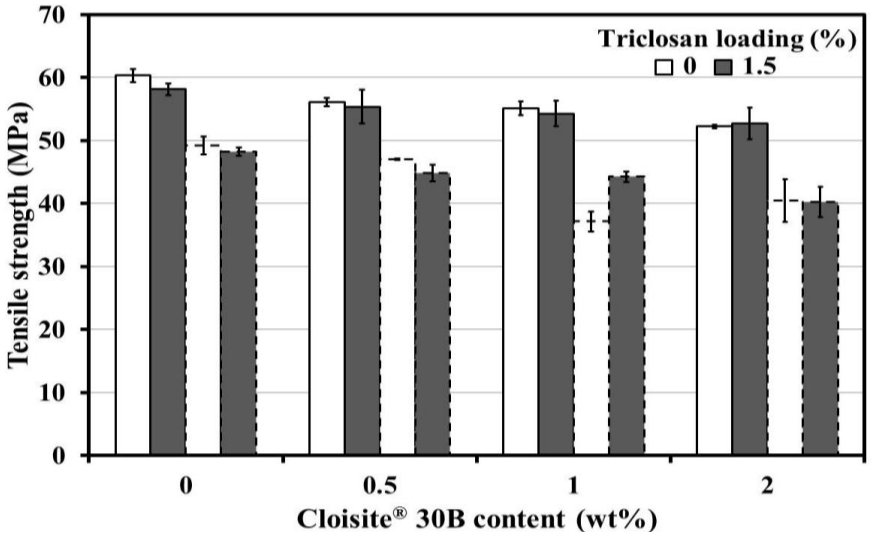

Figure 4.22 Tensile strength of PLA and PLA based composites with different concentration of triclosan and Cloisite® 30B (solid and dashed lines are PLA and wood/PLA systems, respectively)

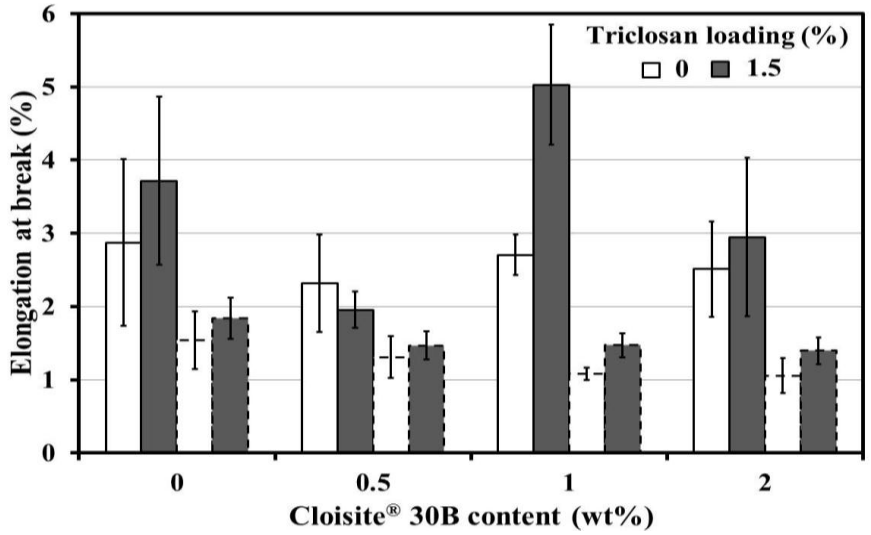

Figure 4.23 Elongation at break of PLA and PLA based composites with different concentration of triclosan and Cloisite® 30B (solid and dashed lines are PLA and wood/PLA systems, respectively)

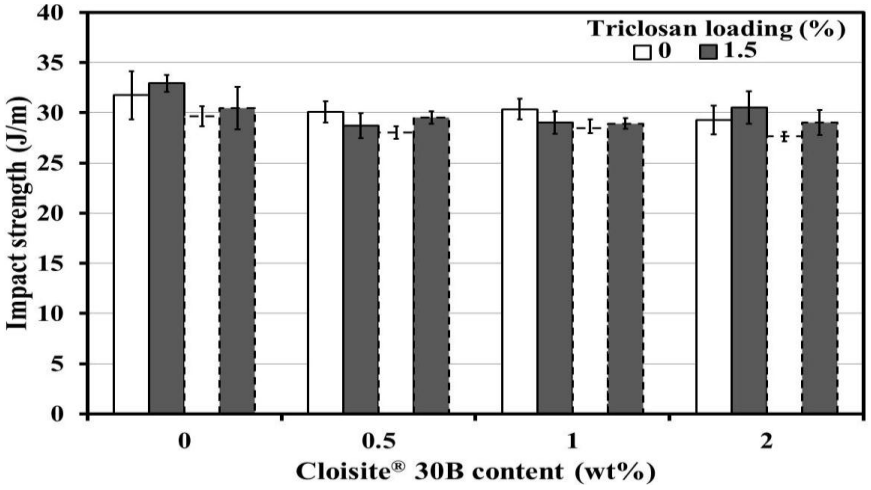

Figure 4.24 Impact strength of PLA and PLA based composites with different concentration of triclosan and Cloisite® 30B (solid and dashed lines are PLA and wood/PLA systems, respectively)

4.2.2 Thermal property and Clay dispersion analysis

The glass transition (T_g), melting (T_m) temperatures and the percentage of crystallinity (X_c) of PLA and PLA composites are given in Table 4.8. The Tg values of the PLA, CP and WP were around 60^{o}C. It can be seen that the addition of clay and triclosan did not affect the T_g values for all loadings used. On the contrary, T_m values of the PLA were affected obviously by the presence of wood and Cloisite® 30B. The T_m peak of the PLA based composites shows a double melting peak (figures not shown) resulting in two T_m values which paid responsibility to crystallinity level of the composites to be increased. The T_m of the neat PLA was split from 153.0 to 143.4 (T_{m1}) and 155.2(T_{m2}) and 148.5(T_{m1}) and 157.8(T_{m2}) when 0.5% clay and 10% wood were compound, respectively. The percentage of crystallinity of the PLA specimens increased when wood and Cloisite® 30B were filled especially, at 10% wood loading. The nucleating agent wood increased the crystallinity level of PLA up to 37.49% and 39.45% for WP

and TWP, respectively. Similar to wood fiber, Cloisite® 30B also increase amount of crystalline of the PLA significantly. The percentage of crystallinity increased with the 0.5% clay and then started to drop when 1% and 2% clay were added. The crystallinity percentage of the neat PLA changed from 20.3% to 29.7%, 15.5% and 22.5% by 0.5%, 1% and 2% clay addition, respectively.

Table 4.8 Thermal properties of PLA and PLA based composites

Specimens	Glass transition temperature (T_g)	Melting temperature (T_m)		Percent of crystallinity ($\%X_c$)
		T_{m1}	T_{m2}	
PLA	60.42	152.98		20.3
0.5CP	60.21	143.37	155.23	29.7
1CP	60.57	143.31	155.59	15.5
2CP	60.99	150.89	160.47	22.3
TP	59.80	151.05		17.3
0.5CTP	59.84	148.60	155.21	27.2
1CTP	59.75	149.41	159.48	27.9
2CTP	59.86	150.20	159.87	22.2
WP	60.63	148.49	157.78	37.5
0.5CWP	60.56	148.62	158.01	39.4
1CWP	60.33	149.52	158.19	26.9
2CWP	59.09	147.79	157.38	28.0
TWP	59.00	147.48	157.09	39.5
0.5CTWP	58.74	146.93	156.88	32.4
1CTWP	58.05	146.26	156.43	24.4
2CTWP	58.17	146.60	156.32	20.9

Figures 4.25a-b shows XRD patterns of pure Cloisite® 30B, PLA and 10% wood/PLA with different concentrations of clay. In general, if there is no clay platelets separation (immiscible), the XRD pattern of the composites would show the same as observed from the clay powder. For the complete dispersion of clay (exfoliation), no X-ray peak scan is exhibited because the distances between platelets would be larger than the limitation of wide angle X-ray can detect. In the case where an “intercalation” occurs,

the peak shifts of lower 2θ or larger d-spacing will exhibit, showing that the platelets have expanded [29].

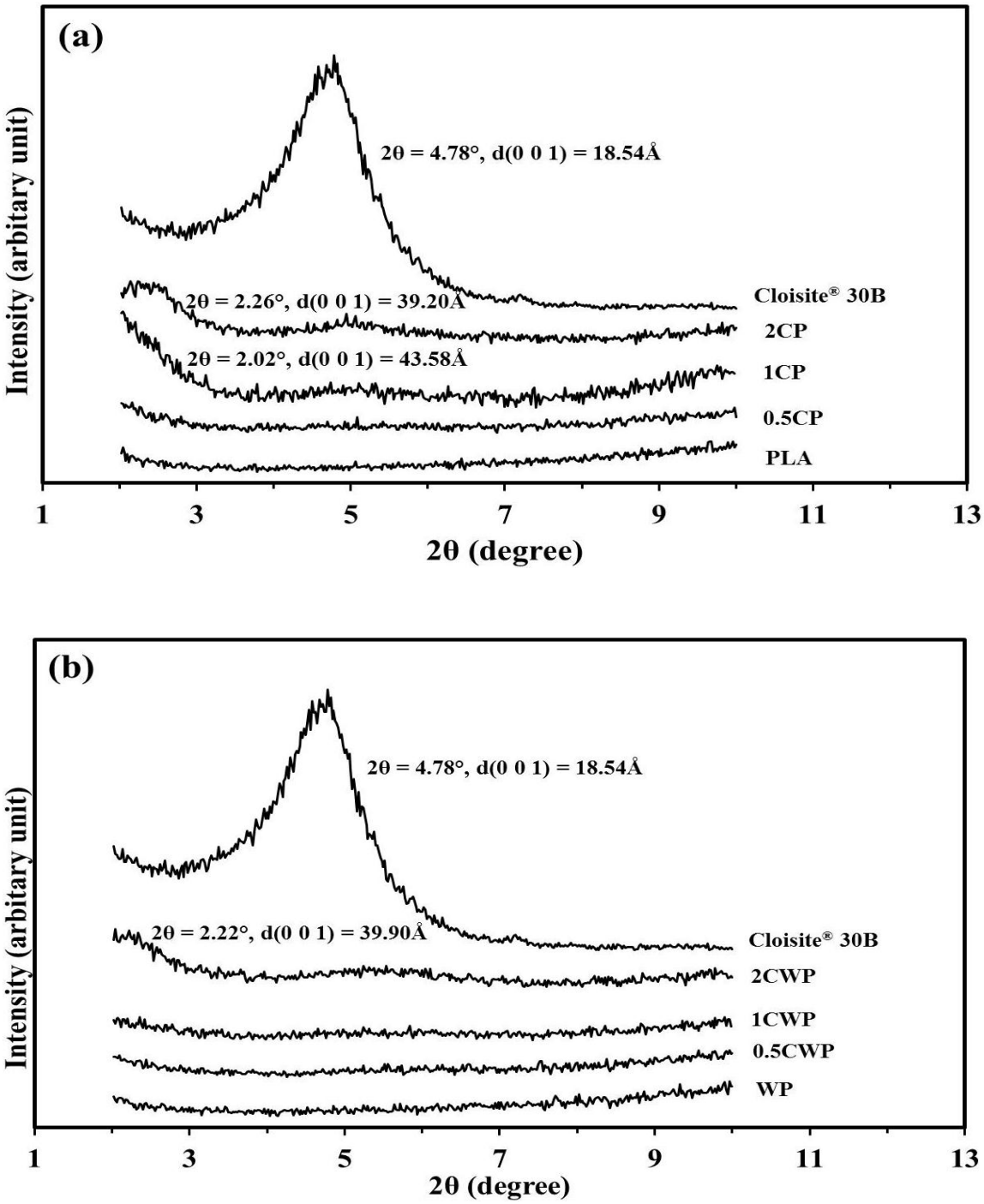

Figure 4.25 XRD patterns of Cloisite® 30B and PLA based composite with Cloisite® 30B loading of 0.5–2%wt: (a) Cloisite® 30B/PLA composites; (b) Cloisite® 30B /W_{10}/ PLA composites

The characteristic peak of Cloisite® 30B occurred at 2θ = 4.78° with the layer distance of d (0 0 1) = 18.54Å. But, in this work, no X-ray peaks were shown for all composite samples, meaning that there were no immiscible composites that occurred. For 1.0% and 2.0% Cloisite® 30B loadings, the specific peak of 1 and 2%wt CP shifted to lower angle from 2θ = 4.78° to 2.02 and 2.26° at d spacing (0 0 1) values of 43.85 and 39.20Å, respectively. The peak of WP added with 2% Cloisite® 30B also shifted to lower angle at 2θ = 2.22° d spacing (0 0 1) value of 39.90Å. These indicated that the intercalation dispersion had exhibited for 1CP, 2CP and 2CWP samples, except for 1CWP sample. For 0.5% Cloisite® 30B loading for PLA, there were no X-ray peak was given for both PLA and WP composites (Figures 4.25a and 4.25b) while the crystallinity level of these specimens raised up from 20.3 to 29.7 and 39.35% for 0.5CP and 0.5CWP, respectively (Table 4.8). This indicated that 0.5% Cloisite® 30B exhibited the exfoliation dispersion which provided more surface area and facilitated nanoparticles to act as nucleating agent for PLA. The similar phenomena also was found by Das. *et al* [95]. In the case of 1CWP, there was no Cloisite® 30B characteristic peak while the percentage of crystallinity dropped from 37.49% to 26.86%, suggesting that this was not the exfoliation dispersion. It was postulated that the influence of high dosage of wood as compared with Cloisite® 30B content disturbed the detection of XRD scan which resulted in the disappearance of the occurrence of intercalated characteristic peak.

4.2.3 Antibacterial property

The quantitative antibacterial evaluations for PLA, 1.5% triclosan/PLA with and without 10% wood at the different concentrations of Cloisite® 30B are given in the Figure 4.26a-d. For all control samples, *E. coli* grew up continuously when contact time was increased. The E. *coli* grown up behavior for pure PLA sample (Figure 4.26a) was similar to the control. This reveals that the neat PLA did not disturb the growth of bacteria. But the growth rate was noted to be slower for Cloisite® 30B added specimens, indicating that the clay could inhibit the bacterial growth rate. The antibacterial activity of organoclay Cloisite® 30B was caused by the operation of quaternary ammonium groups between the silicates layers which are extensively used as cationic bactericide to prohibit the microorganism growth [96]. The viable cell count of *E. coli* in comparison with the control sample for 60 - 240 min. contact time decreased obviously when the clay content was increased (Figure 4.26b). This means that both triclosan and Cloisite® 30B could be active to kill or retard the *E. coli* under the testing conditions. The addition of 10% wood affected the bacterial inhibition of Cloisite® 30B (Figure 4.26c) in CP samples. The changes in *E. coli* viable cell count were not significant in comparison with the control, even when 2% clay was added. But, the *E. coli* colony forming unit of CTP by the presence of 10% wood did not affect significantly (Figure 4.26d). The *E. coli* viable cell count of CTWP decreased with the Cloisite® 30B content and contact time. In comparison between Figure 4.26c and 4.26d, at 240 minute contact time, the *E. coli* viable cell count of control samples of CWP (Figure 4.26c) and CTWP (Figure 4.26d) were about 8.4 and 8.5 log (cfu/ml) while the viable cell count of the same samples were changed to around 8.1 and 7.4 log (cfu/ml) when 2% clay were

compounded, suggesting that the wood could affect the antibacterial activity of the Cloisite® 30B but could not affect the antibacterial efficiency of the triclosan.

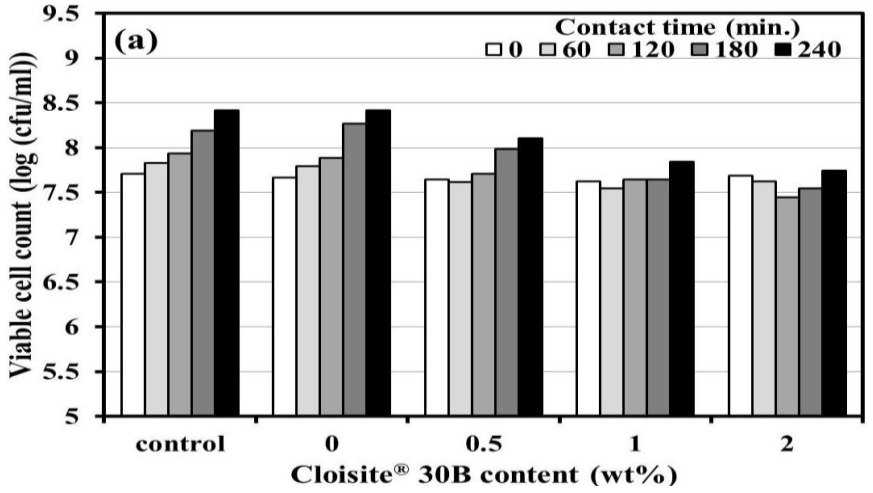

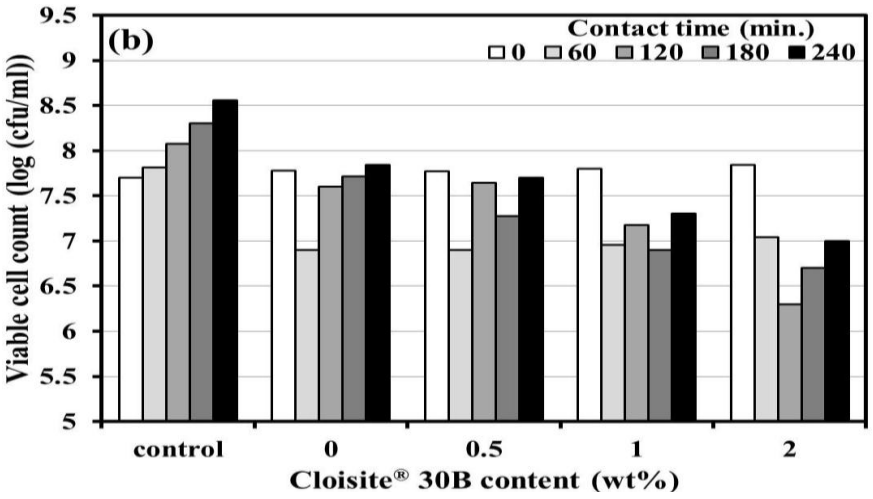

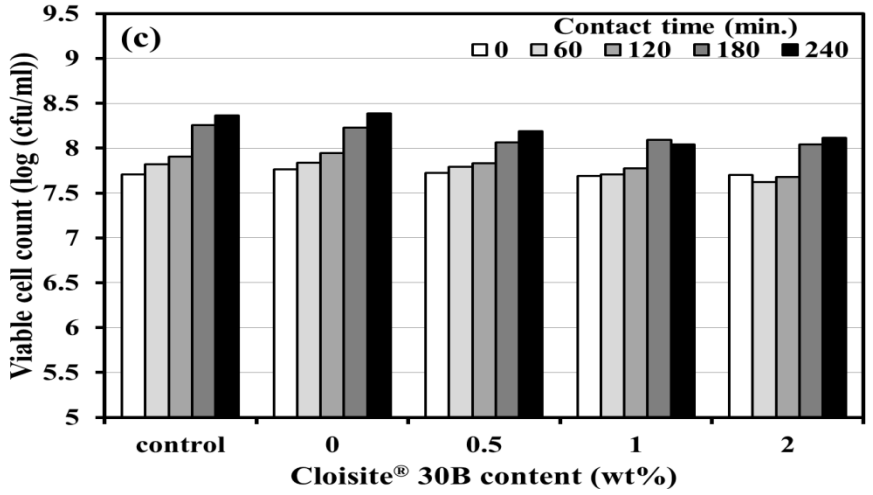

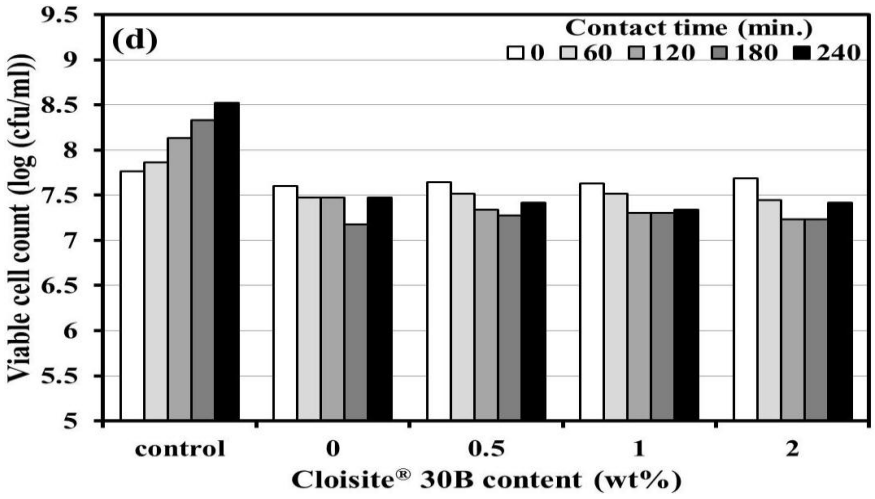

Figure 4.26 Viable cell count of *E.coli* with 0.5–2%wt Cloisite® 30B loading for 0–240 min. contact time: (a) Cloisite® 30B/PLA composites; (b) Cloisite® 30B/1.5% triclosan/PLA composites; (c) Cloisite® 30B/W_{10}/PLA composites; (d) Cloisite® 30B/1.5% triclosan/W_{10}/PLA composites

In order to understand antibacterial performance, the viable cell count was changed to percent bacteria reduction. Table 4.9 shows percent bacterial reductions at different contact times for PLA, 10% wood/PLA and 1.5% triclosan/10% wood composites with Cloisite® 30B loadings of 0.5-2.0 wt%. It can be seen that both neat PLA and WP did not show antibacterial performance, but when the clay was added, the antibacterial performance has been improved greatly with PLA up to 78.85% for 2% clay at 240 min. contact time while the best antibacterial performance of the WP was 52.79% for 1 % clay added at 240 minutes of contact time. Because Cloisite® 30B consists of Quaternary ammonium functional group, the functional group can kill bacteria by denaturing cell membranes and release the intracellular components. The Quaternary ammonium compounds are also show bacteriostatic at low concentrations and bactericidal at high concentrations. For PLA and WP compounded with 1.5% triclosan, it was clear that the triclosan was active under the testing conditions, moreover TWP

showed the better antibacterial activity than the TP. This could be due to the fact that wood could act as the antibacterial promoter for the triclosan/PLA composites by interrupting the interaction between the Triclosan and PLA and absorbs more water molecules to leave triclosan to be free and easy to migrate out of the polymer matrix. However, at the presence of Cloisite® 30B, the antimicrobial result of TWP was slightly worse than that of TP. Antibacterial result of 2CTP and 2CTWP at 240 min. contact time were 92.14% and 97.22, respectively. The wood particles could play a vital role in obstructing the quaternary ammonium groups of Cloisite® 30B to move to the PLA surface and kill the bacteria, resulting in the drop in antibacterial performance of the WP and TWP in a presence of clay.

Table 4.9 Percentage of bacterial reductions at different contact times for PLA, 10%wood/PLA and 1.5% triclosan/10% wood/PLA composites with Cloisite® 30B loadings of 0.0 – 2.0 wt%

Specimens	Contact time (min.)	Percentage of bacterial reduction (%)							
		0.0%		0.5%		1.0%		2.0%	
		0%WF	10%WF	0%WF	10%WF	0%WF	10%WF	0%WF	10%WF
PLA	60	7.46	0.00	38.80	6.06	47.76	22.72	37.31	36.36
	120	10.46	0.00	40.70	15.00	48.84	25.00	67.44	40.13
	180	0.00	5.56	37.66	35.56	71.42	31.11	77.27	38.89
	240	0.38	0.00	50.77	33.48	73.07	52.79	78.85	44.26
1.5TP	60	87.69	58.90	87.66	54.79	86.15	54.79	83.07	61.64
	120	66.39	77.78	63.03	83.70	87.39	85.18	98.32	87.41
	180	74.00	93.06	90.50	91.20	96.00	90.13	97.50	92.13
	240	80.56	90.94	86.11	92.15	94.44	93.35	97.22	92.14

4.2.4 Barrier properties

Water vapor permeability (WVP)

The effect of Cloisite® 30B loading on the WVP of the PLA and PLA based composites are shown in Figure 4.27. At 0% clay, the PLA had the most WVP at 8.24 x 10^{-11} g.mm/mm^2.h.Pa while 1.5% triclosan/PLA had lowest WVP at 7.26 x 10^{-11} g.mm/mm^2.h.Pa. From Table 4.5, it was found that the water contact angle of the pure PLA increased from 58.6° to 68.8° when 1.5% triclosan was added. This indicated that the triclosan made the PLA to be more hydrophobicity and harder for water molecules to penetrate. It was interesting to note that the highly hydrophilic wood also reduced the WVP property of the PLA. This is because the wood particles increase the crystallinity of PLA from 20.3% to about 4 %. The more crystalline and denser polymer structures lead to the lesser water penetration into the polymer surface. WVP of all testing formulations decreased with the Cloisite® 30B loading. For example, WVP of TWP changed from 7.7 x 10^{-11} g.mm/mm2.h.Pa to 6.69 and 6.46 x 10^{-11} g.mm/mm2.h.Pa when 0.5 and 2% clay were added, respectively. Improving water vapor permeability of the clay/PLA composites could be attributed to the impermeable clay silicate layer distributed in the polymer matrix [13]. These clay/polymer composites usually have strong barrier properties because the clay layers retard the diffusing molecule pathway due to tortuosity. Clays are essentially impermeable inorganic crystals, gas molecules have to permeate around the crystals instead of permeation in a straight line path which takes longer mean path and time for gas absorption though these clay/polymer composites [97]. Thus, the water molecules have to take longer time to go through these silicate layers resulting in the improved WVP.

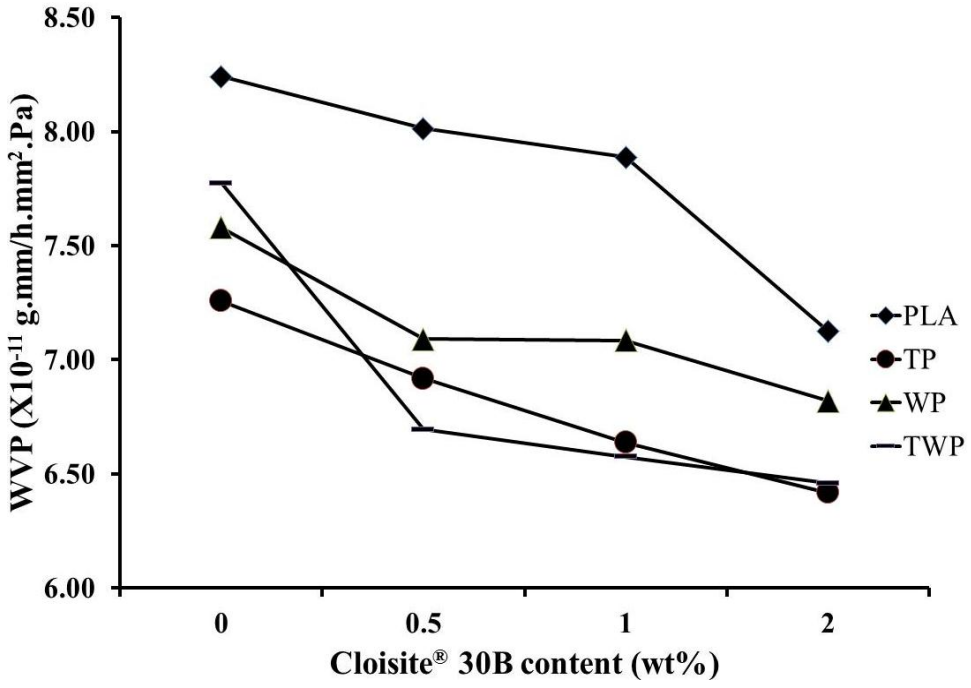

Figure 4.27 Water vapor permeabilities of PLA and PLA based composites as a function of Cloisite® 30B loading

Oxygen permeability

The oxygen permeability results of tested films are shown in Figure 4.28. Oxygen permeability of the PLA decreased when triclosan, wood flour and Cloisite® 30B were added. The oxygen permeability value of the pure PLA was 9.36 cc.mm/m^2.day but decreased to 8.47, 8.74 and 7.18 cc.mm/m^2.day for TP, WP and TWP, respectively. TWP had less oxygen permeability value than WP, TP and neat PLA by 1.56, 1.29 and 2.18 cc.mm/m^2.day, respectively. Hence, the better dispersion of chemical components showed the better films barrier property. This also indicated that all the materials blended affected the oxygen permeability of PLA films by obstruction of oxygen molecules to penetrate through the surface of PLA films. When considering the

Cloisite® 30B content, the oxygen permeability was found to decrease with the clay loading.

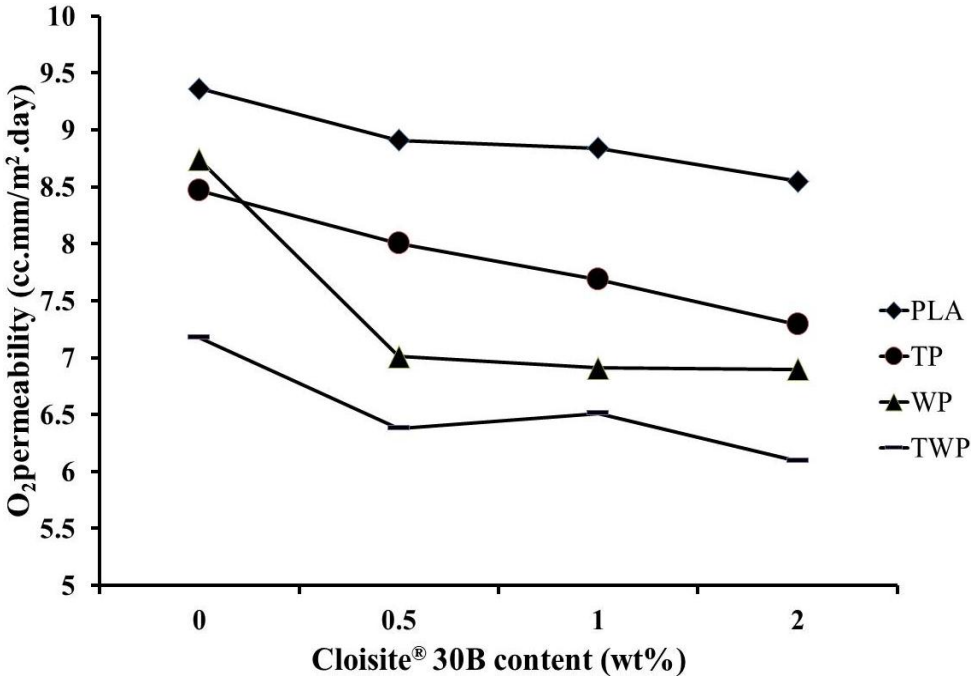

Figure 4.28 The effect of Cloisite® 30B loading on oxygen permeabilities of PLA and PLA based composites

The barrier property of all films increased reasonably when Cloisite® 30B was added as compared with the films without Cloisite® 30B especially, 0.5CWP due to the exfoliated dispersion as discussed in X-ray diffraction pattern. However, the oxygen barrier properties slightly performed with the higher clay loading due to the more impermeable silicate layer content dispersed in the polymer matrix.

CHAPTER 5 CONCLUSIONS AND FUTURE WORKS

5.1 conclusions

Effect of wood flour and antibacterial agents loading on the mechanical, antibacterial and biodegradable properties of PLA and PLA based composites

- Young's modulus was found to increase; and the tensile strength, elongation at break, and impact strength decreased with increasing wood content.
- For Zeomic system, the tensile strength, elongation at break, and impact strength of PLA and wood/PLA incorporated with Zeomic dramatically dropped, especially at a presence of 10% wood, because of the degradation of the PLA matrix as a result of a hydrolysis reaction between PLA, water molecules in the zeolite structure and absorbed water molecules by the wood particles.
- The effect of triclosan loading on the mechanical properties of PLA and wood/PLA did not show a clear trend which could be attributed to the triclosan did not involve in the hydrolysis reaction. Another possible reason is that the dosage of triclosan used was relatively small.
- The wood and Zeomic were found to perform as rigid foreign particles that create crystalline regions of the PLA.
- Triclosan achieved on killing efficiency for both *S.aureus* and *E.coli* bacteria, while Zeomic was ineffective.

- The wood particles promoted bacterial killing efficiency of the triclosan by interruption the hydrogen bond between the triclosan and PLA and also absorbed water molecules which facilitated the triclosan to migrate onto the PLA surface to kill the bacteria
- Wood and Zeomic were found to promote the rates of biodegradation of PLA and wood/PLA composites, whereas triclosan was found to retard their biodegradation.

Effect of Organoclay Incorporation on Mechanical, Barrier and Thermal Properties and Anti-bacterial Performance of PLA and PLA composites with triclosan and Wood Flour

- The effect of triclosan and Cloisite® 30B compounding did not change the mechanical properties and glass transition temperature of the PLA.
- T_m values of the composites exhibited double peak characteristic , by the presence of wood and Cloisite® 30B, which was related to an increase in crystallinity level.
- Antibacterial activity of the PLA composites was improved with the Cloisite® 30B content, and this was attributed to cationic bactericide quaternary ammonium group between the silicates layers.
- The barrier property of all composite films increased reasonably when Cloisite® 30B was added as compared with the films without Cloisite® 30B, especially 0.5CWP as a result of the exfoliate dispersion.

5.2 Future works

According to the dissertation pointed several interesting directions for future work, the present study would be extended as the follows

- Comparative studies for the influences of material variables, e.g. types of polymer matrix, polymer blends (biodegradable polymers, such as, starch and PLA), types and contents of additives (such as, trimethylolpropane triacrylate (TMPTA) as anti-hydrolysis agent) and mixing of antibacterial agents

REFERENCES

1. D'Arcy, N., 2002, "Overview of the Global Biocides Market", **Chimica Oggi-Chemistry Today**, Vol. 20, No. 6, pp. 6-7.
2. Silapasorn, K., Sombatsompop, K., Kositchaiyong, A., Wimolmala, E., Markpin, T., and Sombatsompop, N., 2011, "Effect of Chemical Structure of Thermoplastics on Antibacterial Activity and Physical Diffusion of Triclosan Doped in Vinyl Thermoplastics and Their Composites with Caco3", **Journal of Applied Polymer Science**, Vol. 121, No. 1, pp. 253-261.
3. Jain, P. and Pradeep, T., 2005, "Potential of Silver Nanoparticle-Coated Polyurethane Foam as an Antibacterial Water Filter", **Biotechnology and Bioengineering**, Vol. 90, No. 1, pp. 59-63.
4. Fang, Q. and Hanna, M.A., 1999, "Rheological Properties of Amorphous and Semicrystalline Polylactic Acid Polymers", **Industrial Crops and Products**, Vol. 10, No. 1, pp. 47-53.
5. Pehanich, J.L., Blankenhorn, P.R., and Silsbee, M.R., 2004, "Wood Fiber Surface Treatment Level Effects on Selected Mechanical Properties of Wood Fiber-Cement Composites", **Cement and Concrete Research**, Vol. 34, No. 1, pp. 59-65.
6. Tserki, V., Zafeiropoulos, N.E., Simon, F., and Panayiotou, C., 2005, "A Study of the Effect of Acetylation and Propionylation Surface Treatments on Natural Fibres", **Composites Part a-Applied Science and Manufacturing**, Vol. 36, No. 8, pp. 1110-1118.
7. Duncan, T.V., 2011, "Applications of Nanotechnology in Food Packaging and Food Safety: Barrier Materials, Antimicrobials and Sensors", **Journal of Colloid and Interface Science**, Vol. 363, No. 1, pp. 1-24.

8. Koh, H.C., Park, J.S., Jeong, M.A., Hwang, H.Y., Hong, Y.T., Ha, S.Y., and Nam, S.Y., 2008, "Preparation and Gas Permeation Properties of Biodegradable Polymer/Layered Silicate Nanocomposite Membranes", **Desalination**, Vol. 233, No. 1–3, pp. 201-209.
9. Fukushima, K., Tabuani, D., and Camino, G., 2009, "Nanocomposites of Pla and Pcl Based on Montmorillonite and Sepiolite", **Materials Science and Engineering: C**, Vol. 29, No. 4, pp. 1433-1441.
10. Adame, D. and Beall, G.W., 2009, "Direct Measurement of the Constrained Polymer Region in Polyamide/Clay Nanocomposites and the Implications for Gas Diffusion", **Applied Clay Science**, Vol. 42, No. 3–4, pp. 545-552.
11. Krikorian, V. and Pochan, D.J., 2003, "Poly (L-Lactic Acid)/Layered Silicate Nanocomposite: Fabrication, Characterization, and Properties", **Chemistry of Materials**, Vol. 15, No. 22, pp. 4317-4324.
12. Najafi, N., Heuzey, M.C., and Carreau, P.J., 2012, "Polylactide (Pla)-Clay Nanocomposites Prepared by Melt Compounding in the Presence of a Chain Extender", **Composites Science and Technology**, Vol. 72, No. 5, pp. 608-615.
13. Rhim, J.-W., Hong, S.-I., and Ha, C.-S., 2009, "Tensile, Water Vapor Barrier and Antimicrobial Properties of Pla/Nanoclay Composite Films", **LWT - Food Science and Technology**, Vol. 42, No. 2, pp. 612-617.
14. Chen, G.X. and Yoon, J.S., 2005, "Clay Functionalization and Organization for Delamination of the Silicate Tactoids in Poly(L-Lactide) Matrix", **Macromolecular Rapid Communications**, Vol. 26, No. 11, pp. 899-904.
15. Shah, A.A., Hasan, F., Hameed, A., and Ahmed, S., 2008, "Biological Degradation of Plastics: A Comprehensive Review", **Biotechnology Advances**, Vol. 26, No. 3, pp. 246-265.

16. Kunioka, M., Ninomiya, F., and Funabashi, M., 2006, "Biodegradation of Poly(Lactic Acid) Powders Proposed as the Reference Test Materials for the International Standard of Biodegradation Evaluation Methods", **Polymer Degradation and Stability**, Vol. 91, No. 9, pp. 1919-1928.
17. Avérous, L., 2004, "Biodegradable Multiphase Systems Based on Plasticized Starch: A Review", **Journal of Macromolecular Science, Part C**, Vol. 44, No. 3, pp. 231-274.
18. Lim, L.T., Auras, R., and Rubino, M., 2008, "Processing Technologies for Poly(Lactic Acid)", **Progress in Polymer Science**, Vol. 33, No. 8, pp. 820-852.
19. Auras, R., Harte, B., and Selke, S., 2004, "An Overview of Polylactides as Packaging Materials", **Macromolecular Bioscience**, Vol. 4, No. 9, pp. 835-864.
20. Sinclair, R.G., 1996, "The Case for Polylactic Acid as a Commodity Packaging Plastic", **Journal of Macromolecular Science, Part A**, Vol. 33, No. 5, pp. 585-597.
21. Vert, M., Schwarch, G., and Coudane, J., 1995, "Present and Future of Pla Polymers", **Journal of Macromolecular Science, Part A**, Vol. 32, No. 4, pp. 787-796.
22. Maharana, T., Mohanty, B., and Negi, Y.S., 2009, "Melt–Solid Polycondensation of Lactic Acid and Its Biodegradability", **Progress in Polymer Science**, Vol. 34, No. 1, pp. 99-124.
23. Thwe, M.M. and Liao, K., 2002, "Effects of Environmental Aging on the Mechanical Properties of Bamboo–Glass Fiber Reinforced Polymer Matrix Hybrid Composites", **Composites Part A: Applied Science and Manufacturing**, Vol. 33, No. 1, pp. 43-52.

24. Lee, S.-Y., Kang, I.-A., Doh, G.-H., Yoon, H.-G., Park, B.-D., and Qinglin Wu, 2008, "Thermal and Mechanical Properties of Wood Flour/Talc-Filled Polylactic Acid Composites: Effect of Filler Content and Coupling Treatment", **Journal of Thermoplastic Composite Materials**, Vol. 21, No. 3, pp. 209-223.
25. Côté, W., 1968, "Chemical Composition of Wood", In **Principles of Wood Science and Technology**, Springer Berlin Heidelberg, pp 55-78.
26. Pilla, S., Gong, S., O'Neill, E., Rowell, R.M., and Krzysik, A.M., 2008, "Polylactide-Pine Wood Flour Composites", **Polymer Engineering & Science**, Vol. 48, No. 3, pp. 578-587.
27. Huda, M.S., Drzal, L.T., Misra, M., and Mohanty, A.K., 2006, "Wood-Fiber-Reinforced Poly(Lactic Acid) Composites: Evaluation of the Physicomechanical and Morphological Properties", **Journal of Applied Polymer Science**, Vol. 102, No. 5, pp. 4856-4869.
28. Sinha Ray, S. and Okamoto, M., 2003, "Polymer/Layered Silicate Nanocomposites: A Review from Preparation to Processing", **Progress in Polymer Science**, Vol. 28, No. 11, pp. 1539-1641.
29. Paul, D.R. and Robeson, L.M., 2008, "Polymer Nanotechnology: Nanocomposites", **Polymer**, Vol. 49, No. 15, pp. 3187-3204.
30. Paul, M.A., Delcourt, C., Alexandre, M., Degée, P., Monteverde, F., and Dubois, P., 2005, "Polylactide/Montmorillonite Nanocomposites: Study of the Hydrolytic Degradation", **Polymer Degradation and Stability**, Vol. 87, No. 3, pp. 535-542.
31. Müller, R.-J., 2005, "Biodegradability of Polymers: Regulations and Methods for Testing", In **Biopolymers Online**, Wiley-VCH Verlag GmbH & Co. KGaA.

32. Tokiwa, Y. and Calabia, B., 2006, "Biodegradability and Biodegradation of Poly(Lactide)", **Applied Microbiology and Biotechnology**, Vol. 72, No. 2, pp. 244-251.
33. Tsuji, H. and Miyauchi, S., 2001, "Poly(L-Lactide): Vi Effects of Crystallinity on Enzymatic Hydrolysis of Poly(L-Lactide) without Free Amorphous Region", **Polymer Degradation and Stability**, Vol. 71, No. 3, pp. 415-424.
34. Nakamura, K., Tomita, T., Abe, N., and Kamio, Y., 2001, "Purification and Characterization of an Extracellular Poly(L-Lactic Acid) Depolymerase from a Soil Isolate,Amycolatopsis Sp. Strain K104-1", **Applied and Environmental Microbiology**, Vol. 67, No. 1, pp. 345-353.
35. Sudesh, K., Abe, H., and Doi, Y., 2000, "Synthesis, Structure and Properties of Polyhydroxyalkanoates: Biological Polyesters", **Progress in Polymer Science**, Vol. 25, No. 10, pp. 1503-1555.
36. Lucas, N., Bienaime, C., Belloy, C., Queneudec, M., Silvestre, F., and Nava-Saucedo, J.-E., 2008, "Polymer Biodegradation: Mechanisms and Estimation Techniques – a Review", **Chemosphere**, Vol. 73, No. 4, pp. 429-442.
37. Tsuji, H. and Ikarashi, K., 2004, "In Vitro Hydrolysis of Poly(L-Lactide) Crystalline Residues as Extended-Chain Crystallites: Iii. Effects of Ph and Enzyme", **Polymer Degradation and Stability**, Vol. 85, No. 1, pp. 647-656.
38. De Jong, S.J., Arias, E.R., Rijkers, D.T.S., van Nostrum, C.F., Kettenes-van den Bosch, J.J., and Hennink, W.E., 2001, "New Insights into the Hydrolytic Degradation of Poly(Lactic Acid): Participation of the Alcohol Terminus", **Polymer**, Vol. 42, No. 7, pp. 2795-2802.

39. Thai Industrial Standard (Iso) 17556 : 2003, **Plastic-Determination of the Ultimate Aerobic Biodegradability in Soil by Measuring the Oxygen Demand in a Respirometer of the Amount of Carbon Dioxide Evolved**.

40. American Standard Test Method (Astm) D5338-98, 2003, **Standard Test Method for Determining Aerobic Biodegradation of Plastic Materials under Controlled Composting, Annual**.

41. **Bacterial Cell Structure** [Online, 2014], Available: http://en.wikipedia.org/wiki/ bacterial cell structure [2014, May 6].

42. **Mechanism of Action of Antimicrobials (Overview)** [Online, 2014], Available: http://www.scribd.com/doc/512775/ mechanism-of-antimicrobials [2014, May 6].

43. E.F. Gale, E. Cundliffe, P.E. Reynolds, M.H. Richmond and M.J. Waring, 1981, "Biochemical Targets for Drug Action", **The Molecular Basis of Antibiotic Action**, 2nd Edition, pp.21-65**.**

44. **Nisin,** [Online, 2014] Available: http://en.wikipedia.org/wiki/file:nisin.png [2014, May 6].

45. Morris, S.L., Walsh, R.C., and Hansen, J.N., 1984, "Identification and Characterization of Some Bacterial Membrane Sulfhydryl Groups Which Are Targets of Bacteriostatic and Antibiotic Action", **Journal of Biological Chemistry**, Vol. 259, No. 21, pp. 13590-13594.

46. J.A.C. Expósito, 2006, **Studies on Antimicrobial Activity of Arginine-Based Surfactants and Chemoenzymatic Synthesis of Novel Amphiphiles Based on L-Arginine and D-Fagomine**, Ph.D. Dissertation, Major of Chemistry, Faculty of Science, Autónoma De Barcelona University.

47. **Triclosan Fact** [Online, 2014] Available: http://www.epa.gov/oppsrrd1/reds/ factsheets/triclosan_fs.htm [2014, April 6].

48. Coma, V., 2008, "Bioactive Packaging Technologies for Extended Shelf Life of Meat-Based Products", **Meat Science**, Vol. 78, No. 1–2, pp. 90-103.

49. **Triclosan** [Online, 2014], Available: http://en.wikipedia.org/wiki/file:triclosan.svg [2014, May 6].

50. Heath, R.J., Rubin, J.R., Holland, D.R., Zhang, E., Snow, M.E., and Rock, C.O., 1999, "Mechanism of Triclosan Inhibition of Bacterial Fatty Acid Synthesis", **Journal of Biological Chemistry**, Vol. 274, No. 16, pp. 11110-11114.

51. Kim, J.S., Kuk, E., Yu, K.N., Kim, J.-H., Park, S.J., Lee, H.J., Kim, S.H., Park, Y.K., Park, Y.H., Hwang, C.-Y., Kim, Y.-K., Lee, Y.-S., Jeong, D.H., and Cho, M.-H., 2007, "Antimicrobial Effects of Silver Nanoparticles", **Nanomedicine: Nanotechnology, Biology and Medicine**, Vol. 3, No. 1, pp. 95-101.

52. Sondi, I. and Salopek-Sondi, B., 2004, "Silver Nanoparticles as Antimicrobial Agent: A Case Study on E. Coli as A model for Gram-Negative Bacteria", **Journal of Colloid and Interface Science**, Vol. 275, No. 1, pp. 177-182.

53. Yamanaka, M., Hara, K., and Kudo, J., 2005, "Bactericidal Actions of a Silver Ion Solution on Escherichia Coli, Studied by Energy-Filtering Transmission Electron Microscopy and Proteomic Analysis", **Applied and Environmental Microbiology**, Vol. 71, No. 11, pp. 7589-7593.

54. Appendini, P. and Hotchkiss, J.H., 2002, "Review of Antimicrobial Food Packaging", **Innovative Food Science & Emerging Technologies**, Vol. 3, No. 2, pp. 113-126.

55. Quintavalla, S. and Vicini, L., 2002, "Antimicrobial Food Packaging in Meat Industry", **Meat Science**, Vol. 62, No. 3, pp. 373-380.

56. Chung, D., Papadakis, S.E., and Yam, K.L., 2003, "Evaluation of a Polymer Coating Containing Triclosan as the Antimicrobial Layer for Packaging Materials", **International Journal of Food Science & Technology**, Vol. 38, No. 2, pp. 165-169.

57. Park, E.-S., Moon, W.-S., Song, M.-J., Kim, M.-N., Chung, K.-H., and Yoon, J.-S., 2001, "Antimicrobial Activity of Phenol and Benzoic Acid Derivatives", **International Biodeterioration & Biodegradation**, Vol. 47, No. 4, pp. 209-214.

58. Haugaard, V., Weber, C., Danielsen, B., and Bertelsen, G., 2002, "Quality Changes in Orange Juice Packed in Materials Based on Polylactate", **European Food Research and Technology**, Vol. 214, No. 5, pp. 423-428.

59. Frederiksen, C., Haugaard, V., Poll, L., and Miquel Becker, E., 2003, "Light-Induced Quality Changes in Plain Yoghurt Packed in Polylactate and Polystyrene", **European Food Research and Technology**, Vol. 217, No. 1, pp. 61-69.

60. Brewer, R., Adams, M.R., and Park, S.F., 2002, "Enhanced Inactivation of Listeria Monocytogenes by Nisin in the Presence of Ethanol", **Letters in Applied Microbiology**, Vol. 34, No. 1, pp. 18-21.

61. Broughton, J.D., 1990, "Nisin and Its Uses as a Food Preservative", **Food Technology**, Vol. 44, No. 11, pp. 100–117.

62. Jin, T. and Zhang, H., 2008, "Biodegradable Polylactic Acid Polymer with Nisin for Use in Antimicrobial Food Packaging", **Journal of Food Science**, Vol. 73, No. 3, pp. 127-134.

63. Cutter, C.N., 1999, "Effectiveness of Triclosan-Incorporated Plastic against Bacteria on Beef Surfaces", **Journal of Food Protection**, Vol. 62, No. 5, pp. 474-479.

64. Fernández, A., Soriano, E., Hernández-Muñoz, P., and Gavara, R., 2010, "Migration of Antimicrobial Silver from Composites of Polylactide with Silver Zeolites", **Journal of Food Science**, Vol. 75, No. 3, pp. 186-193.
65. Brody A.L, Strupinsky E.R, and Kline L.R, 2001, "**The Application of Silver-Zeolite to Package Materials**", Active Packaging for Food Applications, 1st Edition, pp. 151-154.
66. Jeong, S., Yeo, S., and Yi, S., 2005, "The Effect of Filler Particle Size on the Antibacterial Properties of Compounded Polymer/Silver Fibers", **Journal of Materials Science**, Vol. 40, No. 20, pp. 5407-5411.
67. Taptim, K., Ansarifar, A., and Sombatsompop, N., 2014, "Effect of Organoclay and Silver-Substituted Zeolite on the Mechanical and Antibacterial Properties of a Silicone Rubber Filled with 2-Hydroxypropyl-3-Piperazinyl-Quinoline Carboxylic Acid Methacrylate", **Polymer Engineering and Science**, Vol. 54, No. 4, pp. 932-941.
68. Finkenstadt, V.L. and Tisserat, B., 2010, "Poly(Lactic Acid) and Osage Orange Wood Fiber Composites for Agricultural Mulch Films", **Industrial Crops and Products**, Vol. 31, No. 2, pp. 316-320.
69. Sykacek, E., Schlager, W., and Mundigler, N., 2010, "Compatibility of Softwood Flour and Commercial Biopolymers in Injection Molding", **Polymer Composites**, Vol. 31, No. 3, pp. 443-451.
70. Lee, S.-Y., Kang, I.-A., Doh, G.-H., Yoon, H.-G., Park, B.-D., and Qinglin, W., 2008, "Thermal and Mechanical Properties of Wood Flour/Talc-Filled Polylactic Acid Composites: Effect of Filler Content and Coupling Treatment", **Journal of Thermoplastic Composite Materials**, Vol. 21, No. 3, pp. 209-223.

71. Petinakis, E., Yu, L., Edward, G., Dean, K., Liu, H., and Scully, A., 2009, "Effect of Matrix–Particle Interfacial Adhesion on the Mechanical Properties of Poly(Lactic Acid)/Wood-Flour Micro-Composites", **Journal of Polymers and the Environment**, Vol. 17, No. 2, pp. 83-94.
72. Mohamed, A.A., Finkenstadt, V.L., and Palmquist, D.E., 2008, "Thermal Properties of Extruded/Injection-Molded Poly(Lactic Acid) and Biobased Composites", **Journal of Applied Polymer Science**, Vol. 107, No. 2, pp. 898-908.
73. Shi, Q.F., Mou, H.Y., Gao, L., Yang, J., and Guo, W.H., 2010, "Double-Melting Behavior of Bamboo Fiber/Talc/Poly (Lactic Acid) Composites", **Journal of Polymers and the Environment**, Vol. 18, No. 4, pp. 567-575.
74. Kositchaiyong, A., Rosarpitak, V., and Sombatsompop, N., 2014, "Antifungal Properties and Material Characteristics of Pvc and Wood/Pvc Composites Doped with Carbamate-Based Fungicides", **Polymer Engineering & Science**, Vol. 54, No. 6, pp. 1248-1259.
75. Krikorian, V. and Pochan, D.J., 2003, "Poly (L-Lactic Acid)/Layered Silicate Nanocomposite: Fabrication, Characterization, and Properties", **Chemistry of Materials**, Vol. 15, No. 22, pp. 4317-4324.
76. Ahn, H.K., Huda, M.S., Smith, M.C., Mulbry, W., Schmidt, W.F., and Reeves, J.B., 2011, "Biodegradability of Injection Molded Bioplastic Pots Containing Polylactic Acid and Poultry Feather Fiber", **Bioresource Technology**, Vol. 102, No. 7, pp. 4930-4933.
77. Ho, K.-L., Pometto, A., III, and Hinz, P., 1999, "Effects of Temperature and Relative Humidity on Polylactic Acid Plastic Degradation", **Journal of Environmental Polymer Degradation**, Vol. 7, No. 2, pp. 83-92.

78. Jarerat, A., Tokiwa, Y., and Tanaka, H., 2003, "Poly(L-Lactide) Degradation by Kibdelosporangium Aridum", **Biotechnology Letters**, Vol. 25, No. 23, pp. 2035-2038.

79. Pongnop, W., Sombatsompop, K., Kositchaiyong, A., and Sombatsompop, N., 2011, "Effects of Incorporating Technique and Silver Colloid Content on Antibacterial Performance for Thermoplastic Films", **Journal of Applied Polymer Science**, Vol. 122, No. 5, pp. 3456-3465.

80. Sin, Lt., Rahmat, Ar., and Rahman, Wa., 2012, "**Polylactic Acid: PLA Biopolymer Technology and Applications**", 1st Edition, Elsevier, pp.125.

81. Sombatsompop, N., Yotinwattanakumtorn, C., and Thongpin, C., 2005, "Influence of Type and Concentration of Maleic Anhydride Grafted Polypropylene and Impact Modifiers on Mechanical Properties of Pp/Wood Sawdust Composites", **Journal of Applied Polymer Science**, Vol. 97, No. 2, pp. 475-484.

82. Bledzki, A.K. and Faruk, O., 2006, "Injection Moulded Microcellular Wood Fibre–Polypropylene Composites", **Composites Part A: Applied Science and Manufacturing**, Vol. 37, No. 9, pp. 1358-1367.

83. Faruk, O. and Matuana, L.M., 2008, "Nanoclay Reinforced Hdpe as a Matrix for Wood-Plastic Composites", **Composites Science and Technology**, Vol. 68, No. 9, pp. 2073-2077.

84. Kim, H., Biswas, J., and Choe, S., 2006, "Effects of Stearic Acid Coating on Zeolite in Ldpe, Lldpe, and Hdpe Composites", **Polymer**, Vol. 47, No. 11, pp. 3981-3992.

85. Sykacek, E., Schlager, W., and Mundigier, N., 2010, "Compatibility of Softwood Flour and Commercial Biopolymers in Injection Molding", **Polymer Composites**, Vol. 31, No. 3, pp. 443-451.

86. Lee, S.Y., Kang, I.A., Doh, G.H., Yoon, H.G., Park, B.D., and Wu, Q.L., 2008, "Thermal and Mechanical Properties of Wood Flour/Talc-Filled Polylactic Acid Composites: Effect of Filler Content and Coupling Treatment", **Journal of Thermoplastic Composite Materials**, Vol. 21, No. 3, pp. 209-223.

87. Kaali, P., Strömberg, E., Aune, R.E., Czél, G., Momcilovic, D., and Karlsson, S., 2010, "Antimicrobial Properties of Ag+ Loaded Zeolite Polyester Polyurethane and Silicone Rubber and Long-Term Properties after Exposure to in-Vitro Ageing", **Polymer Degradation and Stability**, Vol. 95, No. 9, pp. 1456-1465.

88. Sombatsompop, N. and Chaochanchaikul, K., 2004, "Effect of Moisture Content on Mechanical Properties, Thermal and Structural Stability and Extrudate Texture of Poly(Vinyl Chloride)/Wood Sawdust Composites", **Polymer International**, Vol. 53, No. 9, pp. 1210-1218.

89. Pattamasattayasonthi, N., Chaochanchaikul, K., Rosarpitak, V., and Sombatsompop, N., 2011, "Effects of Uv Weathering and a Ceo2-Based Coating Layer on the Mechanical and Structural Changes of Wood/Pvc Composites", **Journal of Vinyl and Additive Technology**, Vol. 17, No. 1, pp. 9-16.

90. Kaali, P., Perez-Madrigal, M.M., Stromberg, E., Aune, R.E., Czel, G., and Karlsson, S., 2011, "The Influence of Ag+, Zn2+ and Cu2+ Exchanged Zeolite on Antimicrobial and Long Term in Vitro Stability of Medical Grade Polyether Polyurethane", **eXPRESS Polymer Letters**, Vol. 5, No. 12, pp. 1028–1040.

91. **Agion Technology**, [Online, 2014] Available:http://www.agion-tech.com/technology.aspx?Id=156 [2014, May 6].

92. Sombatsompop, N., Kositchaiyong, A., and Wimolmala, E., 2006, "Experimental Analysis of Temperature and Crystallinity Profiles of Wood Sawdust/Polypropylene Composites During Cooling", **Journal of Applied Polymer Science**, Vol. 102, No. 2, pp. 1896-1905.

93. Zaidi, L., Bruzaud, S., Bourmaud, A., Médéric, P., Kaci, M., and Grohens, Y., 2010, "Relationship between Structure and Rheological, Mechanical and Thermal Properties of Polylactide/Cloisite 30b Nanocomposites", **Journal of Applied Polymer Science**, Vol. 116, No. 3, pp. 1357-1365.

94. Meng, Q.K., Hetzer, M., and De Kee, D., 2011, "Pla/Clay/Wood Nanocomposites: Nanoclay Effects on Mechanical and Thermal Properties", **Journal of Composite Materials**, Vol. 45, No. 10, pp. 1145-1158.

95. Das, K., Ray, D., Banerjee, I., Bandyopadhyay, N.R., Sengupta, S., Mohanty, A.K., and Misra, M., 2010, "Crystalline Morphology of Pla/Clay Nanocomposite Films and Its Correlation with Other Properties", **Journal of Applied Polymer Science**, Vol. 118, No. 1, pp. 143-151.

96. Hong, S.-I. and Rhim, J.-W., 2008, "Antimicrobial Activity of Organically Modified Nano-Clays", **Journal of Nanoscience and Nanotechnology**, Vol. 8, No. 11, pp. 5818-5824.

97. Bharadwaj, R.K., Mehrabi, A.R., Hamilton, C., Trujillo, C., Murga, M., Fan, R., Chavira, A., and Thompson, A.K., 2002, "Structure-Property Relationships in Cross-Linked Polyester-Clay Nanocomposites", **Polymer**, Vol. 43, No. 13, pp. 3699-3705.

BIOGRAPHY

NAME Mr. Chana Prapruddivongs

DATE OF BIRTH 11 July 1982

EDUCATIONAL RECORD

BACHELOR'S DEGREE Bachelor of Science (Industrial Chemistry),
Faculty of Science,
King Mongkut's Institite of Technology Ladkrabang, 2005

MASTER'S DEGREE Master of Engineering (Chemical Engineering),
Faculty of Engineering,
King Mongkut's University of Technology Thonburi, 2007

DOCTORAL DEGREE Doctor of Philosophy (Materials Technology),
School of Energy, Environment and Materials,
King Mongkut's University of Technology Thonburi, 2013

SCHOLARSHIP The office of Higher Education Commission (OHEC)

PUBLICATION OUTPUTS FROM THIS DISSERTATION

- **JOURNAL PAPERS**

1. C. Prapruddivongs and N. Sombatsompop (2012) Roles and evidence of wood flour as an antibacterial promoter for triclosan-filled poly(lactic acid) **Composites Part B: Engineering,** 43:2730-2737(JIF = 2.143)
2. C. Prapruddivongs, K. Jayaraman, & N. Sombatsompop (2014) Effect of Organoclay Incorporation on Mechanical, Barrier and Thermal Properties and Anti-bacterial Performance of PLA and PLA composites with Triclosan and Wood Flour **Polymers & Polymer Composites**, (accepted) (JIF = 0.309)
3. C. Prapruddivongs and N. Sombatsompop (2014) Wood, Silver-Substituted Zeolite (Zeomic) and Triclosan as Biodegradation Promoters and Antibacterial Agents for PLA and PLA Composites **Journal of Polymers and The Environment** (submitted) (JIF = 1.495)

- **INTERNATIONAL CONFERENCE PAPERS**

1. C. Prapruddivongs and N. Sombatsompop (2011) Effect of wood flour on structural and thermal properties and antibacterial activity of PLA filled with triclosan - **Twentieth International Symposium on Processing and Fabrication of Advanced Materials (PFAM XIX**), 15-18 December 2011, Hongkong China.
2. C. Prapruddivongs and N. Sombatsompop (2013) Biodegradation and Anti-bacterial Properties of PLA and Wood/PLA Composites Incorporated with Zeomic Anti-bacterial Agent - **The 4th International Conference on Multi-Functional Materials and Structures (MFMS 2013),** 14-17 July 2013, Bangkok Thailand